Inaugural dissertation

for

obtaining the doctoral degree

of the

Combined Faculties of Mathematics, Engineering and Natural Sciences

of the

Ruperto – Karls – Univeristy

Heidelberg, Germany

presented by

M.Sc. Siddhi Maniyar (geb. Rathi)

born in Aurangabad, India

Oral examination: 10th of October, 2022

Molecular characterisation of Mck1, a novel Spindle Position Checkpoint (SPOC) protein and mitotic inhibitor.

by

Siddhi Maniyar (geb. Rathi)

Referees:

Prof. Dr. Gislene Pereira

Prof. Dr. Michael Knop

Dr. Sergio P. Acebrón

Dr. Anne Schlaitz

Everything is theoretically impossible until it is done.

-Robert A. Heinlein

To everyone who believed in me

Acknowledgement

This work owes its existence to the unwavering support, help and motivation of several people.

I am most grateful to Prof. Dr. Gislene Pereira for her supervision and mentorship throughout the tenure of my PhD. This would not have been possible without her erudite guidance.

I am also obliged to Prof. Dr. Elmar Schiebel and Prof. Dr. Michael Knop, who were on my Thesis Advisory Committee, for their critical comments and suggestions as well as for sharing laboratory equipment and/or reagents during this thesis.

I am thankful to Irem Polat for her technical assistance and friendly rapport along with making it fun to work in the laboratory. From a mentee to friends, our time together will always be cherished. I would also like to express my gratitude to the Pereira lab members (between 2018-2022) for their help and scientific discussions.

A special thanks to Johanna Streubel for translating the thesis summary into German. For the many exciting meetups, heart-to-heart conversations and friendships, I am in awe of Linda Viol and Mariama M'bengue.

I extend my gratefulness to the German Academic Exchange Service (DAAD) for the financial support throughout the tenure of this PhD.

A big shout out to my friends Karuna Alekhya Pasam and Amrutha Prabodh for bringing out the travel element in my PhD life and the pep talks filled with love, laughter and more ;).

Vriddhi Rathi, Jyoti Grewal and Ankita Kalantri, this would not have been feasible without your constant reassurances even at times when I was unsure about my own

capabilities. Thank you for being a part of my happy moments plus listening to me-crib, complain or cry, during my lows.

During my PhD, I volunteered to work at ‘PhDs of India’ (POI) which gave me some fond experiences of sharing powerful doctoral stories of Indian researchers. I am grateful to the team for letting me be a part of POI which helped pave a way for my progress as a scientist and a writer.

Be it any kind of celebration, I could always count on my Heidelberg family: Sanchita Saxena, Parita Gandhi, Manjunath Satyamurthy, Ashish Jha, Reuben Borisson, Sinéad O’Brien, Gaym Habtemariam, Pratik Patil, Abaya Prakash, Vignesh Viswanathan, Rashi Agrawal, Shivohum Bahuguna, Harshita Mishra and Jidnyasa Gujar. I am beholden to all of you for my life outside of the lab.

To my many friends and family abroad who didn’t let distance matter and filled the emotional void with video calls and messages. My little brother, Kapeel Rathi, thank you for placing your hope and making me smile through thick and thin. To my mother and father-in-law, your encouragement and positive outlook have always raised my spirits high.

I am forever indebted to my parents for believing in me and supporting my aspirations even when they seemed farfetched. I owe this thesis to your undying love, support and inspiration.

Last but not the least, words fall short when I begin to thank my husband, Siddharth Maniyar. I am eternally grateful to you for filling my life with happy colours, adventure and ‘work-life’ balance, but most importantly, for handling me with CARE. Your belief and faith in me have given me the courage to take up new challenges.

Table of Contents

Summary

In *Saccharomyces cerevisiae*, the position of the mitotic spindle is surveyed by the spindle position checkpoint (SPOC). SPOC ensures that cells do not exit mitosis if their anaphase spindle is misaligned thereby ensuring faithful chromosomal segregation. Defects in SPOC can cause multiploidy and decrease cell survival.

The SPOC kinase, Kin4, activates the Bfa1-Bub2 GTPase activating protein (GAP) complex via Bfa1 phosphorylation which in turn inhibits the mitotic exit network (MEN), a pathway that contributes to mitotic exit. Recent work has prompted Kin4-independent mechanisms that engage SPOC. Here, I have investigated the role of glycogen synthase kinase (GSK)-3 homolog, Mck1, as a novel SPOC component that activates SPOC independently of the Kin4 pathway. I show that, Mck1 and Kin4 work in parallel to stop the Cdc14 early anaphase release (FEAR) dependent activation of MEN to promote SPOC in cells with misaligned spindles. The data also indicates that Mck1 prohibits cells with compromised MEN from exiting mitosis.

I illustrate that Mck1 executes its SPOC function by targeting Cdc6, a core component of the pre-replicative complex and a mitotic cyclin-dependent kinase (M-Cdk) inhibitor, for degradation before the cells enter mitosis. I also uncover that the cells overexpressing *CDC6* cannot hold the SPOC arrest and exit mitosis. Moreover, this effect of overproduced Cdc6 was not evident when its N-terminal domain, which inhibits the M-Cdk activity, was lacking. In line with this, overexpression of the N terminal of Cdc6 could prompt SPOC deficiency. Additionally, the elevated levels of Cdc6 in *mck1Δ* cells capture more Clb2 (M phase cyclin) molecules. Altogether this denotes that the association of Cdc6 with Clb2 via the N-terminus seems to be crucial in regulating SPOC and mitotic exit. As cells enter the mitotic phase of the cell cycle, M-Cdk complexes phosphorylate MEN components like Mob1. I observe that the cells lacking Mck1, fail to adequately phosphorylate Mob1, which is an indication

of lower M-Cdk activity. Overall, this suggests that *mck1Δ* cells enter mitosis with higher Cdc6 levels and therefore, lower M-Cdk activity leading to SPOC deficiency and mitotic exit.

This work has contributed to the understanding of Kin4 independent mechanisms that regulate SPOC and govern mitotic exit in the absence of FEAR. I also uncovered a novel function of GSK-3 kinase, Mck1. Given that GSK-3 kinases are highly conserved between organisms, the results obtained using budding yeast may open new directions of investigation into how spindle alignment and mitotic exit are regulated in higher eukaryotes.

Zusammenfassung

Die Position des mitotischen Spindelapparats wird in *Saccharomyces cerevisiae* vom Spindelpositions-Checkpoint (SPOC) überwacht. SPOC stellt sicher, dass Zellen die Mitose nicht verlassen, wenn ihr Spindelapparat in der Anaphase falsch ausgerichtet ist, und sichert damit eine zuverlässige Trennung der Chromosomen. Defekte in SPOC können zu Multiploidie führen und senken die Überlebensrate der Zellen.

Die SPOC-Kinase Kin4 aktiviert den Bfa1-Bub2 GTPase-aktivierendes Protein (GAP)-Komplex durch die Phosphorylierung von Bfa1, der wiederum das mitotic exit network (MEN), einen Signalweg, der zum Verlassen der Mitose beiträgt, inhibiert. Neue Arbeiten haben Mechanismen herausgestellt, die SPOC unabhängig von Kin4 verwenden. Ich habe die Rolle des Glykogen Synthase Kinase (GSK)-3-Homologs Mck1als neue Komponente von SPOC erforscht, die SPOC unabhängig vom Kin4-Signalweg aktiviert. Ich zeige, dass Mck1 und Kin4 parallel arbeiten, um die Aktivierung von MEN in Abhängigkeit von Cdc14 early anaphase release (FEAR) aufzuhalten und SPOC in Zellen mit falsch ausgerichteten Spindeln zu unterstützen. Die Daten weisen auch darauf hin, dass Mck1 Zellen mit defektem MEN davon abhält, die Mitose zu verlassen. Ich zeige auf, dass Mck1 seine Funktion in SPOC ausführt, indem es den Abbau von Cdc6, eine Hauptkomponente des prä-replikativen Komplexes und ein Inhibitor der mitotischen Cyclin-abhängigen Kinase (M-Cdk), fördert, ehe die Zelle mit der Mitose beginnt. Ich decke weiter auf, dass Zellen, die *CDC6* überexprimieren, SPOC nicht aufhalten können, und die Mitose verlassen. Zudem war dieser Effekt der Überproduktion von Cdc6 nicht sichtbar, wenn seine N-terminale Domäne, die die Aktivität von M-Cdk hemmt, fehlte. Dementsprechend konnte die Überexpression der N-terminalen Domäne von Cdc6 einen SPOC-Defekt hervorrufen. Des Weiteren binden die erhöhten Level von Cdc6 in *mck1Δ*-Zellen mehr Clb2 (M phase cyclin) Moleküle.

Zusammengenommen weist das darauf hin, dass die Assoziierung von Cdc6 mit Clb2 über seinen N-Terminus essentiell für die Regulation von SPOC und dem Verlassen der Mitose ist. Wenn Zellen in die mitotische Phase des Zellzyklus gelangen, phosphorylieren M-Cdk-Komplexe Komponenten von MEN, wie Mob1. Ich habe beobachtet, dass Zellen, die kein Mck1 besitzen, Mob1 nicht ausreichend phosphorylieren können, was ein Hinweis auf eine verringerte Aktivität von M-Cdk ist. Zusammengefasst legt dies nahe, dass *mck1Δ*-Zellen mit höheren Leveln von Cdc6 und darum geringerer Aktivität von M-Cdk in die Mitose gehen, was zu einem Defekt von SPOC und dem Verlassen der Mitose führt.

Diese Arbeit hat dazu beigetragen, die Kin4-unabhängigen Mechanismen zu verstehen, die SPOC regulieren und das Verlassen der Mitose in Abwesenheit von FEAR bestimmen. Ich habe auch eine neue Funktion der GSK-3-Kinase Mck1 aufgedeckt. Da GSK3-Kinasen zwischen den Organismen hoch konserviert sind, könnten die Ergebnisse, die mit knospender Hefe erhalten wurden, auch neue Richtungen in der Forschung dazu auftun, wie die Ausrichtung des Spindelapparats und das Verlassen der Mitose in höheren Eukaryoten reguliert werden.

List of abbreviations

APC: Anaphase Promoting Complex
CDK: Cyclin Dependent Kinase
CKI: Cyclin Dependent Kinase Inhibitors
cMT: cytoplasmic Microtubule
FEAR: Cdc-Fourteen Early Anaphase Release
GAP: GTPase Activating Protein
GEF: Guanine Exchange Factor
GSK-3: Glycogen Synthase Kinase 3
MEN: Mitotic Exit Network
MT: Microtubule
ORC: Origin Recognition Complex
pre-RC: pre-Replication Complex
SAC: Spindle Assembly Checkpoint
SCF: Skp-cullin F-box-containing complex
SPB: Spindle Pole Body
SPOC: Spindle Position Checkpoint

1. Introduction

Cell division is a fundamental process that contributes to life. From unicellular to multicellular eukaryotic organisms, this procedure is highly conserved. As a cell prepares to undergo division, it replicates all of its constituent elements and segregates them equally into two new cells. The newly formed daughter cells are then separated from each other by cytokinesis. The systematic and spatiotemporally coordinated sequence of events that contribute to cell division together make up the process of cell cycle. Aberrancy in cell division is the major cause of diseases like cancer and other related diseases. Hence, several studies have contributed to the molecular understanding of cell cycle and the events that ensure accurate segregation of genomic content between the new daughter cells. This PhD work also aims to add to the existing knowledge of cell cycle regulation using budding yeast as a model organism.

1.1 *Saccharomyces cerevisiae* as a model organism

Saccharomyces cerevisiae, also known as budding or baker's yeast has been used to answer cell cycle-related questions (David O. Morgan, 2007). Budding yeast consists of 16 chromosomes and its genome became the first ever completely sequenced eukaryotic genome (Mewes *et al.*, 1997). Yeast proteins that are homologous to their mammalian counterparts are shown to complement their functions (Lee and Nurse, 1987; Osborn and Miller, 2007). Therefore, results obtained in yeast studies can provide an understanding of similar processes in higher-multicellular organisms.

1.1.1 The life cycle of budding yeast

S. cerevisiae cells alter between haploid and diploid forms. Normally they proliferate by asexual budding when in a diploid state but upon starvation give rise to haploid tetrads, two of each mating type: Mat-a and Mat-α (Strathern *et al.*, 1981). These haploid cells bear specific receptors on their plasma membrane that recognise the pheromones (α or a-factor) released from the opposite mating type. Once they sense these pheromones, cells form mating projections called the 'shmoos' and fuse together at the mating sites and give rise to a diploid yeast (a/α) (Bücking-Throm *et al.*, 1973; Mackay and Manney, 1974; Strathern *et al.*, 1981; Rose *et al.*, 1986). This is the homothallic life cycle of budding yeast.

An important characteristic of budding yeast is that both the daughter cells at the end of every cell division vary in size and inherit different cellular contents. This is essentially asymmetric cell division. Although in higher organisms, asymmetric cell division confers to processes like stem cell renewal and cell differentiation, in budding yeast it is just a way to ensure genomic integrity. Cells are polarised prior to undergoing cytokinesis and therefore, have differences in the factors that maintain the polarity during and after the cell division.

1.1.2 Ease of genetic manipulation in budding yeast

The yeast haploid strains that are used in laboratories for experimental analysis have been manipulated to stay stable and cannot alter between mating types. The beauty of this is that unlike in diploids, the characterisation of gene functions is also made easier in the haploid cells. Additionally, gene disruption and integration, promoter replacement as well as epitope-tagging at any specific location in the genome using homologous recombination can be carried out with ease and specificity using established methods (Rothstein, 1991; Knop *et al.*, 1999; Janke *et al.*, 2004; van Driessche *et al.*, 2005). Altogether, this makes budding yeast an excellent model system to study cell cycle.

1.2 Overview of yeast cell cycle

1.2.1 Cell cycle progression

Events in cell cycle are clubbed into four major phases: the Gap phases (G1 and G2), the Synthesis phase (S) and the Mitotic phase (M) as shown in Figure. 1-1. The first gap phase (G1) is where the cell grows in size and prepares itself for a forthcoming cell cycle. Once the cells commit to entering the cell cycle, there is a point of no return called START in yeast and a restriction point in human cells. The presence of mating factors or stress conditions resists the cells from entering the START point (Cross, 1995). When cells move past the START, they initiate polarisation and commence budding along with doubling of the spindle pole body (SPB), the yeast centrosomes, that organise the microtubules (MTs) (Forsburg and Nurse, 1991).

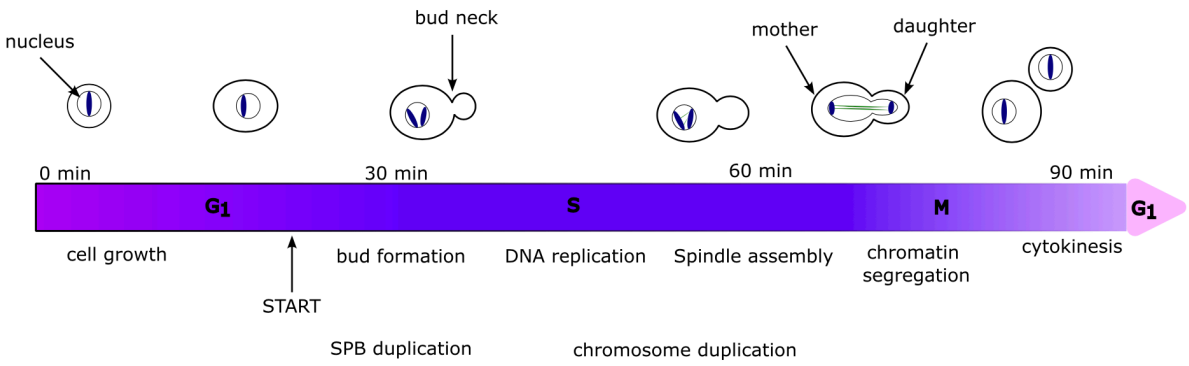

Figure. 1-1. Cell cycle progression in budding yeast. Blue ovals are SPBs that adhere to MTs which are represented in green. Adapted from Alberts *et al.*, 2008. Cells grow during both the gap phases, whereas DNA replication occurs in S phase. The duplicated DNA is segregated equally between the two compartments in M phase after which cells exit mitosis and undergo cytokinesis. Time is indicative of the process at 30°C.

In the S phase, cells duplicate their chromosomes (Hartwell *et al.*, 1974; Huberman, 1996), however, faithful segregation of genomic content into the two compartments occurs later (David O. Morgan, 2007). Mitotic spindle formation is initiated in the G2

phase that coordinates these two events and separates them temporally (Forsburg and Nurse, 1991). Eventually, during the M phase, the chromosomes attach to the cytoplasmic MTs (cMTs) which in turn facilitates equal chromosomal separation (Sharp *et al.*, 2000). This is a classic case of closed mitosis. After this, the cells undergo constriction of the actomyosin-ring at the site of cell division and cause abscission to give rise to two daughter cells (Balasubramanian et al., 2004; Barr and Gruneberg, 2007; Weiss, 2012).

1.2.2 Cyclin-Cdk complexes

The timely occurrence of every step, in the cell cycle, is crucial for a successful cell division. This is regulated by interaction of cyclin-dependent kinases (Cdk) (Cdc28 in yeast) with cyclins (Johnson and Walker, 1999; Jorgensen *et al.*, 2004) as the cell cycle progresses. Although the protein levels of Cdk remain constant, the activity of Cdk oscillates depending on the abundance of phase-specific cyclins that confer its selectivity (Evans *et al.*, 1983; Koch *et al.*, 1996; Morgan, 1997). Unlike in mammalians, Cdc28 is the only Cdk that binds to the nine budding yeast cyclins (Nasmyth, 1993; Bloom and Cross, 2007a) (Figure. 1-2).

In association with Cdk, Cln1-3 initiate the cell cycle progression through G1 phase (Levine *et al.*, 1995) whereas, Clb5 and Clb6 promote entry into S-phase by phosphorylating origin replication complex (ORC) proteins like Orc6 and Orc2 (Epstein and Cross, 1992; Wilmes *et al.*, 2004). Mitotic cyclins, Clb1-4, regulate mitotic advancement, spindle assembly and elongation (Maekawa and Schiebel, 2004; Roostalu *et al.*, 2010). Mitotic cyclins along with Cdk form M-Cdk complex that leads to anaphase onset by activating the E3 ubiquitin ligase-anaphase promoting complex (APC). APC^{Cdc20} targets securin (Pds1) for degradation and causes sister chromatids to separate (Farr and Cohen-Fix, 1999). At the end of M phase, mitotic cyclins are degraded by APC^{Cdc20} and APC^{Cdh1}. Additional inhibition of M cyclins by

the CDK inhibitors (CKIs) like Sic1 and Swe1 is crucial to ensure that the cells exit from the first cycle and are ready to enter the next G1 (Elledge and Harper, 1994; Jaspersen *et al.*, 1998; Wäsch and Cross, 2002).

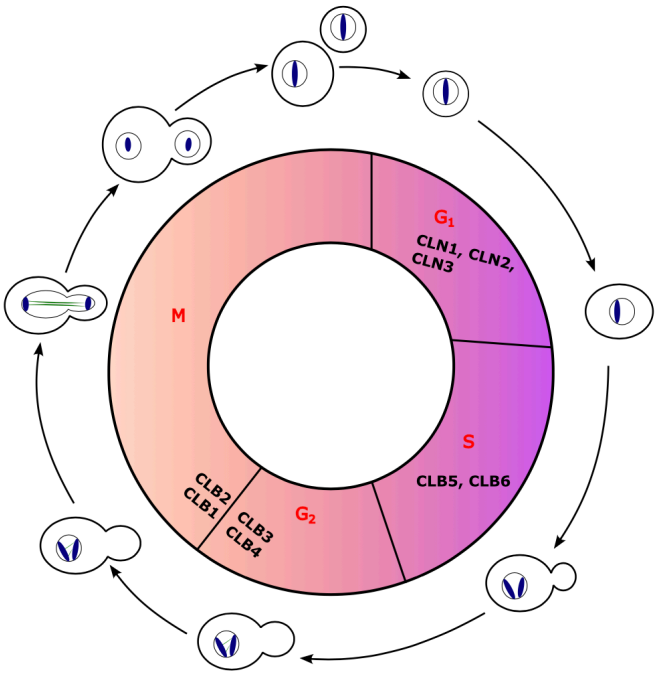

Figure. 1-2. Cyclins with respect to different phases of the cell cycle. Cdk activity is modulated depending on its interaction with different cyclins depending on the stage of the cell cycle. The diagram represents G1 cyclins (Cln1, Cln2 and Cln3) as well as B-type cyclins in S (Clb5, Clb6), G2 (Clb3, Clb4) and M (Clb1, Clb2) phase. Adapted from Morgan, 1997.

1.3 Cell cycle checkpoints

Safeguarding accurate commencement and completion of cell cycle events is a must to prevent defective cells from undergoing cell division. Such surveillance mechanisms are called checkpoints and exist at decisive junctures in the cell cycle.

The G1/S checkpoint safeguards commitment to cell division based on the surrounding conditions like nutrient availability for growth and appropriate cell size. If conditions are not met, cells are stuck in G1 until the adjacent environment is favourable (Forsburg and Nurse, 1991). Cells that have DNA damage induced by UV radiation or any other external factors must be prevented from dividing. Such cells arrest in S phase to repair the DNA damage by activating the DNA damage

checkpoint (Nyberg *et al.*, 2002; Bartek *et al.*, 2004). Problems in the actin-cytoskeleton at the transition of G2-M phase promote the morphogenetic checkpoint which defers nuclear partition (Lew and Reed, 1995). Checkpoints of M phase ensure equal partition of the nuclear content. The spindle assembly checkpoint (SAC) monitors attachment of all chromosomes through their kinetochores to cMTs in a bipolar fashion (Musacchio and Salmon, 2007). Additionally, orientation of mitotic spindle along the mother-daughter polarity axis is surveyed by the spindle position checkpoint (SPOC) (Fraschini *et al.*, 2008). SPOC is explained further in detail in another section.

1.4 Spindle positioning

In *S. cerevisiae*, spindle alignment is assessed by Kar9 or Dynein (Dyn1) dependent pathways (Figure. 1-3). These two pathways are redundant and hence, deletion of both *KAR9* and *DYN1* is lethal whereas, deletion of either one of the two genes leads to a significantly higher percentage of cells with spindle misorientation (Cottingham and Hoyt, 1997; Miller and Rose, 1998). Kar9 is the adenomatous polyposis coli-related spindle-positioning factor required for cytoplasmic microtubule orientation and nuclear migration (Miller *et al.*, 1998). The primary indication of SPOC was seen in mutants with faulty dynein-dependent spindle positioning mechanisms (Yeh *et al.*, 1995). In the absence of Kar9 or Dyn1, cells trust the SPOC pathway to monitor mitotic spindle position (Daum *et al.*, 2000; Pereira *et al.*, 2000).

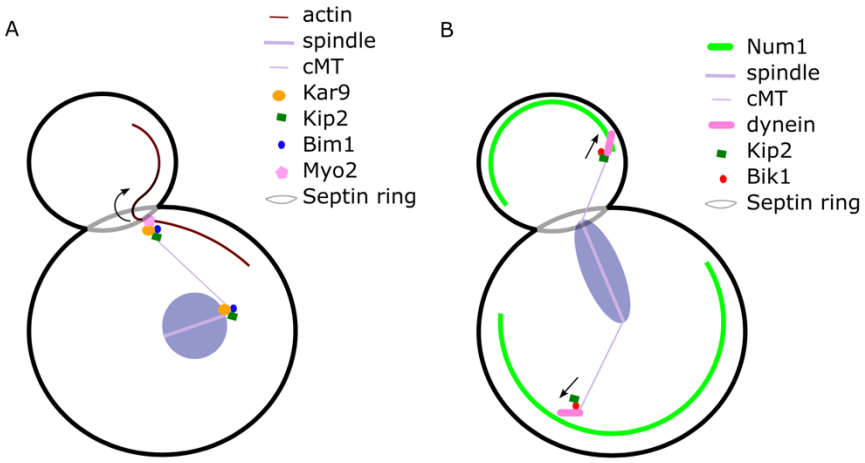

Figure. 1-3. Spindle positioning in *S. cerevisiae*. A) the Kar9 pathway and B) Dynein dependent pathway. Check the text for details. Adapted from Fraschini *et al*., 2008.

Kar9 directs the cMTs protruding from the old SPB to the actin cables, prior to anaphase (Moore and Cooper, 2010) (Figure 1-3A). Bim1 carries Kar9 to the plus ends of cMTs via Kip2-mediated motor transport protein (Lee *et al.*, 2000). Myosin motor protein which is associated with actin cables pulls Kar9 towards the bud neck and eventually the old SPB is carried to the daughter compartment (Pereira *et al.*, 2001; Jaspersen and Winey, 2004; Maekawa and Schiebel, 2004).

Moreover, in anaphase, dynein mediates the connection of the cMTs at the cortex (Siller and Doe, 2009; Moore and Cooper, 2010) (Figure. 1-3B) and Bik1 recruits dynein to carry it towards the plus end with the aid of Kip2 (Lee *et al.*, 2003; Miller *et al.*, 2006). This is where Num1 promotes dynein-facilitated movement of the cMTs along the cortex leading to nuclear and spindle alignment along the polarity axis (Adames and Cooper, 2000; Heil-Chapdelaine *et al.*, 2000). Together this coordinates spindle positioning in budding yeast.

1.5 Spindle position checkpoint (SPOC)

1.5.1 Overview of SPOC

SPOC prevents cells from exiting mitosis if their anaphase spindle is misaligned. This inhibition is released once the spindle realigns along the mother-daughter axis to

facilitate faithful segregation of chromosomes between the mother and the daughter cell (Lew and Burke, 2003; Fraschini *et al.*, 2008). Similar checkpoints are reported to exist in other eukaryotes (Lechler and Fuchs, 2005; Gachet *et al.*, 2006; Yamashita and Fuller, 2008). SPOC postpones mitotic exit by inhibiting the mitotic exit network (MEN) upon spindle misalignment (Piatti *et al.*, 2006) (Figure. 1-4). A cluster of proteins and kinases modify the localisation and phosphorylation of downstream targets that directly regulate MEN and together execute the function of SPOC.

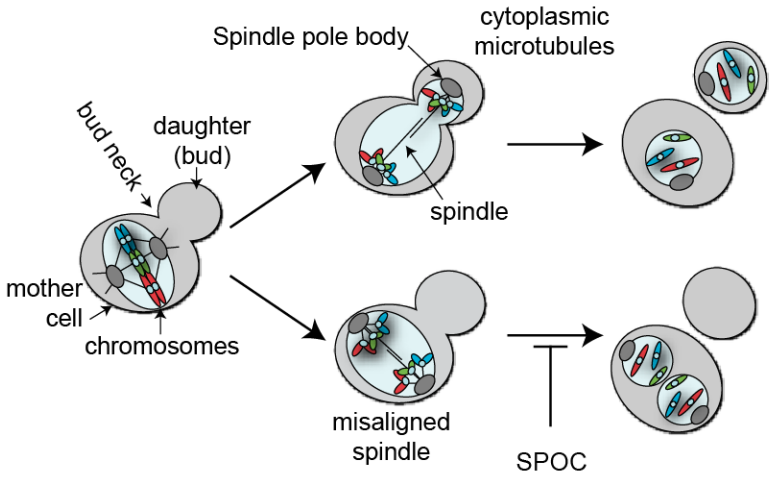

Figure. 1-4. Spindle position checkpoint (SPOC). Cells that align their mitotic spindle along the polarity axis give rise to two cells with equally distributed chromosomes (upper lane). On the contrary, when the anaphase is misaligned, cells activate SPOC to inhibit mitotic exit, which would cause aneuploidy (lower panel). Adapted from Caydasi and Pereira, 2012.

1.5.2 Molecular players that regulate SPOC in a Kin4-dependent manner

Kin4, Bfa1-Bub2 GTPase activating protein (GAP) complex and the polo-like kinase Cdc5 are the core components that localise at the spindle pole bodies (SPBs) and regulate SPOC via the Kin4 pathway.

Kin4 is the central SPOC kinase that is a Par-1 protein homolog, vital for cell polarisation in *D. melanogaster* (Yuan *et al.*, 2012). Kin4 resides in the mother compartment throughout the cell cycle. It shortly also associates with the mSPB and the bud neck during late anaphase (D'Aquino *et al.*, 2005; Pereira and Schiebel,

2005) (Figure. 1-5). In cells with misaligned spindles, Kin4 binds equivalently to both the SPBs (Pereira and Schiebel, 2005) (Figure. 1-5). It is restricted from moving into the bud by Lte1, a guanine exchange factor (GEF) protein and inhibits Kin4 activity in the daughter compartment (Bardin *et al.*, 2000; Pereira *et al.*, 2000) (Figure. 1-5). Lte1 localises to the daughter cell cytoplasm and cortex throughout the cycle and only temporally dissociates to the bud neck after spindle disassociation. When Lte1 location is switched to the mother compartment, SPOC fails to operate (Castillon *et al.*, 2003). Hence, Lte1 regulation over Kin4 is essential to maintain active SPOC.

At SPBs, the SPOC function of Kin4 is to activate the Bfa1-Bub2 GAP complex, which is also a component of the checkpoint (Bloecher *et al.*, 2000; Pereira *et al.*, 2000). Overexpression of both *BFA1* and *KIN4* is lethal to the cells as they arrest in late anaphase (Li, 1999; D'Aquino *et al.*, 2005; Pereira and Schiebel, 2005). Additionally, Kin4 activity is regulated by recently identified SPOC proteins like Elm1 and Rts1 (Caydasi *et al.*, 2010). Action of Kin4 on the GAP complex inhibits the mitotic exit network (MEN) by inducing GTP hydrolysis of its most upstream player, Tem1 (Lee *et al.*, 2001a, 2001b; Geymonat *et al.*, 2002). This inhibition by Bfa1-Bub2 complex largely depends on the phosphorylation status of Bfa1, as the transcription rate and protein abundance of Bfa1 is stable through most of the cell cycle (Spellman *et al.*, 1998; Hu *et al.*, 2001; Lee *et al.*, 2001b). Cdc5-polo-like kinase, hyper-phosphorylates Bfa1 once the spindle starts to elongate and this weakens the affinity of Bfa1-Bub2 complex to Tem1 establishing asymmetry (Hu *et al.*, 2001; Geymonat *et al.*, 2003; Monje-Casas and Amon, 2009), allowing the cells to execute mitotic exit in this scenario (Figure. 1-5; left panel).

On the contrary, in cells with mispositioned anaphase spindles, Kin4 counteracts the inhibitory phosphorylation of Bfa1 by Cdc5 at both the SPBs (D'Aquino *et al.*, 2005; Pereira and Schiebel, 2005). Kin4 phosphorylates Bfa1 which prompts its interaction

with Bmh1, 14-3-3 family protein, leading to dissociation from the SPBs (Caydasi *et al.*, 2014a). This lowers the Bfa1-Bub2 levels at the SPBs and prevents Tem1 activation (Figure. 1-5; right panel). Altogether, cells block mitotic exit in response to misorientation of their mitotic spindles (Figure. 1-5; right panel).

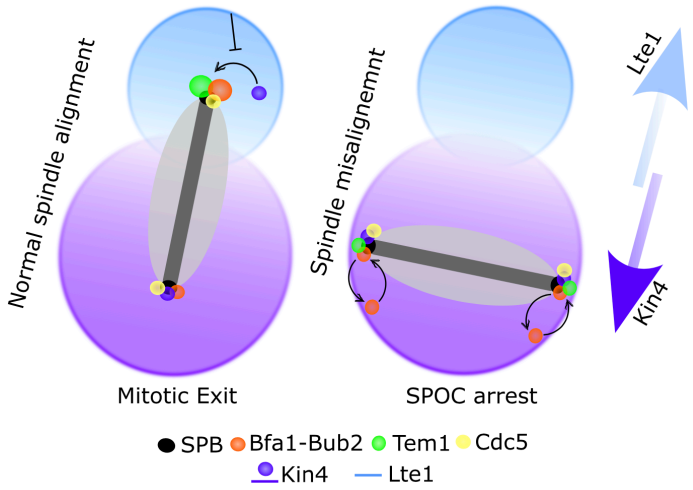

Figure. 1-5. Localisation of key SPOC components. The figure illustrates the localisation of different proteins as indicated upon normal or misalignment of the mitotic spindle. Kin4, Bfa1-Bub2 and Tem1 are asymmetrically localised at the SPBs as the spindle orients correctly along the polarity axis. Adapted from Caydasi and Pereira, 2012.

1.5.3 Kin4 independent regulation of SPOC

Molecular players involved in the Kin4 pathway, sense the position of mitotic spindle and activate SPOC upon spindle misalignment (D'Aquino *et al.*, 2005; Pereira and Schiebel, 2005; Caydasi *et al.*, 2010, 2014b). Cells lacking these components execute mitotic exit without stalling cells in anaphase. Previous reports suggest that mechanisms parallel to Kin4 may hold SPOC in position when cells lack the Cdc-fourteen early anaphase release (FEAR) network (Falk *et al.*, 2016; Caydasi *et al.*, 2017). Independently of Kin4, Glc7 (type 1 protein phosphatase) in conjugation with its regulatory subunit Bud14 has been recently proven to dephosphorylate the Cdc5 mediated repressive phosphorylation of Bfa1 thereby, contributing to SPOC activity (Kocakaplan *et al.*, 2021). On the other hand, studies have reported the role of

chromatin remodelers like Swr1 that sustain the SPOC arrest irrespective of Kin4, by delaying mitotic exit which leads to mitotic slippage (Caydasi *et al.*, 2020).

The work from my PhD contributes to the understanding of another molecular player involved in SPOC modulation autonomously of Kin4.

1.6 Regulation of mitotic exit

At the end of every cell cycle, accurate mitotic exit followed by cytokinesis is a must for a mother cell to give rise to two daughter cells. This is achieved by turning around the cyclin-Cdk mediated changes and dephosphorylating the Cdk substrates that set the stage for mitotic progression. A universally conserved phosphatase, Cdc14 in *S. cerevisiae* is capable of mitigating these changes as well as phosphorylating thereby, preventing the CKIs like Sic1 from degradation (Visintin *et al.*, 1998; Jaspersen *et al.*, 1999; Stegmeier and Amon, 2004a). Therefore, Cdc14 activity is a prerequisite for mitotic exit to occur. Cdc14 is released from its inhibitors by two pathways, namely: Cdc-fourteen early anaphase release (FEAR) network and mitotic exit network (MEN).

1.6.1 FEAR network

Cdc14 is retained in the nucleolus where it is kept torpid by Net1, its inhibitor until cells transition to anaphase (Yoshida *et al.*, 2002; Azzam *et al.*, 2004). Cells transition into anaphase, once Pds1 is set for destruction by the action of APC, (Uhlmann *et al.*, 1999). Protein phosphatase 2-A in conjugation with its subunit Cdc55 ($PP2A^{Cdc55}$) prevents phosphorylation of Net1, a Cdc14 inhibitor which sequesters it in the nucleolus (Azzam *et al.*, 2004; Queralt *et al.*, 2006). Primarily, during the metaphase to anaphase transition, after integrity of SAC is ensured, cells release Cdc14 into the nucleus by FEAR pathway (Pereira *et al.*, 2002; Stegmeier *et al.*, 2002; Rock and Amon, 2009) (Figure. 1-6). Association of FEAR components like

Spo12 with Esp1 and Slk19 result in the partial release of Cdc14 (Queralt *et al.*, 2006; Tomson *et al.*, 2009). This transient Cdc14 release promotes rDNA segregation, spindle elongation and nuclear positioning but is not required for cells to accomplish mitotic exit (D'Amours *et al.*, 2004; Pereira and Schiebel, 2004; Khmelinskii *et al.*, 2007, 2009; Sullivan and Morgan, 2007; Rock and Amon, 2009).

1.6.2 MEN pathway

For mitotic exit and cytokinesis to occur, cells require full release of Cdc14 into the cytoplasm which is facilitated by the mitotic exit network (MEN) (Jaspersen *et al.*, 1998; Shou *et al.*, 1999; Surana *et al.*, 2002; Meitinger *et al.*, 2010, 2012) (Figure. 1-6). A major outcome of the MEN signalling cascade is to cause full release of Cdc14, thereby, promoting the exit of cells from mitosis (Simanis, 2003). MEN is a conserved signalling pathway that functions at the SPB with Ras-like GTPase, Tem1 at its forefront (Stegmeier and Amon, 2004b). Active Tem1, $Tem1^{GTP}$, binds to Cdc15 and further recruits Dbf2 kinase in conjugation with Mob1 to form an active Dbf2-Mob1 complex (Asakawa *et al.*, 2001; Mah *et al.*, 2001). This NDR/LATS kinase complex phosphorylates Cdc14 and dissociates it from Net1 leading to release of Cdc14 into the cytosol (Mohl *et al.*, 2009). Fully released Cdc14 dephosphorylates its targets and contributes to mitotic exit.

Once the cells have concluded mitotic exit, a bud-specific protein called Amn1 interferes and blocks the interaction of Tem1 and Cdc15 in turn inactivating the MEN (Wang *et al.*, 2003). This pathway is known as the antagonist of mitotic exit network (AMEN), which brings back Cdc14 in the nucleus and resets the platform for a new cell cycle to begin.

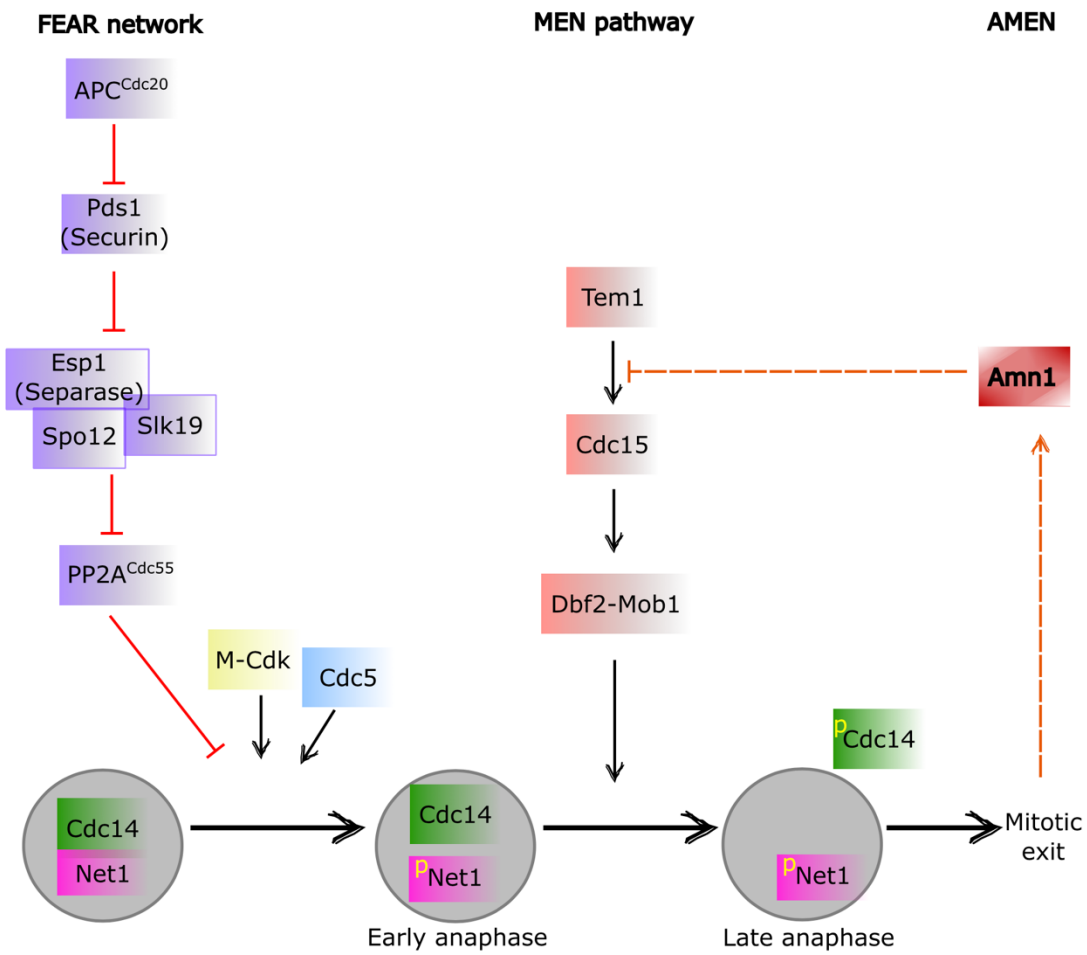

Figure. 1-6. FEAR and MEN pathway. The diagram depicts constituent elements of the FEAR and MEN pathway that contribute to disassociation of Cdc14 from Net1 which results in two succinct waves of Cdc14 release. 'p' represents the phosphorylated forms of the proteins. Adapted from Caydasi and Pereira, 2012.

1.7 Yeast GSK-3 kinases

1.7.1 GSK-3 homologs in budding yeast

Budding yeast has four GSK-3 kinase homologs namely: Mck1, Rim11/Mds1, Ygk3 and Mrk1. All of them share sequence similarities in the kinase domain with mammalian GSK-3 α and β counterparts. The four homologs perform several functions redundantly, for instance, upon starvation, Mds1 and Mck1 regulate meiotic gene expression of *IME1* by phosphorylating the transcription factor Ume6 and stimulating sporulation (Puziss et al., 1994; Bowdish et al., 1994; Malathi et al., 1997; Xiao and Mitchell, 2000). They also take over each other's functions like phosphorylation of Rog1 like kinases, etc. (Andoh et al, 2000).

1.7.2 Mck1 and its known functions

Several functions like chromosome segregation, protein degradation and stress response are conducted solely by Mck1. Mck1 is a serine-threonine protein kinase, that auto-phosphorylates itself on tyrosine residue (Y199) (Dailey et al., 1990; Lim et al., 1993; Rayner et al., 2002). However, this work focuses on exploring the role of Mck1 in cell cycle regulation.

Meiosis and centromere regulatory kinase, Mck1 was recognised as a key player in mitotic chromosomal separation as it showed sensitivity to benomyl treatment and low temperatures (Shero and Hieter, 1991; Puziss *et al.*, 1994; Jiang *et al.*, 1995). However, deletion of *MCK1* did not show any effect on SAC functionality (Gardner *et al.*, 2001). Previous studies showed that Mck1 phosphorylates the inhibitor of Calcineurin, Rcn1, and targets it for SCF^{Cdc4} mediated degradation (Hilioti *et al.*, 2004; Kishi *et al.*, 2007). Moreover, it has been anticipated to regulate Swe1 and Mih1 (Pal *et al.*, 2008). Mck1 is also implicated in blocking multiple replications of DNA and monitoring the DNA damage checkpoint function (Archambault *et al.*, 2005; Delgado and Toczyski, 2019; Li *et al.*, 2019). Another report determined that Mck1 modulates calcineurin signalling and along with transcription factors, Msn2 and Msn4 (multicopy suppressor of *SNF1*) promote the osmotic stress induced gene expression (Estruch and Carlson, 1993; Hilioti *et al.*, 2004; Gutin *et al.*, 2019). Mck1 is also involved in the plasma membrane signalling pathway as mutants are sensitive to SDS treatment (Kono *et al.*, 2016).

Along with these functions, Mck1 functions in similar mechanisms to the human GSK-3. For instance, Mck1 also phosphorylates its targets (Rcn1, Hsl1, Rog1 and Cdc6) at the fourth position in the S/T-x-x-x-S/P consensus GSK-3 site (Fiol *et al.*, 1987; Andoh *et al.*, 2000; Mizunuma *et al.*, 2001; Hilioti *et al.*, 2004; Ikui *et al.*, 2012). Mck1 blocks the pyruvate kinase A (PKA) pathway whereas, in mammals, PKA has

been shown to inhibit GSK-3 kinase (Fang *et al.*, 2000; Rayner *et al.*, 2002). The uncanny similarities between the two GSK-3s make it important to study Mck1 and its involvement in cell cycle regulation in budding yeast.

1.8 Cdc6

DNA replication in eukaryotic cells occurs due to a series of highly coordinated steps that ensure correct duplication of the genome. This process is initiated by appropriate assembly and anchorage of the pre-replicative complex (RC) (Bell and Dutta, 2003). One of the core components of the pre-RC is Cdc6 and it is essential for DNA replication (Bell and Dutta, 2003). It belongs to a conserved group of nucleotide-dependent loading factor proteins that make use of ATP hydrolysis to dissociate from DNA (Perkins and Diffley, 1998; Weinreich *et al.*, 1999; Speck *et al.*, 2005; Chang *et al.*, 2015).

1.8.1 Cdc6 and its regulation

To prevent aberrant and multiple rounds of DNA replication, the transcription timing and stability of Cdc6 are tightly regulated across different phases of the cell cycle (Dalton and Whitbread, 1995; McInerny *et al.*, 1997). Cdc6 is only transcribed later in mitosis owing to the presence of an early cell cycle box in its promoter (McInerny *et al.*, 1997). In the rest of the cell cycle phases, Cdc6 is degraded by multiple methods. Early in G1, Cdc6 is degraded by E3 ligase Tom1 and SCF^{Dia2} (Kim *et al.*, 2012), whereas, during S-phase and mitosis Cdc6 is phosphorylated by Cdk which primes it for SCF^{Cdc4} mediated destruction (Drury *et al.*, 2000).

In S phase, Clb5-Cdk (S-Cdk) recognises the ^{30}RxL^{32} motif in the N-terminus of Cdc6 and phosphorylates it at T7 and subsequently creating phospho-degrons at the CDK sites (S/T-P) in the N and C-terminal (Drury *et al.*, 2000; Perkins *et al.*, 2001; Örd *et al.*, 2019). Later, Clb2 binds Cdc6 at the ^{47}LxF^{49} motif in the N-terminal domain and

along with Cdk (M-Cdk) phosphorylates Cdc6 at S372 (Elsasser *et al.*, 1996; Mimura *et al.*, 2004; Örd *et al.*, 2019). This serves as a priming site for Mck1 to phosphorylate the C-terminal GSK-3 consensus site at T368 and mark it for SCF^{Cdc4} mediated proteasomal degradation (Ikui *et al.*, 2012; Al-Zain *et al.*, 2015). Moreover, in late anaphase, M-Cdk complex associates with Cdc6 via the N-terminal region and keeps it stable by guarding the T39-S43 phopho-degron (Örd *et al.*, 2019).

The significance of maintaining low Cdc6 levels prior to mitotic entry has not been clearly understood yet. The results from this study provide insight into this query.

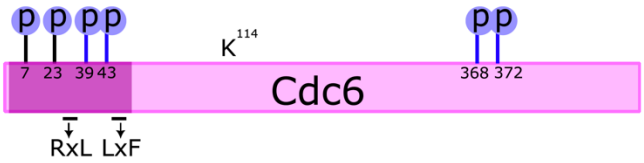

Figure. 1-7. Cdc6 domain architecture. Cdc6 is a member of the AAA+ family of proteins (ATPase associated with diverse cellular activities) (Neuwald *et al.*, 1999). It has six Cdk phosphorylation sites as shown in the figure. The phosphorylated residues at 39-43 form the N-terminal phospho-degron whereas, at 368-372 form the C-terminal phospho-degron (represented in blue bars). Cyclins, Clb5 (S phase) and Clb2 (M phase) in association with Cdk bind to Cdc6 at ^{30}RxL^{32} and ^{47}LxF^{49} motifs, respectively. The lysine (K) residue at 114th amino acid position is essential for Cdc6's replicative function (Weinreich *et al.*, 1999).

1.8.2 Role of Cdc6 in mitotic exit

Of the other possible ways like APC^{Cdh1} arbitrated Clb2 destruction and downregulation of M-Cdk activity by Sic1, the inhibitory effect of Cdc6 on M-Cdk activity appears to be vital for mitotic exit. A truncated version of Cdc6 that lacks the N-terminal domain has been proved to abrogate its interaction with Clb2 and therefore, fails to obstruct the M-Cdk activity (Elsasser *et al.*, 1996; Calzada *et al.*, 2001). This mutant Cdc6 is also further stabilised. Reports also suggest that Cdc6, Sic1 and APC^{Cdh1} synergistically stop M-Cdk activity and prepare cells for admission into the next G1 (Calzada *et al.*, 2001; Archambault *et al.*, 2003). $PP2A^{Cdc55}$ has been

recently implicated in Cdc6 dephosphorylation which prompts Cdc6 degradation later in mitosis (Philip *et al.*, 2022).

However, the function of Cdc6 and the consequences of its stability throughout the cell cycle conferred by deletion of *MCK1*, in governing correct spindle orientation and mitotic exit is not yet explored. The aim of this work was to address this question.

2. Aims and objectives of the study

The asymmetric distribution of cell fate determinants largely depends on the orientation of the mitotic spindle with respect to the intrinsic and extrinsic polarity cues. In budding yeast, the position of the mitotic spindle is surveyed by the spindle position checkpoint (SPOC) (Caydasi *et al.*, 2010). When the anaphase spindle is misaligned, localisation of the Bfa1-Bub2 complex is perturbed due to the phosphorylation by Kin4 kinase (Molk *et al.*, 2004; Caydasi and Pereira, 2009; Valerio-Santiago and Monje-Casas, 2011). This invokes SPOC in wild type cells ensuring faithful chromosome segregation, while mutants where if the SPOC is not functional exit mitosis and lead to accumulation of multipolar and multinucleated cells.

Work from the Pereira group and other laboratories has advanced the understanding of SPOC function and the underlying molecular players that regulate SPOC activity. To investigate the underlying mechanisms of Kin4 activity, a genome wide screen was performed in the lab that contributed in cataloguing several potential SPOC regulators (Caydasi *et al.*, 2010). *MCK1*, a budding yeast GSK-3 kinase, was one of the genes found in the screen. The role of Mck1 in meiosis, DNA damage and cell wall integrity checkpoints has been well characterised. Although, its importance in spindle orientation checkpoint was elusive.

Therefore, in this PhD project, I set out to decipher whether Mck1 is a bona fide SPOC component and subsequently, how Mck1 works in SPOC at a molecular level. As Mck1 is a protein kinase, I hypothesised that phosphorylation of key components by Mck1 contributes to this regulation. Mck1 is known to target Cdc6, a pre-RC protein for degradation and Cdc6 has been implicated in driving cells out of mitosis (Calzada *et al.*, 2001; Archambault *et al.*, 2003; Ikui *et al.*, 2012). Therefore, I asked if

the regulation of Mck1 over Cdc6 governs mitotic exit and/or SPOC. Moreover, I also planned to identify Mck1 interaction partners which may contribute to its function in sensing spindle misorientation and blocking mitotic exit. After the identification of putative Mck1 substrates, validating some of these substrates was my aim. Another important question I asked was whether the Mck1 regulation in SPOC was via the Kin4 dependent or independent pathway.

3. Results

3.1 Mck1 is a novel SPOC component

3.1.1 Deletion of *MCK1* rescues the lethality of *KIN4* overexpression

Bfa1, Bub2 and Kin4 are very well characterised core SPOC components, which inhibit MEN in cells with misaligned spindles (Hu *et al.*, 2001; D'Aquino *et al.*, 2005; Pereira and Schiebel, 2005). In cells with normally aligned spindles, the Bfa1-Bub2 GAP complex is inhibited by Cdc5-dependent phosphorylation, which activates the MEN at the dSPB (Hu *et al.*, 2001) (Figure. 3-1A). Upon spindle misalignment, Kin4 counteracts the Cdc5 mediated phosphorylation of Bfa1, thereby activating the GAP complex to inactivate MEN on both the SPBs (Hu *et al.*, 2001) (Figure. 3-1A). This ensures that the cells with mis-orientated spindles do not undergo mitotic exit. On the other hand, overexpression of *KIN4* keeps the Bfa1-Bub2 GAP complex constitutively active at both the SPBs leading to persistent inactivation of MEN pathway. Eventually, this arrests the cells in late anaphase and causes a cell cycle block (D'Aquino *et al.*, 2005; Pereira and Schiebel, 2005) (Figure. 3-1B).

To discover novel players involved in Kin4 regulation, a genome wide screen was performed in the lab to uncover the genes whose deletion rescued the lethality of *KIN4* overexpression (Caydasi *et al.*, 2010). Mck1 was one of the identified genes. It is a dual specificity serine/threonine and tyrosine kinase homologous to the mammalian glycogen synthase kinase-3 (GSK-3). Budding yeast Mck1 is known to perform many diverse biological functions like promoting meiotic gene expression and regulating the DNA damage and cell wall integrity checkpoint (Neigeborn and Mitchell, 1991; Delgado and Toczyski, 2019). But its role in SPOC and mitotic exit has not been characterized yet.

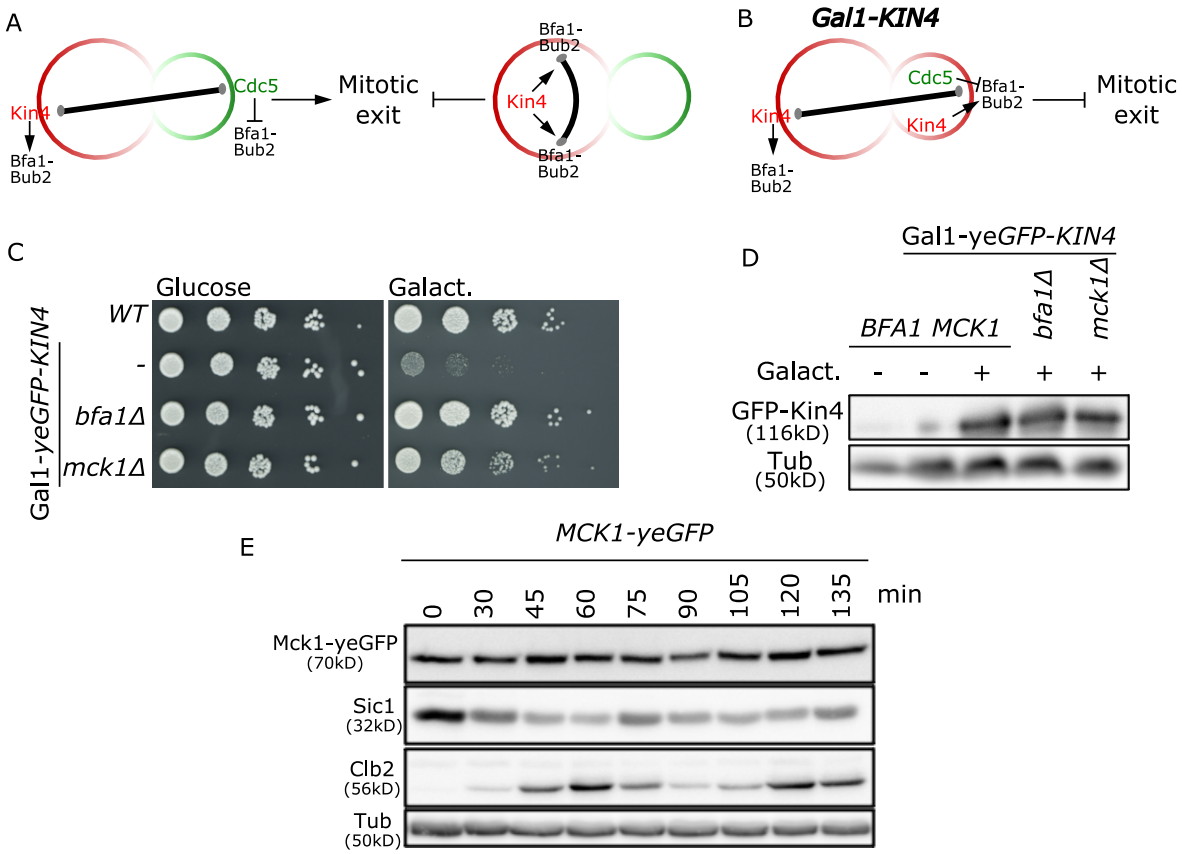

Figure. 3-1. *MCK1* deletion can rescue the lethality of *KIN4* overexpression. A) Schematic representation of cells co-ordinating mitotic exit upon correct spindle alignment or misalignment via regulating Bfa1-Bub2 activity at the SPBs. B) Schematic representation of lethality caused by *KIN4* overexpression at a molecular level. C) Serial dilutions of indicated strains on Galactose containing, Gal1-*KIN4* inducing (Galact.) or repressing (Glucose) plates. D) Immunoblots of strains used in C depicting Kin4 levels upon Galactose induction for 4 hours. Tubulin (Tub) served as a loading control. E) Cells were arrested in G_1 phase by alpha-factor synchronisation and released in fresh medium. Samples were collected at indicated time points to be analysed by western blotting. The immunoblots represent Mck1-yeGFP levels at indicated time points. Clb2 and Sic1 serve as markers for cell cycle progression and Tub is a loading control. (Experiment in E was conducted with the help of Irem Polat).

To validate that lack of Mck1 rescues Kin4 overproduction lethality, I analysed the growth of *mck1Δ* Gal1-*KIN4* cells on galactose inducing conditions. I observe that *mck1Δ* cells survive this toxicity similar to cells bearing *BFA1* deletion (Figure. 3-1C). The levels of Kin4 upon galactose induction were comparable in cells harbouring wild type *MCK1* or its deletion (Figure. 3-1D). I also confirmed that Mck1 protein levels remain constant throughout the cell cycle (Figure. 3-1E). This suggests that Mck1 is

essential to inhibit mitotic exit in cells with abundant Kin4, but it does not do so by perturbing Kin4's expression levels.

3.1.2 *mck1Δ* cells are SPOC deficient

I further examined if Mck1 is a bona fide component in SPOC. In S. cerevisiae, spindle alignment is regulated by Kar9 or Dynein dependent pathways. These two pathways are redundant and hence, deletion of both *KAR9* and *DYN1* is lethal whereas, deletion of either one of the two genes leads to increase in spindle misorientation (Cottingham and Hoyt, 1997; Miller and Rose, 1998). Kar9 is the adenomatous polyposis coli-related spindle-positioning factor required for cytoplasmic microtubule orientation and nuclear migration (Miller *et al.*, 1998). To induce spindle misalignment, like in other studies, I used cells that lacked Kar9 (*kar9Δ*) (Daum *et al.*, 2000; Pereira *et al.*, 2000). *kar9Δ* cells with misaligned spindles activate SPOC and arrest the cells until the mitotic spindle is re-orientated parallel to the polarity axis. In cases when the SPOC is not functional, cells do not sense the spindle misorientation and exit mitosis to undergo cytokinesis despite inappropriate chromosome segregation. Therefore, the SPOC-deficient cells in *kar9Δ* background accumulated multinucleated, enucleated as well as multi-budded cells (Figure. 3-2A-a).

To assess the SPOC integrity, I tagged tubulin ((yeast-enhanced) *yeGFP-TUB1*) as a marker for the anaphase spindle. I enumerated the SPOC deficient cells along with normal and misaligned anaphase spindles in *kar9Δ*, *kar9Δ kin4Δ* and *kar9Δ mck1Δ* cells to calculate the percentage of SPOC deficient cells for each strain (Figure.3-2A-b). I observe ~ 35 % of cells are deficient for SPOC in *kar9Δ mck1Δ* in contrast to the SPOC proficient *kar9Δ and mck1Δ* cultures. And nearly 40% of cells in *kar9Δ kin4Δ* showed SPOC deficiency, which served as a positive control in the experiment

(Figure. 3-2B). Thus, Mck1 is required to regulate SPOC in *kar9Δ* cells with misaligned spindles.

Mck1 was predicted to be involved in spindle positioning by regulating astral microtubule dynamics (Drechsler *et al.*, 2015). To validate this in our strain background and growth conditions, I determined the percentage of metaphase and anaphase cells with mis-orientated spindles. I did not observe any spindle positioning defects in cells devoid of Mck1, unlike *kar9Δ* cells that portray a higher percentage (~30- 35%) of disorientated metaphase/anaphase spindles.

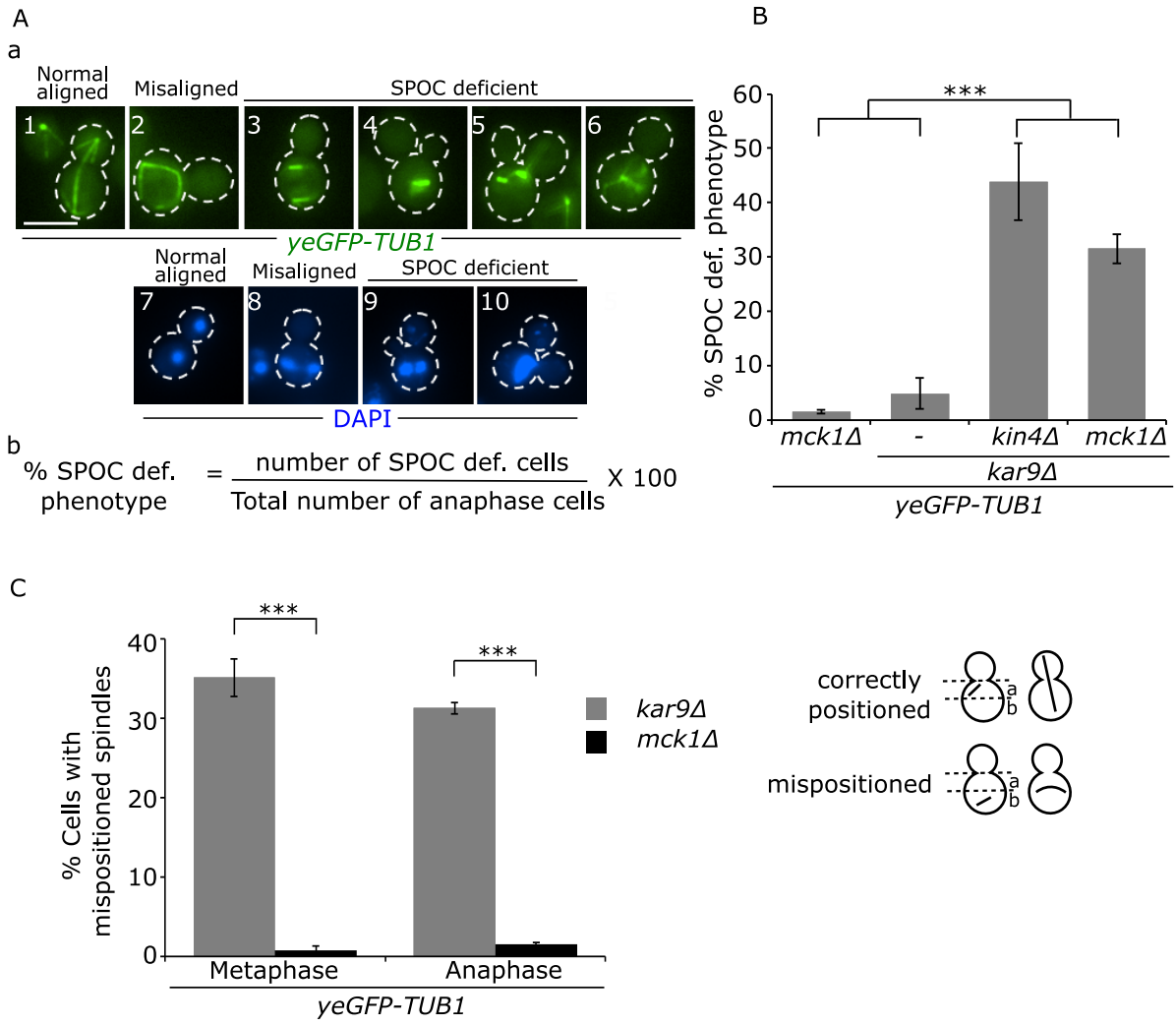

Figure. 3-2. *mck1Δ* cells are SPOC deficient. A) a) Representative images of tubulin tagged with yeGFP (1:6) and nucleus stained by DAPI (7:10), respectively, in cells with normally aligned (1,7), misaligned spindles (2,8) or SPOC deficiency (3:4; 9:10). Cell boundaries are marked in dashed white lines. Scale bars- 3 µm. b) The formula used to calculate percentage of SPOC deficient (def.) cells of the total anaphase cells. B) Graph represents the average percentage of SPOC deficient cells in

indicated strains from three independent experiments. 100 anaphase cells were counted per strain and the error bars show standard deviation between the three experiments. C) The positioning of metaphase (3-4 µm: short) and anaphase (>5 µm: long) spindles was monitored by their location with respect to the bud neck as shown in the cartoons on the right. The metaphase spindles in section 'a' were determined as correctly oriented, whereas, their presence in section 'b' was considered as mispositioned spindles. Spindles were visualised by yeGFP-Tubulin. The graph depicts average ± s.d. of cells with mispositioned spindles from three independent experiments. N=100 cells per strain and experiment. Asterisks mark significant difference based on Student's two-tailed t-test (* = $p<0.05$, ** = $p<0.001$, *** = $p<0.0001$).

Next, the anaphase duration of *kar9Δ yeGFP-TUB1* cells was investigated using live-cell imaging. The time from start of spindle elongation until the spindle break was measured as the anaphase duration. In all cell types, when the spindle was normally aligned, the anaphase duration was ~22 mins (Figure. 3-3A). In *kar9Δ* cells, the misaligned spindle stays intact for >35 minutes and did not disassemble until it was reoriented along the mother-daughter axis. Contrary to this, the time taken by the misaligned anaphase spindles to disassemble in the mother cell compartment (giving rise to multinucleation) in *kar9Δ mck1Δ* cultures did not significantly vary in comparison to cells with correctly aligned spindles (Figure. 3-3B). The behaviour of *kar9Δ mck1Δ* cells is similar to *kar9Δ kin4Δ* (Figure. 3-3A, 3-3B). Altogether, this shows that Mck1 is a novel SPOC component essential to stall mitotic exit in cells with misaligned anaphase spindle.

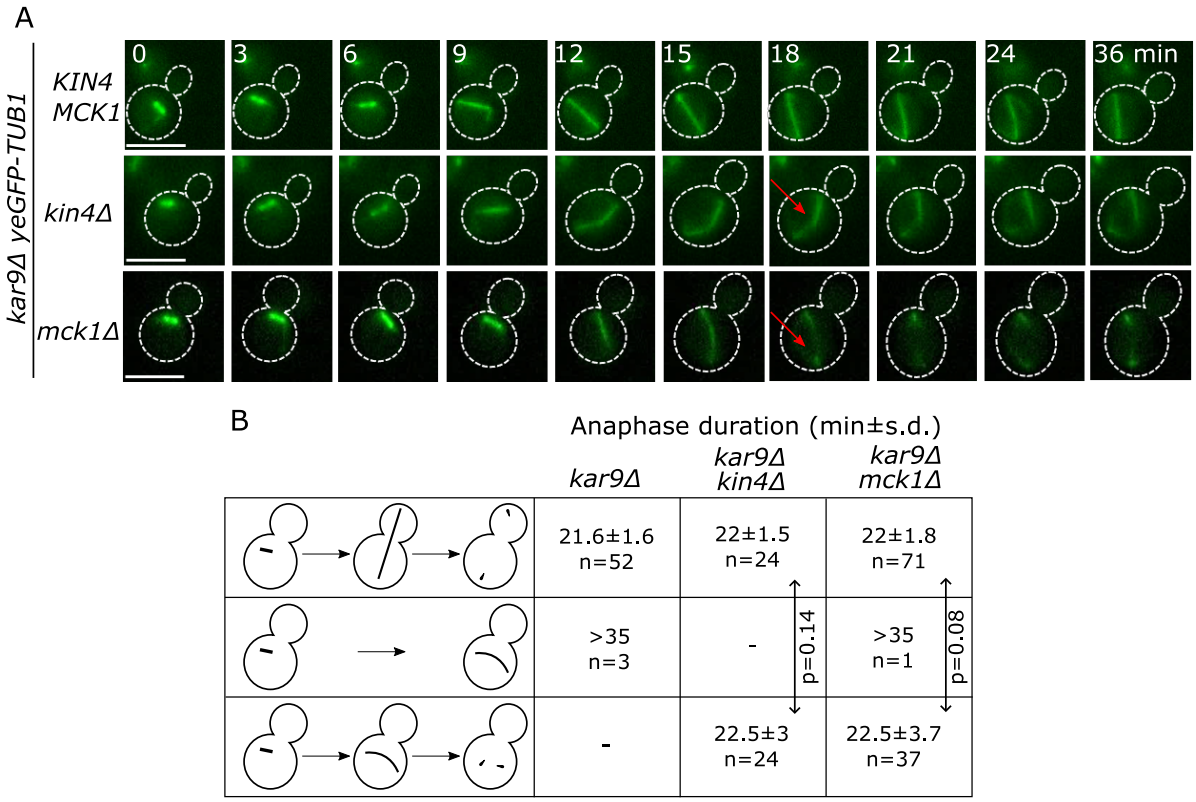

Figure. 3-3. Mck1 is essential to halt mitotic exit in cells with mis-orientated anaphase spindles. A) Representative images from live cell imaging of indicated strains harbouring yeGFP tagged Tubulin to visualise the anaphase spindles. Red arrows point to spindle disassembly in the mother compartment and Cell boundaries are marked by dashed lines. Scale bars- 3 µm. B) Quantification of the anaphase duration of cells imaged in A, where anaphase duration was defined as the time before beginning of spindle elongation until spindle disassembly.

3.1.3 The kinase activity of Mck1 is essential for its SPOC function

Next, I questioned if the kinase activity of Mck1 is essential for this function. The aspartic acid (D) residue at 181st position in mammalian GSK-3β forms the active site in the catalytic subunit of the Ser/Thr kinase domain (Dajani *et al.*, 2001). This reside aligns perfectly with D164 in Mck1, so I created a kinase-dead form of Mck1, *mck1-KD (D164A)* (Rayner *et al.*, 2002). I observe that the expression of the wild type Mck1, could revert the growth of *mck1Δ* Gal1-*KIN4* cells under galactose inducing conditions, but the plasmid carrying *mck1-KD* could not (Figure. 3-4A). Cells with the mutant form of Mck1, *mck1-KD*, behaved like the *mck1Δ* and were able to grow (Figure. 3-4A). Therefore, the kinase activity of Mck1 is essential to rescue the *KIN4*

overexpression. Additionally, the SPOC deficiency of *mck1Δ* cells was reverted upon integrating wild type *MCK1* in the Leucine locus but not *mck1-KD* (Figure. 3-4B). These findings, therefore, confirm that the rescue of the *KIN4* overexpression lethality arose because of *MCK1* deletion and is dependent upon its kinase activity. And that the SPOC function of Mck1 also relies on its kinase activity.

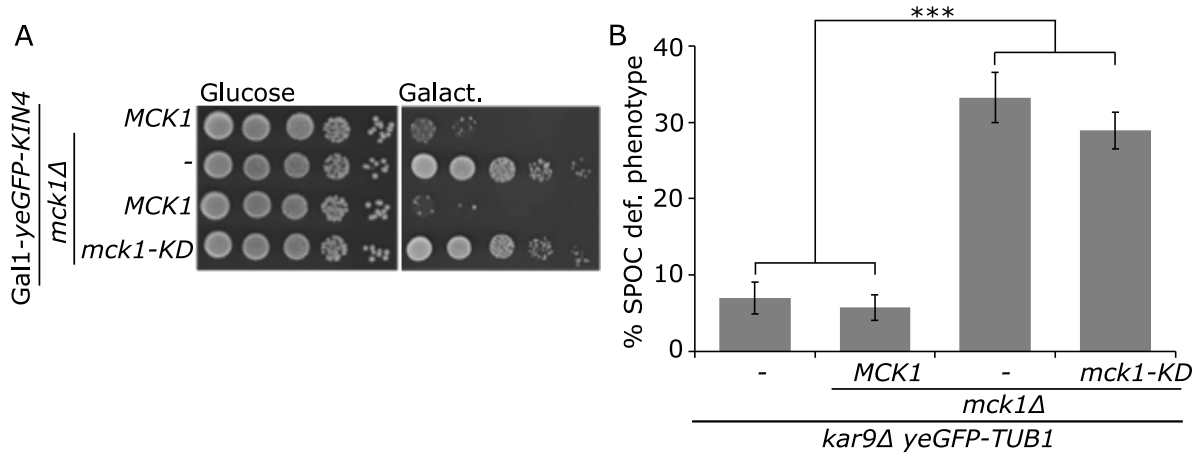

Figure. 3-4. Mck1 kinase activity is required for its SPOC function. A) Serial dilutions of indicated strains on Galactose containing Gal1-*KIN4* inducing (Galact.) or repressing (Glucose) plates. B) Graph represents the average percentage of SPOC deficient cells in indicated strains from three independent experiments. 100 anaphase cells were counted per strain and the error bars show standard deviation between the three experiments. Asterisks mark significant difference based on Student's two-tailed t-test (* = p<0.05, ** = p<0.001, *** = p<0.0001).

3.1.4 The function of SPOC is not shared by other GSK-3 homologs

In *S. cerevisiae*, there are four GSK-3 kinase homologues namely, Mck1, Mds1 (Rim11), Mrk1 and Ygk3. All four homologs have very similar domain architecture, with a central Ser/Thr kinase domain, like their mammalian GSK-3β counterparts. They are known to perform overlapping functions in budding yeast (Neigeborn and Mitchell, 1991; Malathi *et al.*, 1997; Rubin-Bejerano *et al.*, 2004). These homologs namely Mds1/Rim11, Mrk1 and Ygk3 share 59%, 61% and 65% similarity with Mck1, respectively, in the central kinase domain but are all very diverse at the C termini. So, I wanted to see if the SPOC function is unique to Mck1 or is redundant between the other family members.

First, I sought to see if the single deletions of the other three family members could rescue the lethality of *KIN4* overexpression like *mck1Δ*. Surprisingly, deletion of none of the homologues could rescue the lethality of *KIN4* overexpression like *mck1Δ* could, indicating that this is unique to Mck1 (Figure. 3-5A). To know whether they have a role in SPOC, I also counted the percentage of cells with SPOC deficient phenotype in *kar9Δ* cells depleted for the three homologs, one at a time. *kar9Δ mck1Δ* cells showed a significantly higher percentage of SPOC deficient cells as compared to the other homologues (Figure. 3-5B). Thus, from these results, we conclude that the role of Mck1 in regulating SPOC is unique and is not shared with any of the other GSK-3 family members.

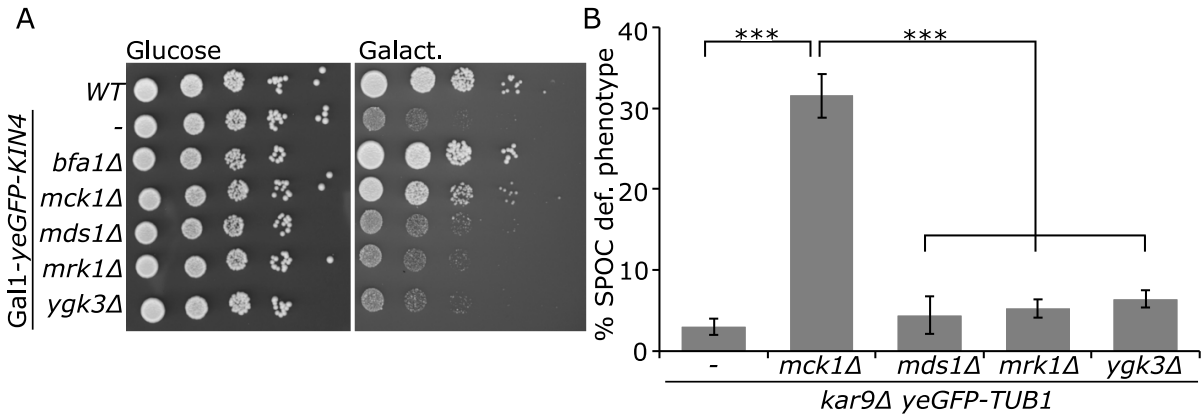

Figure. 3-5. SPOC function of Mck1 is not shared by other budding yeast GSK-3 homologs. A) Serial dilutions of indicated strains on Galactose containing Gal1-*KIN4* inducing (Galact.) or repressing (Glucose) plates. B) Graph represents the average percentage of SPOC deficient cells in indicated strains from three independent experiments. 100 anaphase cells were counted per strain and the error bars show standard deviation between the three experiments. Asterisks mark significant difference based on Student's two-tailed t-test (* = p<0.05, ** = p<0.001, *** = p<0.0001).

3.1.5 Spindle Assembly Checkpoint (SAC) is intact in *mck1Δ* cells

The spindle assembly checkpoint (SAC) restricts sister chromatin separation until all kinetochores during metaphase are attached to the opposing microtubules (Foley and Kapoor, 2013). I asked if Mck1 was vital for SAC activity or not. To test this, I assessed the growth of cells lacking Mck1 upon nocodazole treatment that causes microtubule depolymerisation. Similar to the wild type cells, these cells are also

arrested as large budded cells, unlike the SAC-deficient *bfa1Δ* cells which progressed through the cell cycle (Figure. 3-6A).

Another indicator of SAC activity is the inhibition of Pds1/securin degradation upon microtubule depolymerisation (Foley and Kapoor, 2013). As reported earlier, we see that in wild type cells arrested with high levels of Clb2 and Pds1 (Figure. 3-6B), unlike *mad2Δ* cells that degrade Pds1 and Clb2 (Figure. 3-6B; 60 min marked with an asterisk) leading to mitotic exit. The *mck1Δ* culture, behaved like the wild type culture in this scenario strengthening the conclusion that Mck1, does not influence the SAC. Therefore, similar to Bmh1 and Kin4 (D'Aquino *et al.*, 2005; Pereira and Schiebel, 2005; Caydasi *et al.*, 2010), Mck1 is essential for SPOC but not SAC.

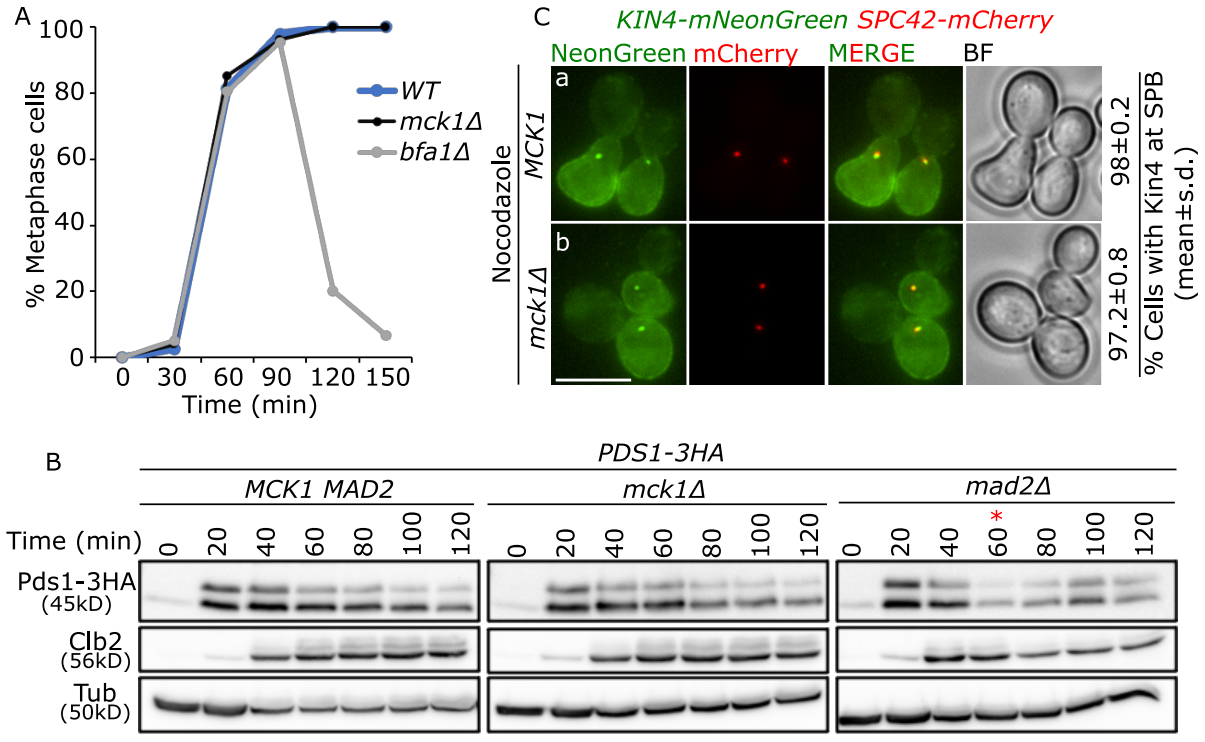

Figure. 3-6. Mck1 does not regulate SAC or Kin4 localisation. A) The indicated strains were arrested in G_1 by alpha-factor and released in fresh medium containing nocodazole. Samples were collected at indicated time points and the percentage of cells that were arrested as large buds and carried one DAPI stained nucleus at each time point are represented in the linear plot. B) Immunoblots to visualise Pds1-3HA degradation. Cells were arrested in G_1 by alpha-factor and released in fresh medium containing nocodazole. Samples were collected at indicated time points for protein extraction. Clb2 served as marker for cell cycle progression and Tub as loading control. C) Representative images of Kin4 localisation in nocodazole treated, metaphase arrested. Spc42-mCherry served as an

SPB marker. The quantification of cells bearing SPB localisation of Kin4 is represented in the right corner. Scale bars- 5 µm.

3.2 Mck1 does not affect the Kin4 kinase activity

3.2.1 Kin4 localisation remains unperturbed in *mck1Δ* cells

SPOC is activated only upon binding of Kin4 to the mother cortex and at the mSPB (Pereira and Schiebel, 2005; Maekawa *et al.*, 2007). Its localisation to the mSPB and cortex is promoted by Rts1, a PP2A phosphatase subunit, a gene whose deletion also leads to SPOC deficiency in cells (Bertazzi *et al.*, 2011). Therefore, I wanted to assess if Mck1 could also directly or indirectly regulate Kin4 localisation. To mimic SPOC activation and get a large number of cells with Kin4 at mSPB and mother cortex, I monitored the localisation of Kin4-mNeonGreen in nocodazole-treated, metaphase arrested cells (Pereira and Schiebel, 2005). The SPB protein Spc42, tagged with mCherry served as an SPB marker. Kin4-mNeonGreen localised to the mother cell cortex and SPBs in WT cells (Figure. 3-6C-a). A similar localisation pattern was observed in the majority of *mck1Δ* cells (Figure. 3-6C-b). Thus, Mck1 is not required for proper recruitment of Kin4 to the cortex or SPB when SPOC is activated.

3.2.2 Mck1 does not influence Bfa1 phosphorylation and localisation

After identifying the role of Mck1 in regulating SPOC, I aimed to understand if it affects Kin4 activity. To evaluate Kin4 activity in vivo, I assessed the phosphorylation profile of Bfa1 by monitoring Bfa1 mobility shift on 8% SDS-PAGE gels. It is known that Kin4 phosphorylates Bfa1 to prevent it from inhibitory phosphorylation by polo-like-kinase Cdc5 (Hu *et al.*, 2001; Pereira and Schiebel, 2005). The Cdc5-dependent phosphorylated forms of Bfa1 migrate slowly on protein gels. In metaphase-arrested, nocodazole treated cells, these slowly migrating forms of Bfa1 become apparent only

upon deletion of *KIN4* (Pereira and Schiebel, 2005; Maekawa *et al.*, 2007). Accordingly, slow migrating forms of Bfa1-3HA can be seen in metaphase-arrested *kin4Δ* cells (Figure. 3-7A, asterisk). These slow-migrating forms of Bfa1 are absent in *mck1Δ* like the wild type cells (Figure. 3-7A). Importantly, in the double mutant *kin4Δ mck1Δ* the phospho-shift of Bfa1 was promoted (Figure. 3-7A, asterisk, last panel). Thus, the phosphorylation profile of Bfa1 that is maintained by Kin4 and Cdc5 is not affected upon deletion of *MCK1*. Phospho-regulation of Bfa1 by Kin4 and Cdc5 govern the SPB localisation of the Bfa1-Bub2 GAP complex.

SPOC is engaged upon phosphorylation of Bfa1 by Kin4 which then disrupts the asymmetric SPB localisation of Bfa1-Bub2 complex. To decipher if Mck1 controls the localisation of Bfa1, I determined Bfa1-yeGFP SPB localisation in *mck1Δ* cells upon spindle misalignment. As has been reported earlier (Caydasi and Pereira, 2009; Monje-Casas and Amon, 2009), I observe that Bfa1 localised symmetrically (with equal intensity at both SPBs) in most of the *kar9Δ* cells with misaligned spindles (Figure. 3-7B). In contrast, Bfa1 localised asymmetrically at SPBs in the majority of *kar9Δ kin4Δ* cells with misoriented mitotic spindles. Of importance, I observe that *kar9Δ mck1Δ* cells show Bfa1 localisation behaviour similar to that of the WT cells (Figure. 3-7B, 3-7C). Altogether, these data suggest that Mck1 is not involved in regulating the phosphorylation of Bfa1 and its Cdc5 and Kin4-dependent phosphorylation remain unperturbed in *mck1Δ* cells.

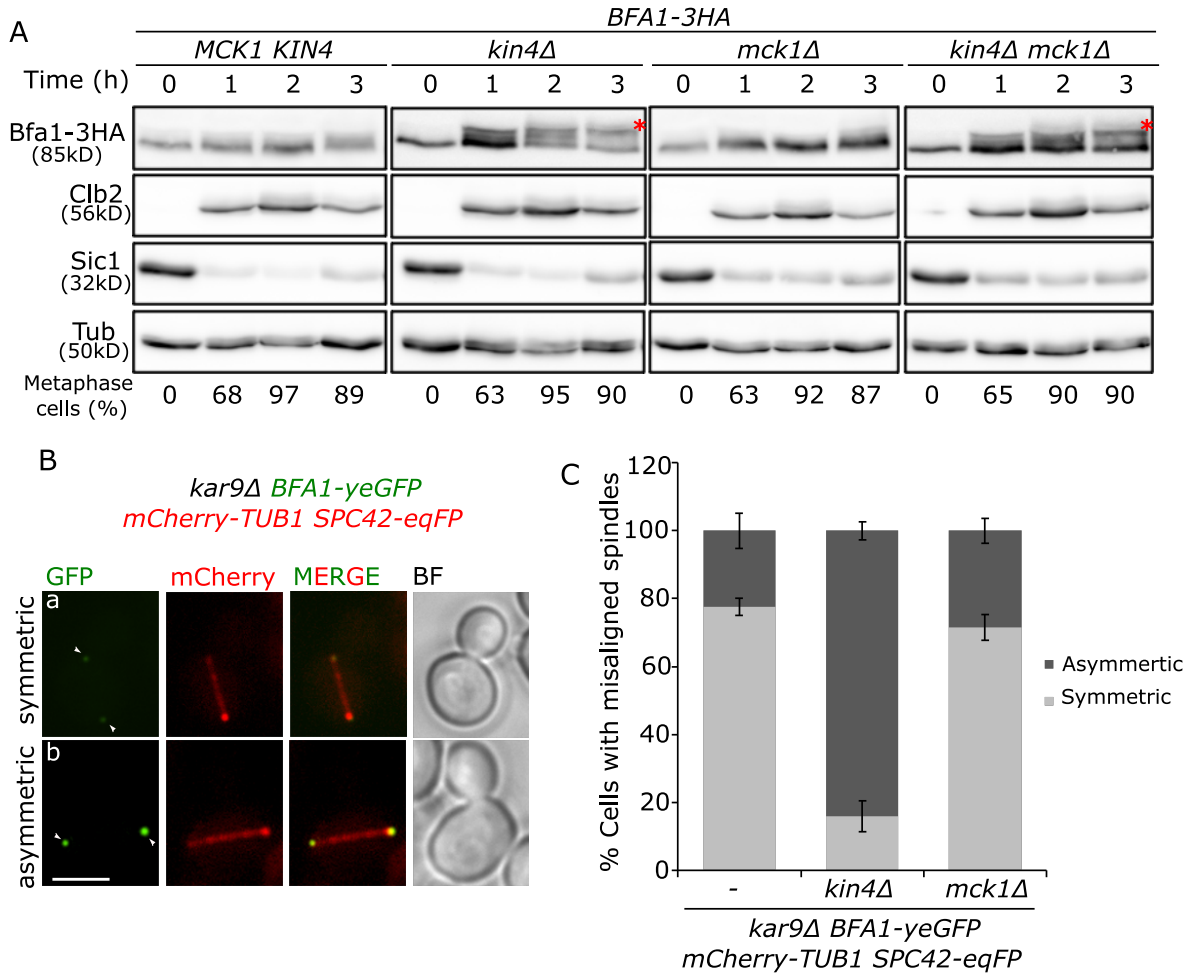

Figure. 3-7. Mck1 does not modulate Kin4 activity *in vivo*. A) Immunoblots representing the phosphorylation of Bfa1-3HA. Cultures were arrested in G_1 by alpha factor synchronisation and released in fresh medium containing nocodazole. Samples were collected every hour to visualise slow migrating band on Bfa1, marked with red asterisks, on SDS-PAGE. Clb2 and Sic1 served as cell cycle markers and Tub served as a loading control. B) Still images representing symmetric and asymmetric localisation of Bfa1-yeGFP in cells with misaligned spindles. mCherry-Tub1 and Spc42-eqFP marked spindles and SPBs, respectively. Scale bars- 3 µm. C) Graphical representation of indicated strains containing asymmetric or symmetric Bfa1 localisation as shown in B. Data represented is average from three independent experiments and 100 cells with misaligned spindles were counted for each strain.

3.3 Deletion of *MCK1* activates MEN in cells with mis-orientated spindles

Cells lacking *MCK1* do not influence Kin4 or Bfa1 activity upon spindle misalignment. This finding might imply that Mck1 functions downstream of Bfa1, acting upon the MEN components. Therefore, I next sought to look at the localisation of MEN components like Mob1.

3.3.1 Mob1 localises at the SPBs in *mck1Δ* cells with misaligned spindles

FEAR released Cdc14 enhances MEN activity by recruiting Cdc15 to the SPBs which further promotes accumulation of Dbf2-Mob1 (Menssen *et al.*, 2001; Visintin and Amon, 2001; Molk *et al.*, 2004; König *et al.*, 2010; Rock *et al.*, 2013). In cells with normally aligned spindles, Mob1 localises at both the SPBs (Figure. 3-8A-a; arrows) and briefly before cytokinesis at the bud-neck (Figure. 3-8A-a; asterisk). Therefore, I looked at Mob1-yeGFP localisation at SPBs in cells with misaligned spindles. In the presence of Mck1, upon spindle misalignment, the levels of Mob1 remained low at SPBs (Figure. 3-8A-b; arrows). It has been shown earlier that Mob1 accumulates at SPBs in *kin4Δ* cells with misaligned spindles (Caydasi *et al.*, 2017), and I observe that deletion of *MCK1* also promoted sequestration of Mob1 at SPBs (Figure. 3-8A-c; arrows). Notably, spindle disassembly in the mother compartment also leads to bud-neck accumulation of Mob1 in *mck1Δ* cells (Figure. 3-8A-d; asterisk). Similar to *kin4Δ* cells, majority of cells with misaligned spindles showed accumulation of Mob1-yeGFP at both SPBs in *mck1Δ* cells (Figure. 3-8B). This serves as the first evidence for *mck1Δ* cells exiting SPOC arrest upon spindle misalignment by activating MEN.

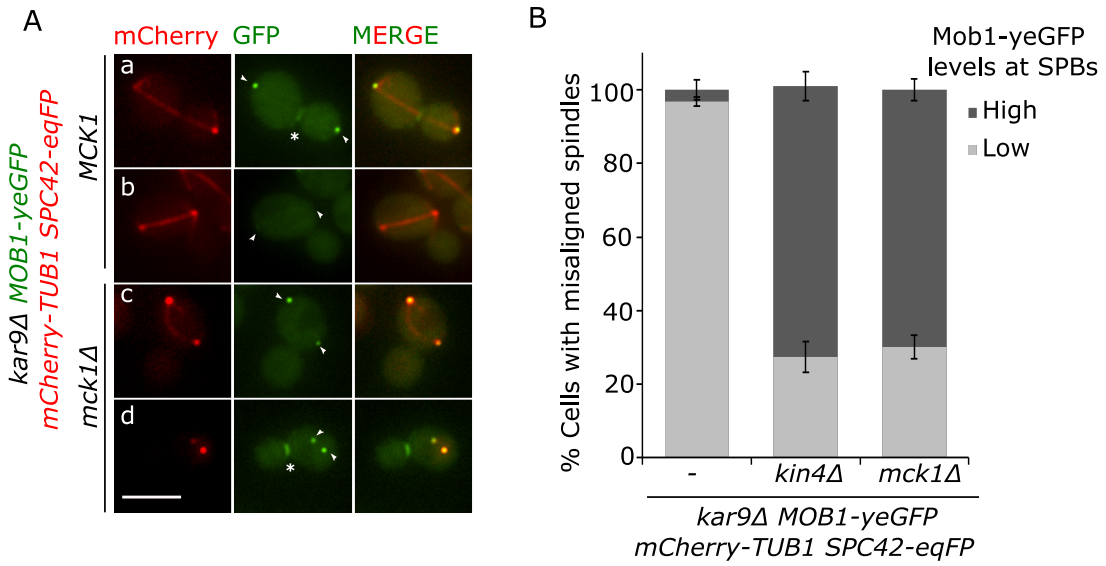

Figure. 3-8. *mck1Δ* cells accumulate Mob1 at the SPBs upon spindle misalignment. A) Still images representing localisation of Mob1-yeGFP in cells. Low Mob1 levels at SPBs (b) and

accumulation of Mob1 at SPBs (a,c,d). White arrows mark SPBs and asterisks mark the bud neck localisation of Mob1. mCherry-Tub1 and Spc42-eqFP marked spindles and SPBs, respectively. Scale bars- 3 µm. B) Graphical representation of indicated strains containing low or high Mob1 at SPBs upon spindle misalignment as shown in A. Data represented is average from three independent experiments and 100 cells with misaligned spindles were counted for each strain.

3.3.2. Full release of Cdc14 occurs upon spindle misalignment in *mck1Δ* cells

Cdc14 is an ultimate effector of MEN activation, the release of which promotes cytokinesis and mitotic exit (Shirayama *et al.*, 1994b; Jaspersen *et al.*, 1998; Shou *et al.*, 1999; Meitinger *et al.*, 2012). I, therefore, questioned if deletion of *MCK1* led to the full release of Cdc14 upon spindle misorientation. Most of the *kar9Δ* cells with misaligned spindles retained Cdc14-mCherry in the nucleus (Figure. 3-9A-a,b), thereby inhibiting mitotic exit. On the other hand, 81% of *mck1Δ* cells showed full Cdc14 full release in cells with misaligned spindles (Figure. 3-9A-a,b; marked with arrows). Thus, *mck1Δ* cells cannot hold SPOC arrest due to activation of MEN (Figure. 3-8, 3-9A). And this is strong proof that Mck1 inhibits mitotic exit by regulating the full release of Cdc14 upon spindle misalignment.

Cdc14 resides largely in the nucleolus in an inactive state (Figure. 3-9B-a) and in early anaphase, the Cdc-fourteen early anaphase release (FEAR) network promotes a brief release of Cdc14 into the nucleus (Figure. 3-9B-b,c). I wanted to check whether deleting Mck1 affects this FEAR-dependent Cdc14 release. To investigate this, I used *cdc15-1* temperature-sensitive (ts) strains, where cells grow normally at permissive temperatures (23°C) and are stuck in late mitosis at non-permissive temperature (37°C) due to failure in Cdc14 full release (Jaspersen *et al.*, 1998). I first arrested the cells in the G_1 phase by alpha-factor synchronisation at 23°C and later released them in fresh media at 37°C. Samples were taken until 3 hours and cells that showed FEAR release of Cdc14 were counted with respect to their pole-pole distance (spindle length). My analysis shows that wild type and *mck1Δ* cells have

comparable Cdc14-FEAR release in each spindle length category (Figure. 3-9C). Additionally, in contrast to the *spo12Δ* cells, we observe that *mck1Δ* cells have normal FEAR-dependent Cdc14 release, which is lost in mck*1Δ spo12Δ* cells (Figure. 3-9C). This implies that Cdc14 full release upon spindle misalignment in *mck1Δ* cells (Figure. 3-9A) is due to activation of MEN and not an aberrant FEAR release of Cdc14.

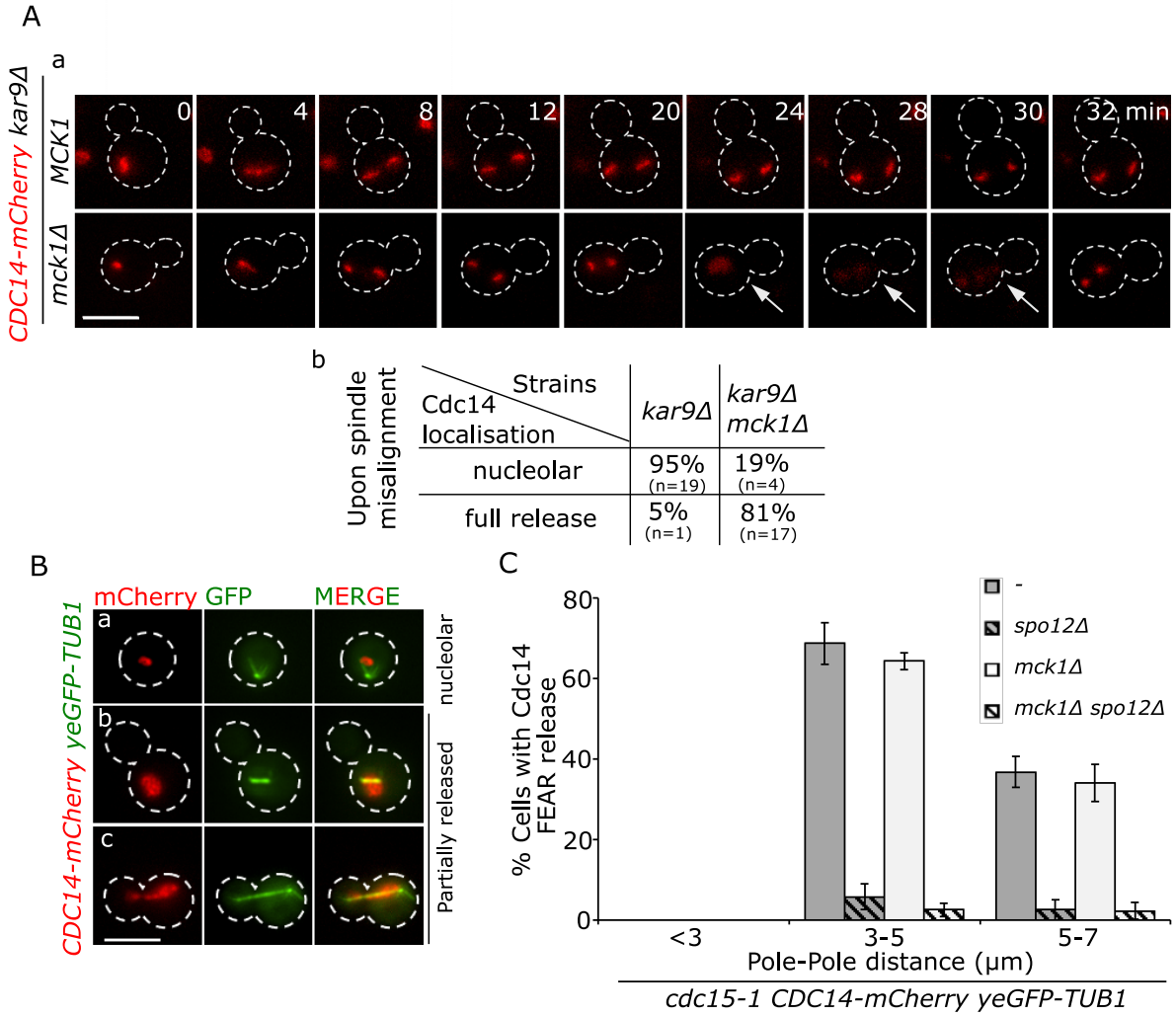

Figure. 3-9. Cells lacking Mck1 activate the full release of Cdc14 upon spindle misalignment. A) (a) Representative images from live cell imaging of indicated strains harbouring mCherry tagged Cdc14 to visualise its release. White arrows point to the full release of Cdc14. Scale bars- 3 μm. (b) Quantification of the cells from A. B) Images representing Cdc14 nucleolar localisation (a) and partial release (c,d). Scale bars- 3 μm. C) Quantification of cells exhibiting partial (FEAR mediated) Cdc14 release in indicated strains with respect to the spindle length (pole-pole distance). Data represents an average from three independent experiments and error bars show standard deviation between them.

3.4 Mck1 is dispensable for SPOC in the absence of FEAR

It has been established that Kin4 functions to counterbalance MEN activation by the FEAR network in the mother cell compartment. Thus, it becomes dispensable for SPOC function in absence of FEAR (Falk *et al.*, 2016; Caydasi *et al.*, 2017).

Spo12 is a component of the FEAR network, and overexpression of it promotes mitotic exit in a Cdc14-dependent manner without bypassing MEN (Falk *et al.*, 2016; Caydasi *et al.*, 2017). As for *kin4Δ* cultures, I wanted to understand if *SPO12* deletion could also prompt SPOC proficiency along with *MCK1* deletion. I observe that the otherwise SPOC deficient *kar9Δ mck1Δ* cultures became SPOC proficient when SPO12 was deleted in them (Figure. 3-10). This behaviour of Mck1 in inhibiting FEAR-dependent MEN activation upon SPOC activation is similar to Kin4. Therefore, implying that Mck1 and Kin4 could function either in the same or independent, parallel pathways to engage SPOC.

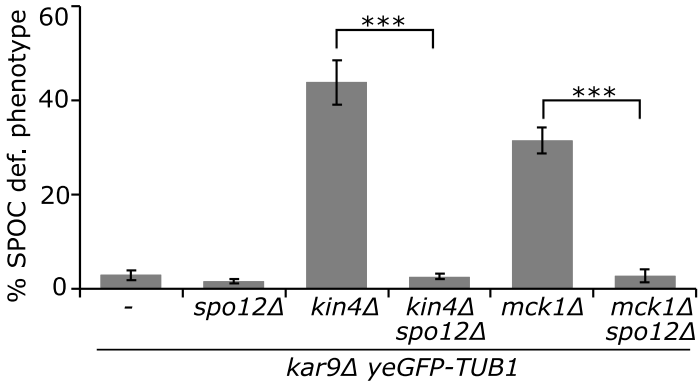

Figure. 3-10. Mck1 is not essential for SPOC in the absence of FEAR. The graph represents the average percentage of SPOC deficient cells in indicated strains from three independent experiments. 100 anaphase cells were counted per strain and the error bars show standard deviation between the three experiments. Asterisks mark significant difference based on Student's two-tailed t-test (* = p<0.05, ** = p<0.001, *** = p<0.0001).

3.5 Mck1 inhibits mitotic exit independent of the spindle orientation

From the results mentioned above, the role of Mck1 in inhibiting MEN upon spindle misalignment is evident. I next asked if Mck1 is a general mitotic inhibitor, preventing

mitotic exit also in cells with a normally aligned spindle. To assess this, I tested the survivability of mitotic exit mutants, upon deletion of *MCK1*.

3.5.1 The MEN temperature-sensitive mutants

MEN activation is essential for cells to exit mitosis (Shirayama *et al.*, 1994b; Shou *et al.*, 1999). Tem1, Mob1, Cdc15, Cdc5 and some core MEN components and temperature sensitive mutants of these components block cell cycle progression in a temperature-dependent manner (Jaspersen *et al.*, 1998) (Figure. 3-11A). Cells lacking Mck1 could rescue the lethality of *tem1-3, cdc15-1, cdc5-10 and mob1-67* at non-permissive temperatures (33-35°C) (Figure. 3-11A). This implies that Mck1 inhibits the exit of cells from mitosis via MEN or possibly independent of it. To test the latter, I checked for the growth of cells lacking *MOB1*, *TEM1* or *CDC15* upon *MCK1* deletion (Figure. 3-11B). To this end, *MCK1* deletion could not rescue their lethal phenotype (Figure. 3-11B), indicating that *mck1Δ* cells require residual MEN activity to exhibit growth in MEN ts mutants.

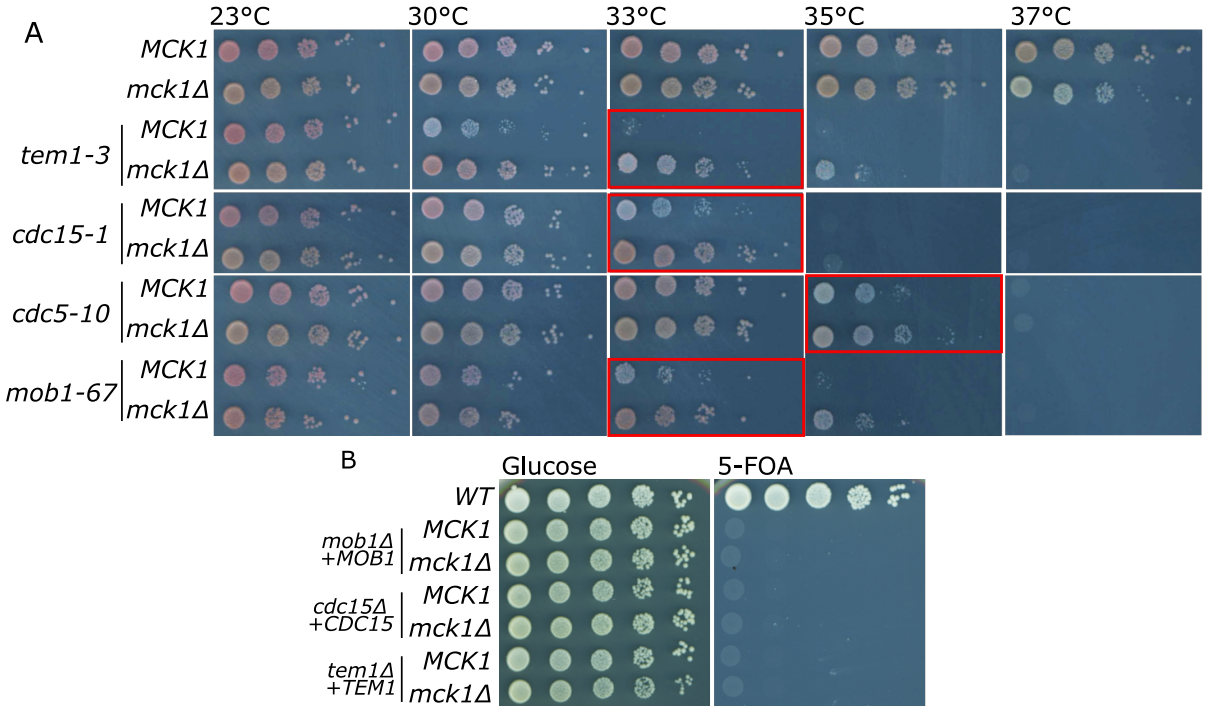

Figure. 3-11. Mck1 does not bypass MEN to inhibit mitotic exit. A) Serial dilutions of MEN ts mutants with or without Mck1 on agar plates at specified temperatures. B) Growth analysis of indicated strains on plates in the presence (SC-Complete) or absence (5-FOA) of *URA3*-based: *MOB1*/ *CDC15*/ *TEM1* plasmids. Red boxes mark the reversal of growth lethality upon *MCK1* deletion.

3.5.2 Cold sensitivity of *LTE1* deletion

Mitotic exit is regulated in a spatiotemporal manner, with several components occupying distinct intracellular sites. Lte1 is one such daughter-cell specific MEN regulator, that localises to the bud cortex and inhibits Kin4 activity in the daughter compartment (Shirayama *et al.*, 1994a; Bardin *et al.*, 2000; Bertazzi *et al.*, 2011; Falk *et al.*, 2011). *LTE1* deletion has been reported to be lethal at cold temperatures, as cells fail to exit mitosis (Shirayama *et al.*, 1994a). However, Lte1 is not essential at 30°C for cell survival indicating that are parallel pathways activating MEN (Shirayama *et al.*, 1994a; Höfken and Schiebel, 2002). This cold sensitivity of *lte1Δ* cells has been reported to be reverted by the deletion of *KIN4, BUB2* or *BFA1* like mitotic inhibitors (Stegmeier *et al.*, 2002; D'Aquino *et al.*, 2005) (Figure. 3-12A). Likewise, I observe that *lte1Δ mck1Δ* cells are not cold sensitive and rescue the lethality of *lte1Δ* in cold (Figure. 3-12A). This reinserts the role of Mck1 as a general mitotic inhibitor.

3.5.3 Lethality of *lte1Δ FEARΔ* mutants

The absence of Lte1 along with FEAR components like Spo12 and Slk19 leads to arrest of cells in anaphase thereby, blocking mitotic exit (Stegmeier *et al.*, 2002). This states that the cells either of the two mechanisms to activate MEN. The lethality of *lte1Δ spo12Δ* and *lte1Δ slk19Δ* cells can be rescued by *KIN4, BFA1* or *BUB2* deletion (Caydasi *et al.*, 2017). Similarly, deleting *MCK1* in these double mutants (*lte1Δ FEARΔ*) also reverts their growth phenotype (Figure. 3-12B). Implying that Mck1 inhibits mitotic exit in cells irrespectively of the spindle orientation.

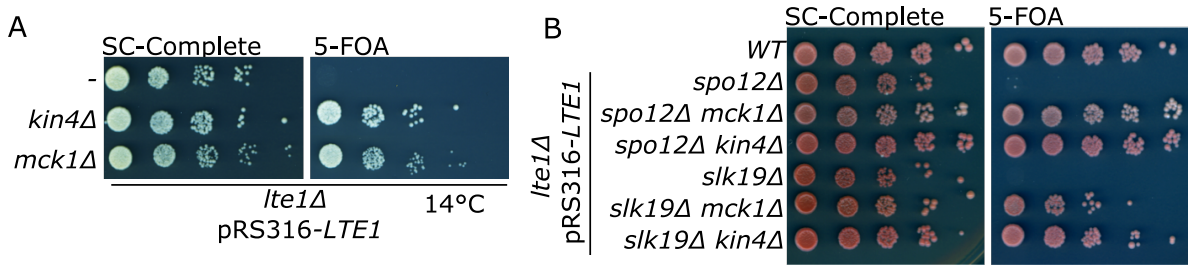

Figure. 3-12. Mck1 inhibits mitotic exit irrespective of spindle orientation. (A, B) Growth analysis by serial dilutions of indicated strains in the presence (SC-Complete) or absence (5-FOA) of pRS316-*LTE1*.

3.5.4 Synthetic lethality caused by *BFA1* overexpression

Based on the understanding so far, that *MCK1* deletion can rescue the lethality of *KIN4* overexpression but does not interfere with Kin4 activity or Bfa1 phospho-regulation, I questioned to see if it may work downstream of Bfa1.

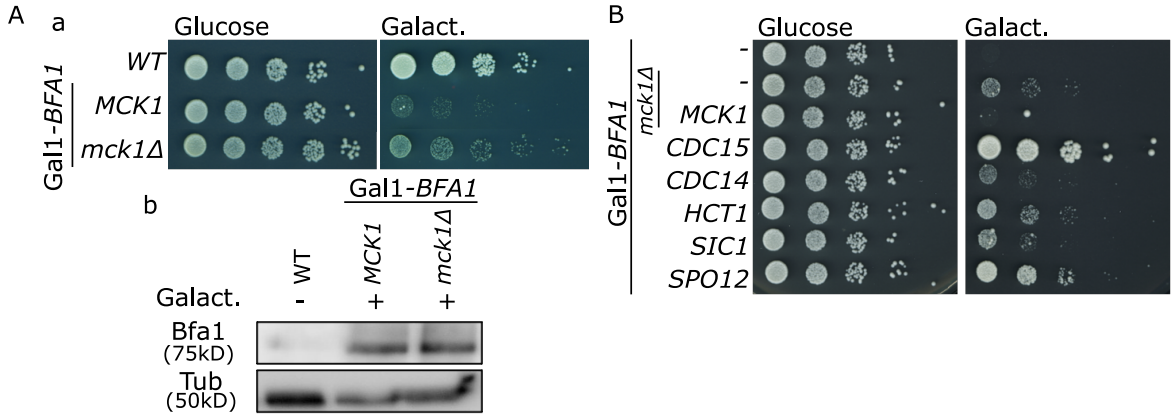

Figure. 3-13. *MCK1* deletion can moderately rescue the growth lethality of *BFA1* overexpression. A-a, B) Growth analysis by serial dilutions of indicated strains on Gal1-*BFA1* inducing (Galact.) or repressing (Glucose) plates. (A-b) Immunoblot to visualise the protein levels of Bfa1 in the indicated strains.

BFA1 overexpression severely blocks mitotic exit due to failure of Cdc14 full release in late anaphase (Li, 1999; Whalen *et al.*, 2018). I sought to investigate if *MCK1* deletion could rescue the dosage lethality of overproduced Bfa1. Surprisingly, the synthetic lethality of *BFA1* overexpression was reverted in cells lacking Mck1 (Figure. 3-13A-a). This wasn't due to a change in Bfa1 protein stability, as confirmed by the comparable levels in both wild type and *mck1Δ* cells (Figure. 3-13A-b). Expression of

positive regulators of mitosis like Cdc15 and Spo12 along with overproduced Bfa1 led to a better rescue of the lethality (Figure. 3-13B). This finding may impose the idea that Mck1 can contribute to the negative regulation of MEN, by acting either downstream of Bfa1 or modulating the Bfa1-Bub2 GAP complex activity.

Altogether this confirms the hypothesis that Mck1 is a negative regulator of mitosis and inhibits mitotic exit irrespectively of the anaphase spindle alignment.

3.6 Mck1 works in a FEAR-dependent manner to inhibit MEN

We know that other than Kin4, cells with misaligned spindles require Mck1 to activate SPOC in the absence of the FEAR (Figure. 3-10). I asked if this dependence on FEAR of Mck1 is also important irrespective of spindle position. As observed earlier (Figure. 3-11; 3-12; 3-13), *MCK1* deletion prompted the growth rescue of genetically lethal MEN mutants. This ability of *mck1Δ* cells was compromised by deletion of *SPO12* in the temperature sensitive (ts) mutants of Tem1 and Cdc15 (Figure. 3-14A), the lethality caused by overexpression of *KIN4* (Figure. 3-14B) and *BFA1* (Figure. 3-14C). Therefore, Mck1 requires FEAR to promote mitotic exit.

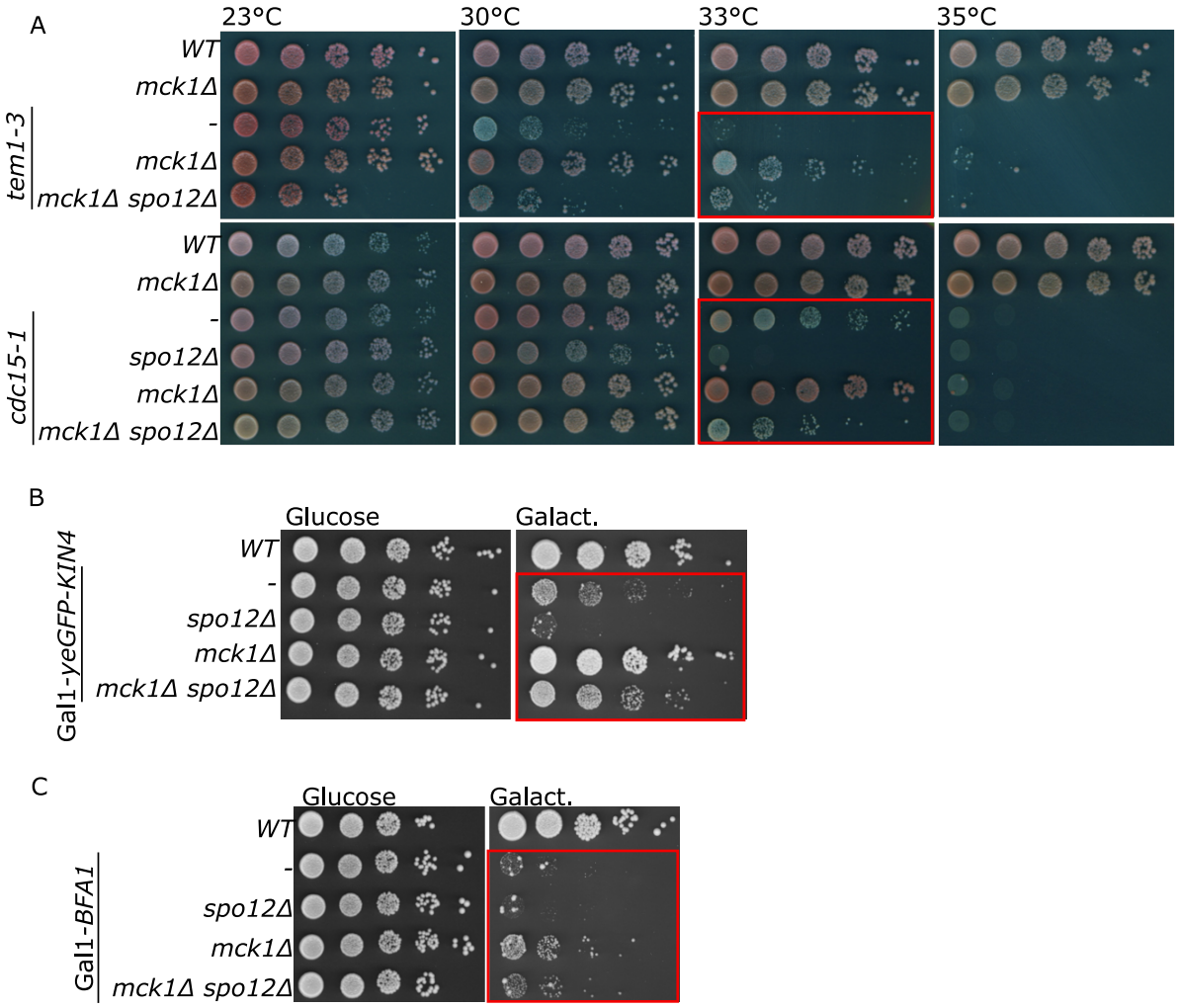

Figure. 3-14. Mck1 requires FEAR to promote mitotic exit. A) Serial dilutions of indicated MEN ts strains on plates at specified temperatures. (B, C) Serial dilutions of indicated strains on Galactose containing Gal1-*KIN4* (B) or Gal1-*BFA1* (C) inducing (Galact.) or repressing (Glucose) plates. Red boxes mark the reversal of growth lethality upon *MCK1* or *SPO12* deletion, or in combination.

3.7 Mck1 regulates SPOC and mitotic exit independently of Kin4

The analysis so far, portrayed a lot of similarities between Mck1 and Kin4, suggesting its function in the Kin4-dependent SPOC pathway. For instance, similar anaphase durations in cells with misaligned or normally aligned spindles (Figure. 3-3), no role in SAC regulation (Figure. 3-7A, C) and inhibition of FEAR-dependent MEN activation in cells with misaligned spindles (Figure. 3-10:14). Altogether this strongly supports the notion of Mck1 promoting SPOC via Kin4-pathway. However, I do not observe any changes in Kin4 activity upon *MCK1* deletion (Figure. 3-6B; 3-7). Therefore, I further looked into investigating the dependency of Mck1 on the Kin4-pathway.

lte1Δ spo12Δ ste20Δ is a genetically lethal strain whose lethality was reported to be reverted by the deletion of *BFA1* but not *KIN4* (Caydasi *et al.*, 2017) (Figure. 3-15A). To understand if Mck1 and Kin4 worked together to inhibit MEN, I assayed the survivability of this triple mutant. Like Kin4, Mck1 could not rescue the growth lethal phenotype of *lte1Δ spo12Δ ste20Δ*, however, when *KIN4* was deleted in combination with *MCK1*, these cells survived (Figure. 3-15A). This suggests that Mck1 and Kin4 inhibit MEN independent of each other.

As shown previously, *kar9Δ spo12Δ* cultures remained SPOC proficient after single gene deletions of *MCK1* or *KIN4* (Caydasi *et al.*, 2017) (Figure. 3-10). Next, I performed a SPOC assay in *kar9Δ spo12Δ,* SPOC proficient cells upon deletion of both *MCK1* and *KIN4*. This quadrupole deletion strain was deficient for SPOC (Figure. 3-15B), indicating that Mck1 and Kin4 work independently to block mitotic exit and to engage SPOC in FEARless cells.

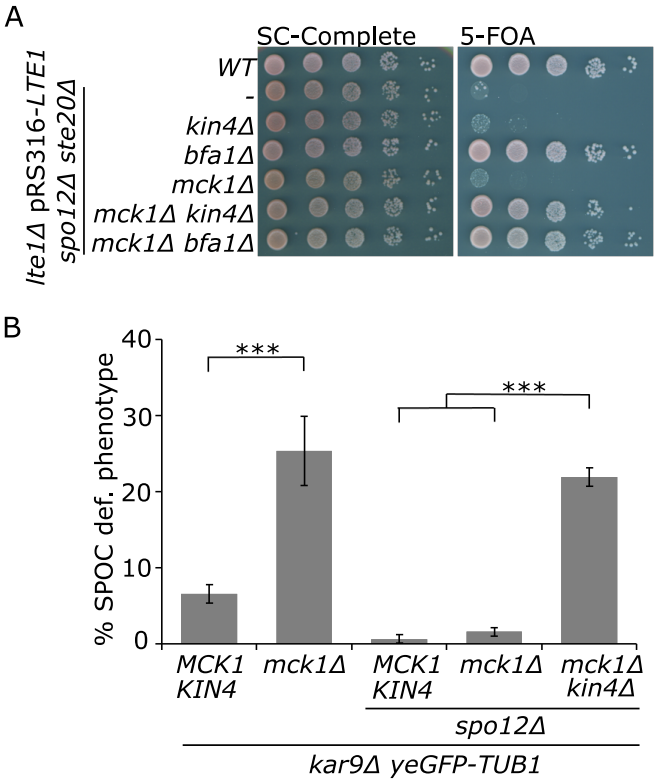

Figure. 3-15. Mck1 regulates SPOC independently of Kin4. A) Growth analysis by serial dilutions of indicated strains in the presence (SC-Complete) or absence (5-FOA) of pRS316-*LTE1*. B) Graph represents the average percentage of SPOC deficient cells in indicated strains from three independent

experiments. 100 anaphase cells were counted per strain and the error bars show standard deviation between the three experiments. Asterisks mark significant difference based on Student's two-tailed t-test (* = p<0.05, ** = p<0.001, *** = p<0.0001).

I also, asked if the MEN ts mutants could exit mitosis upon *KIN4* deletion, like Mck1 (Figure. 3-11A). Conversely, MEN ts mutants with or without Kin4 grew to a similar extent at different temperatures (Figure. 3-16; marked in red boxes). This strengthens my conclusion that Mck1 and Kin4 work independently of each other.

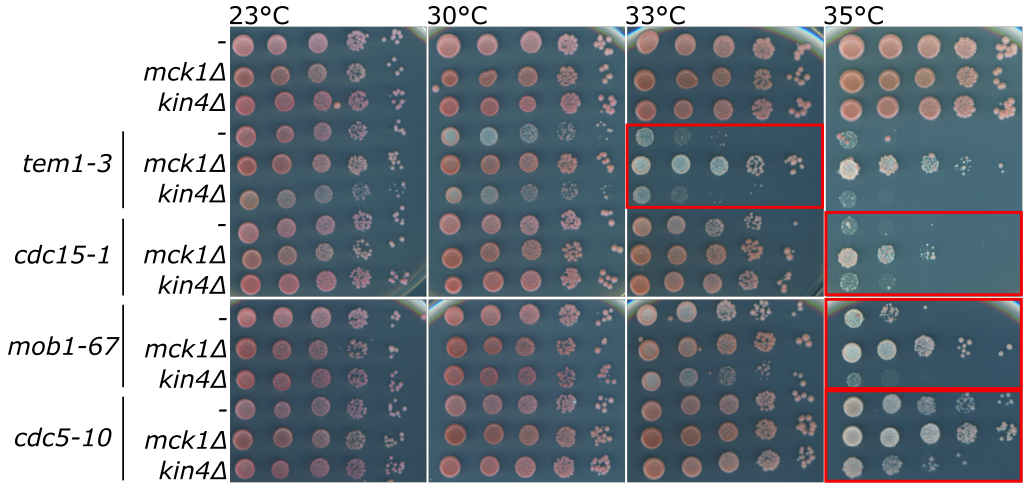

Figure. 3-16. *KIN4* deletion cannot rescue the MEN ts mutants. Growth analysis by serial dilutions of the MEN ts strains at specified temperatures. Red boxes mark the reversal of growth lethality upon *MCK1* but not by *KIN4* deletion.

3.8 Cdc6 accumulation in *mck1Δ* cells prompts failure in SPOC activation

3.8.1. Cdc6 accumulates in cells lacking Mck1

Mck1 kinase activity seemed to be crucial in engaging SPOC (Figure. 3-4B). Therefore, it was essential to elucidate the substrates that contribute to Mck1's SPOC function. Of all the known substrates that Mck1 phosphorylates, Cdc6, an essential component of the pre-RC, is identified as an interesting candidate (Cocker *et al.*, 1996; Bell and Dutta, 2003; Ikui *et al.*, 2012). Cdc6 has been reported to be involved in the regulation of mitotic exit apart by cooperating with other mitotic inhibitors - Sic1 and Hct1, independently of its role in DNA replication (Bueno and Russell, 1992; Calzada *et al.*, 2001; Archambault *et al.*, 2003). Cdc6 is an unstable

protein and its levels are tightly regulated throughout the cell cycle to prevent DNA re-replication (Luo *et al.*, 2003). Phosphorylation of Cdc6 by Cdc28 and Mck1, creates phospho-degrons at the N and C-terminus, respectively, thereby, targeting it for SCF^{Cdc4} mediated degradation between G1/S and mitosis (Piatti *et al.*, 1995; Elsasser *et al.*, 1996; Drury *et al.*, 1997; Sánchez *et al.*, 1999; Perkins *et al.*, 2001; Ikui *et al.*, 2012; Al-Zain *et al.*, 2015).

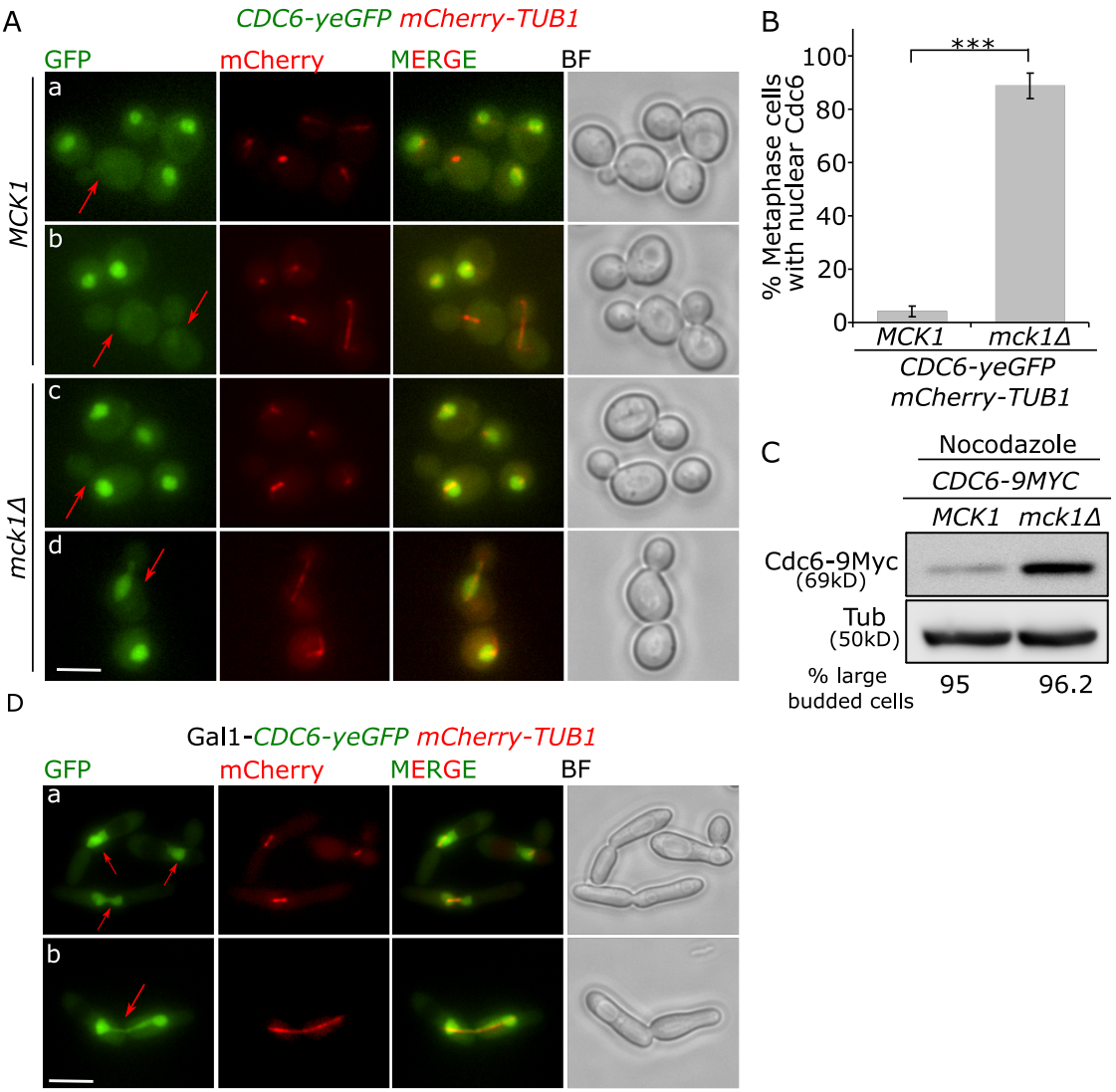

Figure. 3-17. Cdc6 accumulates in mitosis upon *MCK1* deletion. A) Still images representing endogenous Cdc6 localisation in indicated strains. Wild type cells do not show nuclear Cdc6-yeGFP localisation (a,b) in metaphase or early anaphase cells, unlike in *mck1Δ* cells (c,d). Red arrows mark the mitotic cells and mCherry-Tubulin marks spindles. Scale bars- 5 µm. B) Graphical representation of the average number of mitotic cells with nuclear Cdc6-yeGFP from A, from three independent experiments. Error bars show standard deviation and asterisks mark significant differences based on Student's two-tailed t-test. Asterisks mark significant difference based on Student's two-tailed t-test (* = $p<0.05$, ** = $p<0.001$, *** = $p<0.0001$). C) Immunoblots to visualise Cdc6-9Myc in indicated strains

upon nocodazole arrest. Tubulin served as a loading control. D) Still images represent localisation of galactose induced (Gal1-*CDC6-yeGFP*), overproduced Cdc6. Red arrows mark the cells with nuclear Cdc6-yeGFP and mCherry-Tubulin marks spindles. Scale bars- 5 µm.

It has been shown that due to failure in degradation of the protein, Cdc6 remains stabilised in *mck1Δ* cells (Ikui *et al.*, 2012). Similarly, unlike the *MCK1* cells, Cdc6 localised in the nucleus at all times in *mck1Δ* cells in our strain background as well (Figure. 3-17A; marked in red arrows). Notably, majority of the mitotic cells upon *MCK1* deletion showed nuclear Cdc6 localisation (Figure. 3-17B) and increased stability in the protein levels as confirmed by immunoblotting (Figure. 3-17C). Hence, Cdc6 accumulated in cells lacking Mck1. Cells constitutively overexpressing *CDC6* also show nuclear Cdc6 throughout the cell cycle (Figure. 3-17D) (Bueno and Russell, 1992). This may be due to an insufficient amount of Mck1 or other Cdc6 phosphorylating proteins that influence Cdc6's stability.

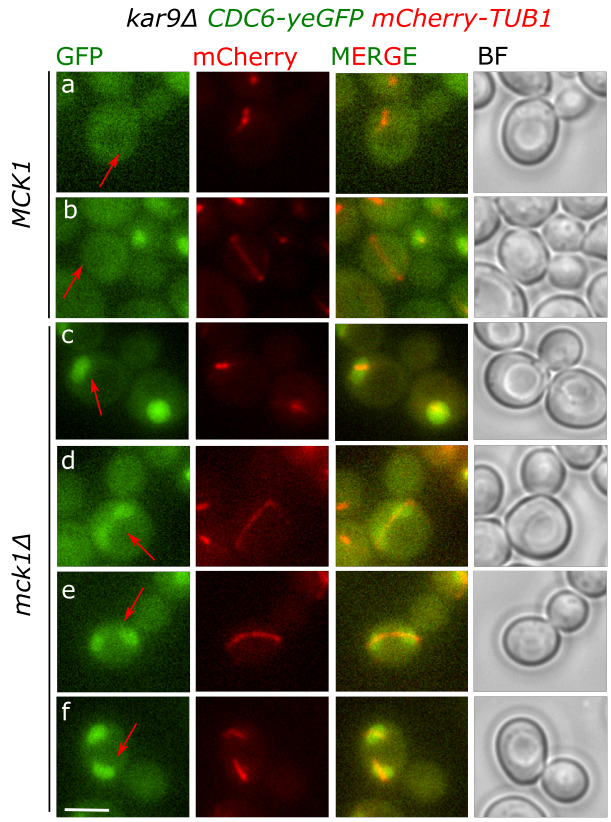

Figure. 3-18. Cdc6 accumulates upon spindle misalignment in *mck1Δ* cells. A) Still images representing endogenous Cdc6 localisation in indicated strains. Wild type cells do not show nuclear

Cdc6-yeGFP localisation (a,b) in metaphase or early anaphase cells with misaligned spindles, unlike in *mck1Δ* cells (c,d,e). Red arrows mark the mitotic cells and mCherry-Tubulin marks spindles. Scale bars- 3 µm.

I further investigated whether the stabilisation of Cdc6 in *mck1Δ* cells was dependent on the orientation of mitotic spindles. Indeed, Cdc6 accumulated in all mitotic cells of *mck1Δ kar9Δ* but not in the *kar9Δ* cultures (Figure. 3-18; marked in red arrows). This implies that the regulation of Mck1 over Cdc6 is independent of the spindle alignment.

3.8.2 Abundant levels of Cdc6 in *mck1Δ* cells bind to more Clb2

Cdc6 is degraded rapidly at the onset of S phase by early cyclin-Cdk mediated phosphorylation to prevent DNA re-replication (Bueno and Russell, 1992; Dalton and Whitbread, 1995; Piatti *et al.*, 1995; Drury *et al.*, 1997). Later, Cdc6 is transcribed again when it binds to the mitotic cyclin, Clb2, via its N terminal LxF (47-49 amino acids) motif thereby, preventing M-Cdk activity (Calzada *et al.*, 2001; Mimura *et al.*, 2004; Örd *et al.*, 2019). It has been recently shown that stabilisation of Cdc6 led to higher levels of Cdc6-Clb2 complexes being formed (Philip *et al.*, 2022), thereby, inhibiting M-Cdk activity. As *mck1Δ* cells also have elated levels of Cdc6, I hypothesised that these Cdc6 molecules may similarly, bind to more Clb2 in mitosis.

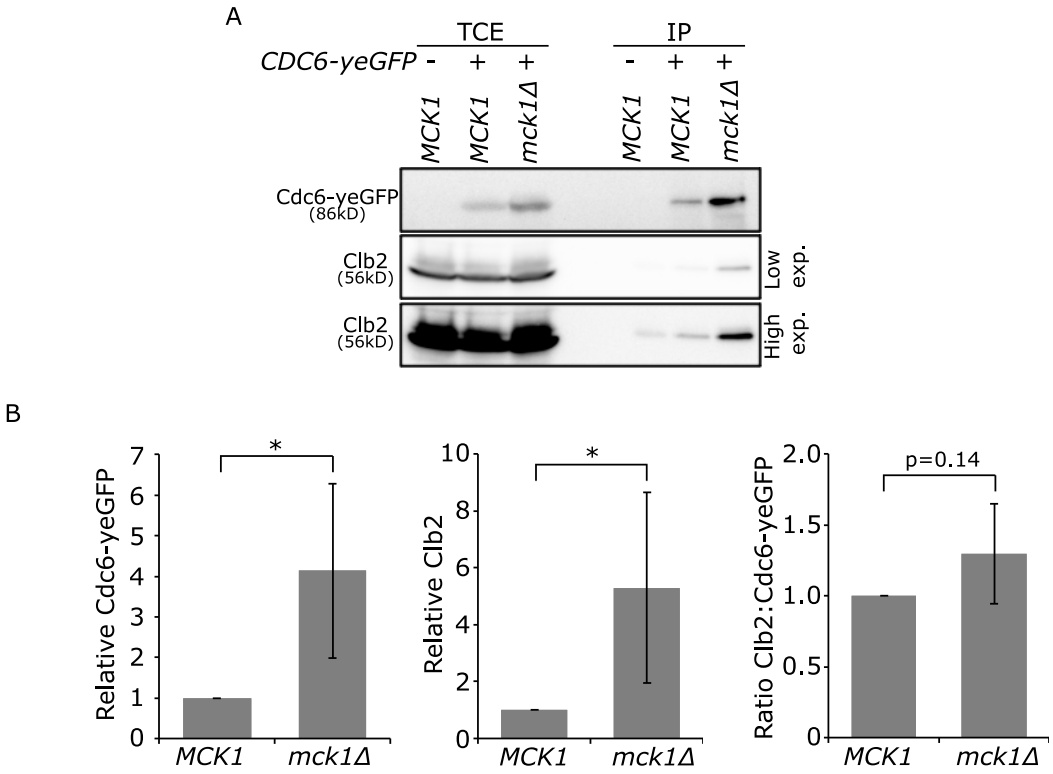

Figure. 3-19. *mck1Δ* cells accumulate abundant Cdc6 that associates with Clb2. A) Immunoblots represent the co-immunoprecipitation of Cdc6 with Clb2 in lysates from indicated strains. TCE represents the total cell extracts of the strains that were arrested in metaphase by nocodazole treatment for 2.3-3 hours. The TCEs were incubated with anti-GFP beads to Immuno-precipitate Cdc6-yeGFP; IP samples are these samples. B) Graphical analysis of data from four independent experiments in A. Relative Cdc6 and Clb2 intensities (a,b, respectively) are represented. (c) The relative ratio of Clb2:Cdc6 intensities. Error bars indicate standard deviation and asterisks show significant difference as measured by Student's two-tailed t-test (* = $p<0.05$, ** = $p<0.001$, *** = $p<0.0001$). (Experiments were conducted with the help of Irem Polat).

To answer this, I strategized to pulldown Clb2 along with Cdc6 in a co-immunoprecipitation experiment using wild type cells and cells lacking *MCK1*. As expected, higher levels of Cdc6 in the total cell extracts (TCE) of *mck1Δ* cells were observed, which prompted more Cdc6 immunoprecipitation as compared to the wild type (Figure. 3-19A, B). Clb2 levels remained comparable in TCEs of both the strains, however, more Clb2 molecules were immunoprecipitated with Cdc6 upon deletion of *MCK1* (Figure. 3-19A, B). Overall, when I compared the Clb2:Cdc6 complex formation, the proportion of Cdc6 and Clb2 association remained similar

(Figure. 3-19B). This supports the conclusion that a higher fraction of Clb2 associates with Cdc6 in cells depleted for Mck1.

3.8.3 Lower Clb2 levels are not sufficient to inhibit SPOC

Based on the above data, we can conclude that deletion of *MCK1* causes SPOC deficiency in cells with misaligned spindles and leads to accumulation of Cdc6 in miotic cells which binds to more Clb2. If more Clb2 binds to Cdc6, this may quench the amount of Clb2 available to associate with Cdc28 to form mitotic cyclin-dependent kinase (M-Cdk). To this end, I asked if lowering Clb2 levels in cells could cause SPOC deficiency. As Clb2 is an essential gene, diploid budding yeast was used to create a heterozygotic deletion for Clb2 (*clb2*$^{+/-}$). These heterozygotes demonstrated a 40% reduction of Clb2 levels than wild type diploid cells when visualised on an immunoblot (Figure. 3-20A, B).

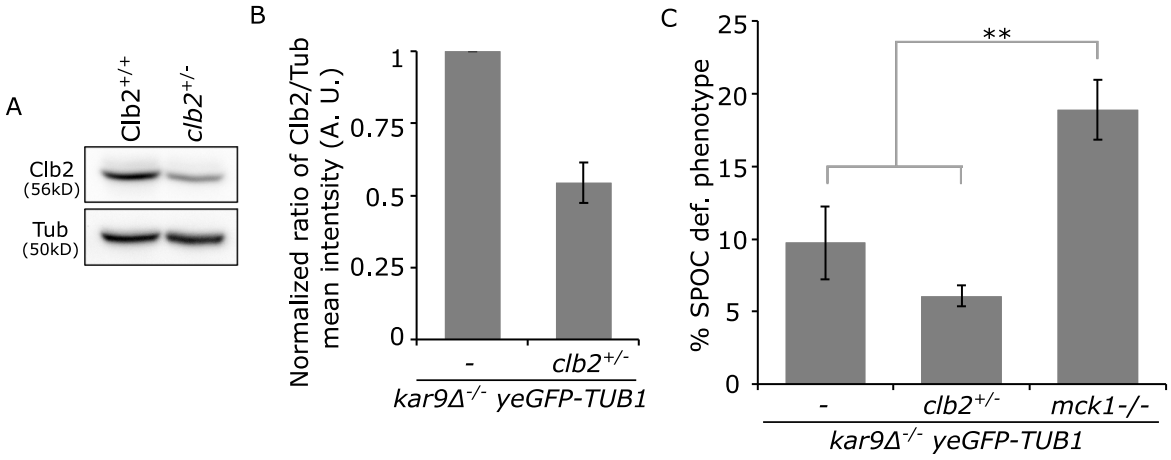

Figure. 3-20. Lower Clb2 levels do not have an effect on SPOC regulation. A) Immunoblot showing Clb2 levels in indicated strains. Tubulin served as loading control. B) Graphical representation of Clb2 signal intensities from three independent experiments in A. C) Graph represents the average percentage of SPOC deficient cells in indicated strains from three independent experiments. 100 anaphase cells were counted per strain and the error bars show standard deviation between the three experiments. Asterisks show significant difference as measured by Student's two-tailed t-test (* = p<0.05, ** = p<0.001, *** = p<0.0001). (Experiments were conducted with the help of Irem Polat).

Next, a SPOC assay using *kar9*$^{-/-}$ *yeGFP-TUB1* diploid cells was conducted. In this background, homozygotic deletion for *MCK1* (*mck1*$^{-/-}$) served as a control for SPOC

deficiency, and heterozygotic deletion for *CLB2* (*clb2*$^{+/-}$) was made, as *CLB2* is an essential gene. *mck1*$^{-/-}$ *kar9*$^{-/-}$ cultures showed nearly 20% SPOC deficient cells whereas, clb2$^{+/-}$ *kar9*$^{-/-}$ and *kar9*$^{-/-}$ cultures could maintain the SPOC arrest (Figure. 3-20C). This could imply that just depletion of Clb2 levels isn't sufficient to regulate SPOC. However, in this case, we cannot be certain of the fraction of Clb2 that is actively bound to Cdc28. It may be that these cells compensate for the lower levels of Clb2 for some other unknown reasons and can still attain adequate M-Cdk activity. Further experiments need to be done in this context to check for the M-Cdk activity in the cells with lower Clb2 levels.

3.8.4 Overexpression of *CDC6* phenocopies characteristics of *mck1Δ* cells

I next asked if the characteristics displayed by *mck1Δ* cells are a mere effect of elevated Cdc6 levels. To investigate this, I used a 2μ plasmid (pRS425-*CDC6*) carrying a Leucine selection marker to achieve moderate overexpression of *CDC6*. Unlike deletion of *MCK1*, I observe that overproduced Cdc6 could not rescue the lethality of *KIN4* or *BFA1* overexpression (Figure. 3-21A, B). However, similar to *mck1Δ* cells, 2μ-*CDC6* could rescue to growth lethal phenotype of *lte1Δ spo12Δ* cells (Figure. 3-21C) and temperature dependent lethality of MEN ts mutants (Figure. 3-21D; marked in red boxes).

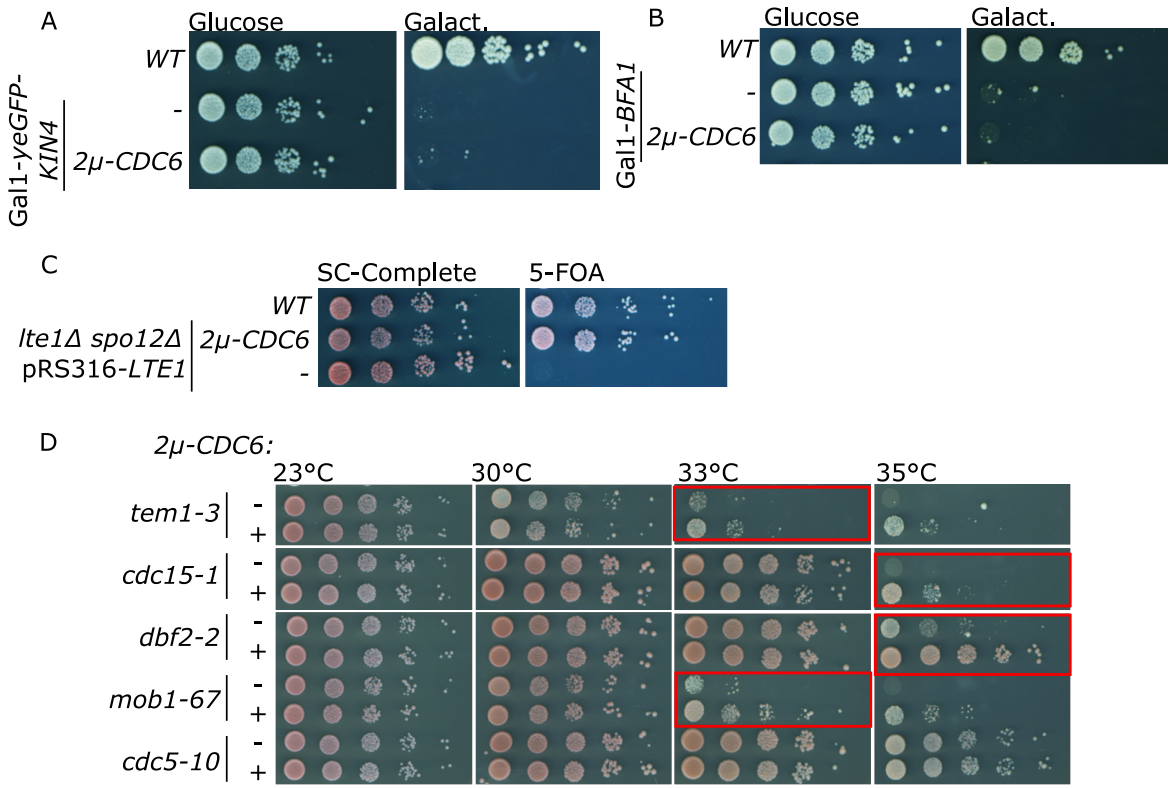

Figure. 3-21. Moderate overexpression of CDC6 rescues some mitotic exit mutants. (A, B) Serial dilutions of indicated strains on Galactose containing Gal1-*KIN4* (A) or Gal1-*BFA1* (B) inducing (Galact.) or repressing (Glucose) plates. (C) Growth analysis by serial dilutions of indicated strains in the presence (SC-Complete) or absence (5-FOA) of pRS316-*LTE1*. D) Growth analysis by serial dilutions of MEN ts mutants with or without 2μ-*CDC6* at indicated temperatures. Red boxes mark the reversal of growth lethality upon moderate overexpression of *CDC6*.

As mentioned earlier, Cdc6 is reported to bind Clb2 via its N terminal LxF motif (Mimura *et al.*, 2004; Örd *et al.*, 2019). I sought to see if the activation of mitotic exit in the MEN ts mutants was dependent on the interaction of Cdc6 with Clb2. To achieve this, I created an N terminal deletion in *CDC6*, to get a *cdc6*$^{N\Delta}$ construct (Figure. 3-22A), lacking 2-49 amino acids from its coding region. *cdc6*$^{N\Delta}$ construct has been reported to show abrogated binding with Clb2 in mitotic cells (Elsasser *et al.*, 1996; Archambault *et al.*, 2003). Indeed, expression of 2μ-*cdc6*$^{N\Delta}$ in the *tem1-3* ts mutants failed to rescue the growth lethality that expression of 2μ-*CDC6* could cause (Figure. 3-22B).

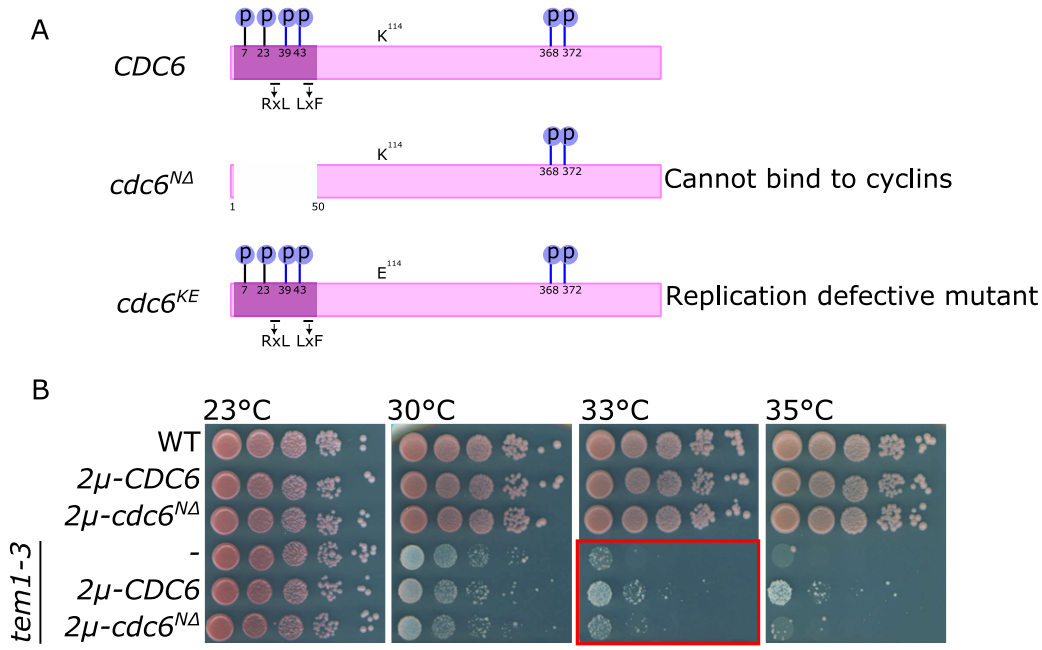

Figure. 3-22. N terminal of Cdc6 is crucial to activate mitotic exit in MEN ts mutants. A) Domain architecture of Cdc6 constructs used in this study. B) Serial dilutions of wild-type or *tem1-3* strains carrying 2μ-*CDC6,* 2μ-*cdc6* ^{NΔ} or empty *LEU2-based* 2μ plasmid at specified temperatures. Red boxes mark the reversal of growth lethality upon moderate overexpression of *CDC6*.

cdc6^{NΔ} had been reported to support growth with similar kinetics as *CDC6* in the absence of endogenous Cdc6 (Elsasser *et al.*, 1996). Therefore, I checked the functionality and expression levels of these constructs. Unlike 2μ-*cdc6*^{KE} (K114E), a replication defective Cdc6 (Weinreich *et al.*, 1999), overproduced *CDC6* and *cdc6*^{NΔ} could rescue the lethality of cells deleted for endogenous *CDC6* (Figure. 3-22A, 3-23A). These Cdc6 constructs were tagged with 9Myc tag at the C terminal and the expression levels were examined by immunoblotting. As is evident in the immunoblots, Cdc6-9Myc levels in *mck1Δ* cells were equivalent to that produced by the 2μ-*CDC6* construct (Figure. 3-23B). As expected, Cdc6^{NΔ} was stabilised (Figure. 3-23B) due to a lack of Cdc28 phosphorylation sites in the N terminal region.

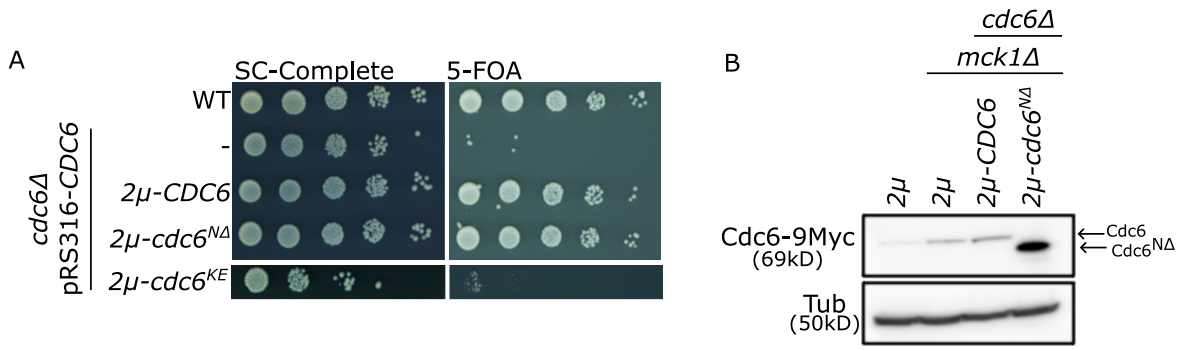

Figure. 3-23. 2μ-*CDC6* and 2μ-*cdc6*^{NΔ} can compensate for endogenous Cdc6 and achieve moderate overexpression. A) Growth analysis by serial dilutions of the indicated strains in the presence (SC-Complete) or absence (5-FOA) of pRS316-*CDC6*. B) Immunoblots representing the levels of Cdc6 as expressed by the constructs in the given strains. Tubulin served as a loading control.

3.8.5 Overexpression of *CDC6* causes SPOC deficiency via its N-terminal domain

The results from overexpression of *CDC6*, drive me to question whether the defect in SPOC of *mck1Δ* cells arises due to elevated levels of Cdc6. I observe that expression of 2μ-*CDC6* was sufficient to promote a higher percentage of SPOC deficient cells in *kar9Δ* cultures (Figure. 3-24A). Cdc6^{KE}, the replication inactive Cdc6, when overproduced also accumulated SPOC deficient cells (Figure. 3-24A). However, 2μ-*cdc6*^{NΔ} could not prompt SPOC deficiency in *kar9Δ* cells (Figure. 3-24A). This suggests that the role of Cdc6 in DNA replication and SPOC regulation/mitotic exit is independent of each other. Additionally, this result emphasises the importance of the N-terminal region of Cdc6 in promoting mitotic exit. Furthermore, I analysed if the SPOC deficiency of cells lacking Mck1 was due to the N terminal activity of the stabilised Cdc6. To this extent, I overproduced Cdc6^{NΔ} in cells lacking both, endogenous Mck1 and Cdc6. Mitotic exit inhibition and SPOC activation were achieved in the *kar9Δ mck1Δ* cultures expressing only Cdc6^{NΔ} (Figure. 3-24B). Implying that the Mck1 may promote SPOC and mitotic exit by regulating Cdc6 levels.

Furthermore, I asked if expression of the N terminal of Cdc6 could promote SPOC deficiency in *kar9Δ* cells. For this purpose, I cloned the first fifty amino acids of Cdc6

in the 2μ (pRS425) plasmid: 2μ-*N50-cdc6*. Surprisingly, I observe that overexpressing 2μ-*N50-cdc6* lead to SPOC deficiency (Figure. 3-24C). This inferred that the stabilisation of Cdc6, especially the N terminal, promotes mitotic exit.

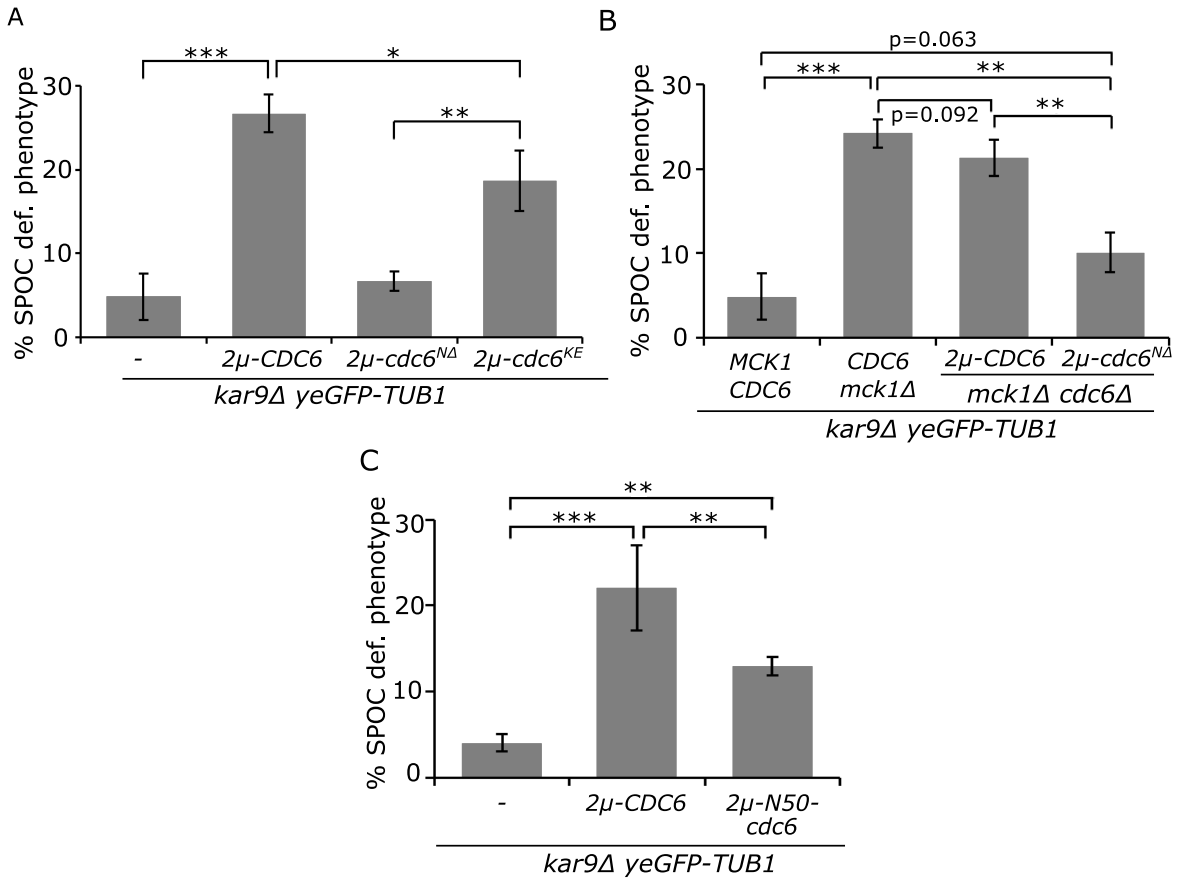

Figure. 3-24. SPOC deficiency of *mck1Δ* cells is a consequence of Cdc6 stabilisation. (A, B, C) The graphs represent an average percentage of SPOC deficient cells in indicated strains from three independent experiments. 100 anaphase cells were counted per strain and the error bars show standard deviation between the three experiments. Asterisks show significant difference as measured by Student's two-tailed t-test (* = p<0.05, ** = p<0.001, *** = p<0.0001).

Altogether, these results suggest that the N terminal of Cdc6 is critical in promoting mitotic exit and failure to degrade Cdc6 in *mck1Δ* cells promotes SPOC deficiency in these cultures. Cdc6, may therefore, be one of the key substrates of Mck1 that it targets for degradation in order to inhibit mitotic exit.

3.8.6 Failure to dephosphorylate Cdc6 by PP2A^{Cdc55} is irrelevant to SPOC

Recent studies have shown that Cdc55*,* a protein phosphatase 2A (PP2A) regulatory subunit, interacts with Cdc6 and dephosphorylates Cdc6 to release it from the M-Cdk complex (Boronat and Campbell, 2007; Philip *et al.*, 2022). They observe that cells lacking Cdc55 accumulate Cdc6 later in mitosis and therefore, show a higher association of Cdc6 with Clb2 (Philip *et al.*, 2022). As mentioned earlier, *mck1Δ* cells also stabilise Cdc6 and pull more Clb2 molecules with it (Figure. 3-19A). Therefore, to understand if I see the same in my strains and culture background, I checked the Cdc6 localisation in cells devoid of Cdc55. It is evident that similar to wild type, *cdc55Δ* cells did not show nuclear localisation of Cdc6 in metaphase/early anaphase cells (Figure. 3-25A). However, cells bearing a double deletion of *MCK1* and *CDC55* showed premature Cdc6 nuclear localisation (Figure.3-25A), suggesting that the Mck1 dependent regulation on Cdc6 occurs prior to that of Cdc55. Next, I compared the Cdc6 levels in *mck1Δ* and *cdc55Δ* cells in log phase cultures. It is notable that Cdc6 was stabilised to a greater extent upon Mck1 depletion than upon Cdc55 depletion (Figure. 3-25B). Altogether, implying that Mck1 maintains lower mitotic Cdc6 by targeting it for degradation and Cdc55 contributes to sustaining its stability later in mitosis.

Although *cdc55Δ* cells displayed lower protein levels of Cdc6 than in *mck1Δ*, the levels were still higher than in the wild type cells (Figure. 3-25B). Therefore, I questioned if this moderately high Cdc6 in cells lacking Cdc55 could affect SPOC activity. I assessed the SPOC proficiency of *kar9Δ* cells lacking Cdc55 alone or in combination with Mck1. Surprisingly, *cdc55Δ* cells could engage SPOC upon spindle misalignment whereas *cdc55Δ mck1Δ* cells were SPOC deficient (Figure. 3-25C). This suggests that the regulation of Cdc55 over Cdc6 does not affect SPOC integrity and that Mck1 mediated Cdc6 regulation sets the ground for SPOC to function.

However, raises the question of how cells coordinate the spatiotemporal regulation of Cdc6 by Cdk, Mck1 and Cdc55 to maintain SPOC arrest and stop mitotic exit.

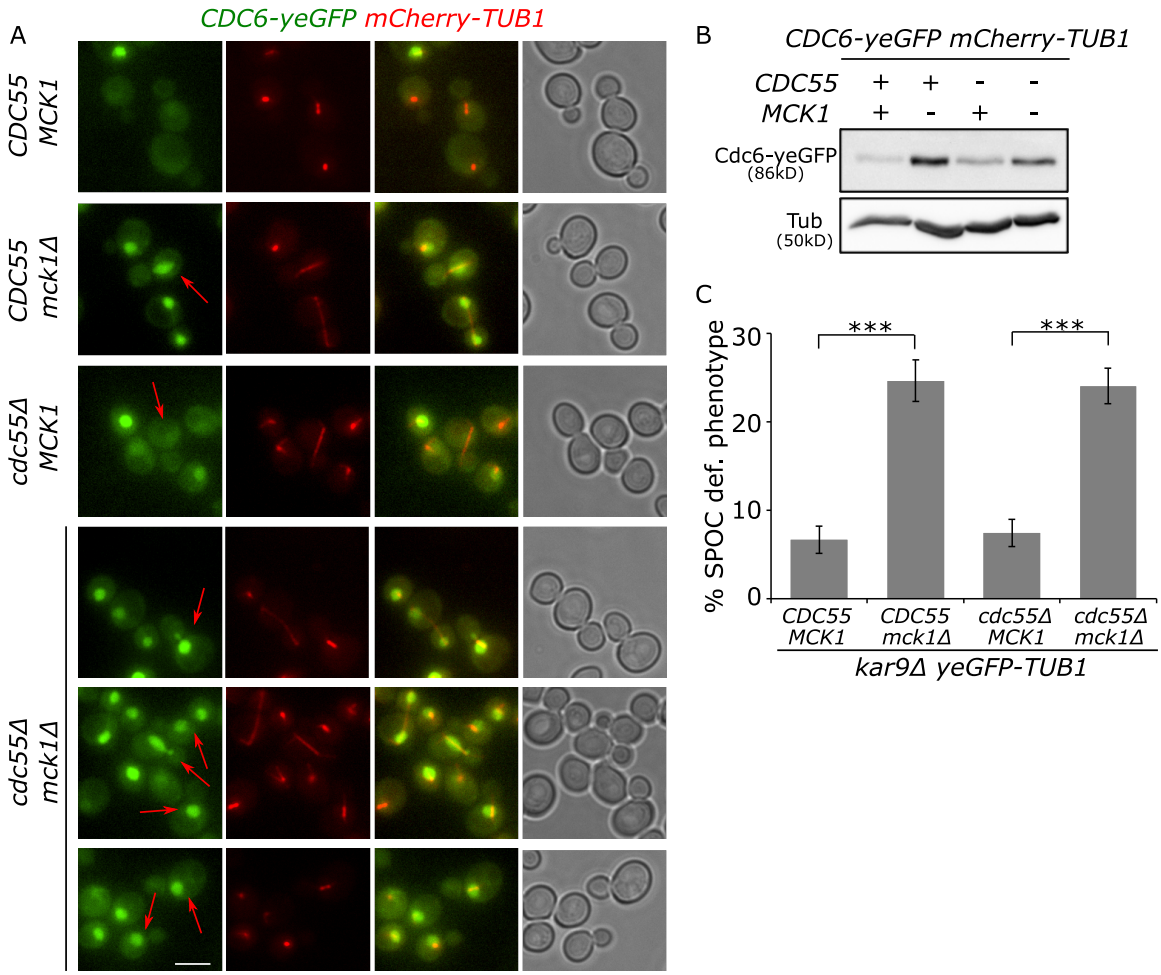

Figure. 3-25. Cdc55 mediated regulation on Cdc6 does not contribute to SPOC. A) Still images representing endogenous Cdc6 localisation in indicated strains. Wild type cells do not show nuclear Cdc6-yeGFP localisation (a,b) in metaphase or early anaphase cells, unlike in *mck1Δ* cells (c,d). Red arrows mark the mitotic cells and mCherry-Tubulin marks spindles. Scale bars- 5 µm. B) Immunoblots to visualise Cdc6-yeGFP in indicated strains. Tubulin served as a loading control. C) Graph represents the average percentage of SPOC deficient cells in indicated strains from three independent experiments. 100 anaphase cells were counted per strain and the error bars show standard deviation between the three experiments. Asterisks show significant difference as measured by Student's two-tailed t-test (* = p<0.05, ** = p<0.001, *** = p<0.0001).

3.9 Investigating the phosphorylation of key mitotic regulators in *mck1Δ* cells

3.9.1 Mck1 does not modulate Cdc5 activity

I further wanted to investigate if Mck1 modulates the phosphorylation and thereby, the activity of SPB components like Bfa1, Nud1 and Spc72. Bfa1, Nud1 and Spc71

are phosphoproteins that are Cdc5 substrates (Gruneberg *et al.*, 2000; Ho *et al.*, 2002; D'Aquino *et al.*, 2005; Maekawa *et al.*, 2007, 2017; Snead *et al.*, 2007).

From earlier data, we know that Mck1 does not affect the Cdc5-dependent phosphorylation of Bfa1 (Figure. 3-7A). Recently, Bfa1 has also been reported to be phosphorylated by Cdc28 in late mitosis (Caydasi *et al.*, 2017). I aimed to see if Mck1 could regulate the phosphorylation of Bfa1 in late mitosis. *cdc14-2* cells were arrested in late mitosis following release from G_1 phase at 37°C. Bfa1 migrated as a single hypo-phosphorylated band (marked as Bfa1) until 80 minutes after the release and we see that slower migrating forms of Bfa1 became abundant later after 120-160 minutes (Figure. 3-26A; marked as Bfa1-p) (Caydasi *et al.*, 2017). *mck1Δ* cells also showed a similar phosphorylation profile of Bfa1 indicating that Mck1 does not regulate mitotic exit by modulating Bfa1 phosphorylation.

I aimed to confirm if the phosphorylation of Bfa1 was directly abrogated by *MCK1* deletion in the absence of its Cdc28 dependent phosphorylation. To this end, I used a strain carrying an analog-sensitive Cdc8 allele, *cdc28-as*, which aids conditional inhibition of Cdc28 activity in the presence of 1NM-PP1, its inhibitor (Bishop *et al.*, 2000). It is notable that upon 1NM-PP1 treatment, the slow migrating forms of Bfa1 (Figure. 3-26B; marked by red asterisks) disappeared significantly and the Bfa1 protein profile as visualised on immunoblots remained comparable in cells with or without Mck1 (Figure. 3-26B).

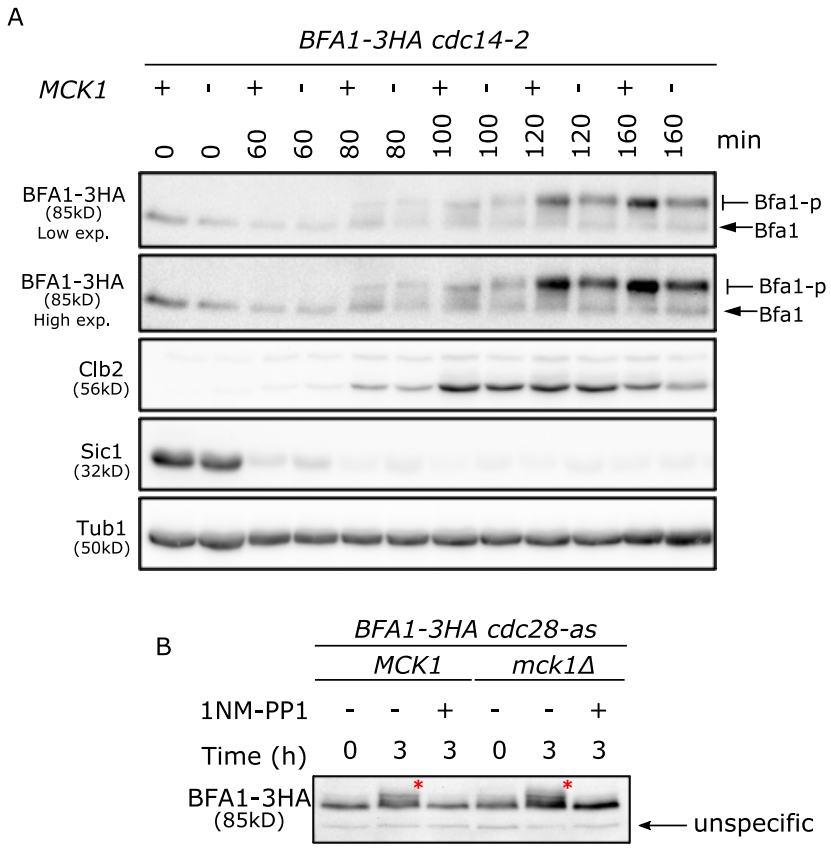

Figure. 3-26. Bfa1 phosphorylation status remains unperturbed in cells deleted for *MCK1*. A) Cultures were arrested in G_1 phase by alpha-factor synchronisation at 23°C and released in fresh medium at 37°C. Samples were collected at indicated time points to be analysed by western blotting. The immunoblots represent phosphorylation of Bfa1, slower migrating forms are labelled as Bfa1-p. Clb2 and Sic1 serve as markers for cell cycle progression and Tub is a loading control. B) Indicated strains were arrested in G_1 phase by alpha-factor synchronisation and released in fresh medium containing DMSO or 1NM-PP1. Samples were collected at indicated time points for immunoblotting analysis. Red asterisks mark the slow migrating forms of Bfa1.

Nud1 and Spc72 are two critical SPB components that are phosphorylated by Cdc5 irrespective of the mitotic spindle orientation (Maekawa *et al.*, 2007). Nud1 serves as a scaffold for the MEN components to govern MEN activation (Rock *et al.*, 2013) whereas, Spc72 recruits Kin4 at the SPBs upon spindle misalignment (Maekawa *et al.*, 2007). Perturbation to the activity of both can lead to defective MEN signalling. A recent study showed that a hyperactive Nud1 mutant, *nud1-A308T*, could rescue the growth lethality of *BFA1* overexpression (Vannini *et al.*, 2022), similar to what I observed upon *MCK1* deletion (Figure. 3-13A-a). Therefore, it becomes important to

examine the Nud1 phosphorylation in cells lacking Mck1. Finally, I set out to examine the phosphorylation of Nud1 and Spc72 in cells lacking Mck1. In wild type cells, Nud1 and Spc72 became phosphorylated as soon as cells enter mitosis (Figure. 3-27A; marked by Nud1-p and Spc72-p) (Maekawa *et al.*, 2007). A similar phosphorylation trend was observed in cells lacking Mck1 (Figure. 3-27A). When the lysates of wild type and *mck1Δ* cells were loaded side by side the phosphorylation status of Nud1 and Spc72 appeared comparable (Figure. 3-27B). Hence, Mck1 does not inhibit mitotic exit by modulating Nud1, Bfa1 or Spc72.

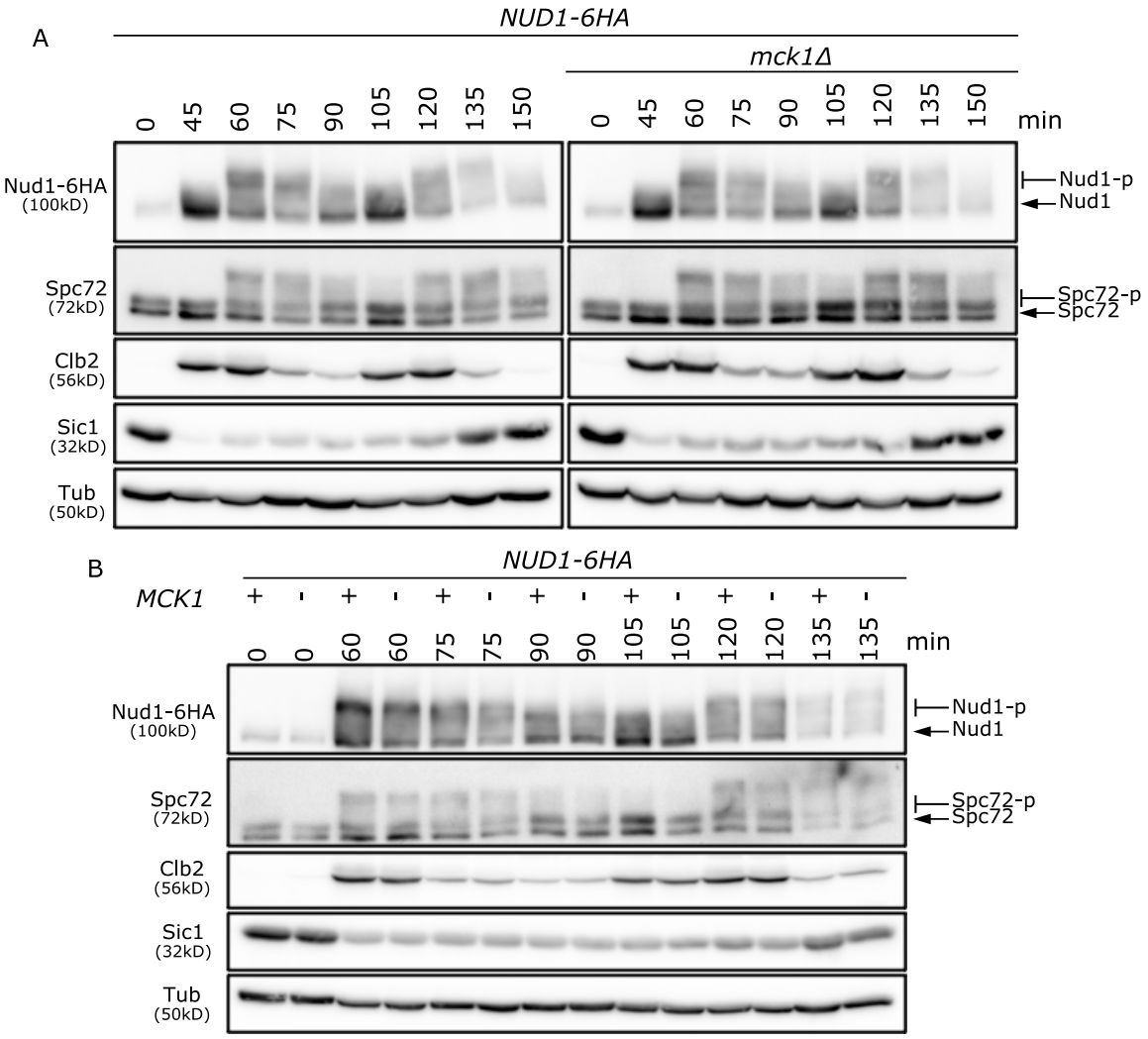

Figure. 3-27. Phosphorylation profile of SPB components, Nud1 and Spc72 remains unaltered in *mck1Δ* cells. A) Cultures were arrested in G_1 phase by alpha-factor synchronisation and released in fresh medium. Samples were collected at indicated time points to be analysed by western blotting. The immunoblots represent phosphorylation of Nud1 and Spc72, slower migrating forms are labelled as Nud1-p and Spc72-p. Clb2 and Sic1 serve as markers for cell cycle progression and Tub is a

loading control. B) Samples from experiment in A were run on an SDS-PAGE side by side for better comparison.

3.9.2 *mck1Δ* cells exhibit lower Clb2-Cdc28 but not Clb5-Cdc28 activity

From all the above data, it becomes evident that *mck1Δ* cells enter mitosis with higher levels of Cdc6 and these Cdc6 molecules associate with more Clb2. Studies have shown that the N terminal of Cdc6 is sufficient to interact with Clb2 which thereby, inhibits the Clb2-Cdc28 complex (mitotic cyclin dependent kinase (M-Cdk)) activity (Elsasser *et al.*, 1996). This may also imply that *mck1Δ* cells enter mitosis with lower Clb2-Cdc28 activity. To assess the consequence of M-Cdk activity, I decided to look at the phosphorylation status of its downstream substrates using protein mobility shifts on SDS-PAGE.

Mob1 is one such substrate of Cdc28 that is phosphorylated before cells enter anaphase and is dephosphorylated by Cdc14 as soon as cells commit to mitotic exit (König *et al.*, 2010). In the absence of Cdc14 in *cdc14-2* temperature-sensitive strain, at non-permissive temperatures (37°C), it also shows that Mob1 remains hyperphosphorylated (König *et al.*, 2010). I used this background to understand the Mob1 phosphorylation profile in *mck1Δ* cells. The cells were arrested in G_1 by alpha-factor synchronisation at 23°C and released into fresh medium at 37°C (non-permissive temperature). It can be observed that Mob1 migrates as a single band until 20 mins after the release. As cells start budding, Clb2 accumulates and the higher bands corresponding to Mob1 hyperphosphorylation (marked as Mob1-p) begin to appear in wild-type cells (Figure. 3-28A) (König *et al.*, 2010). On the contrary, in *mck1Δ* cells, the Mob1 bands seem to be dominant as compared to the hyper-phosphorylated, slow migrating Mob1 bands (Figure. 3-28A). The difference between phosphorylation of Mob1 in cells with or without Mck1 becomes evident when samples were run next to each other (Figure. 3-28B). This indicates that upon

MCK1 deletion, cells cannot adequately phosphorylate Mob1 before entering mitosis. This may be a consequence of lower Clb2-Cdc28 activity and not due to the possibility of early dephosphorylation by Cdc14, as these cells lack Cdc14 activity at 37°C.

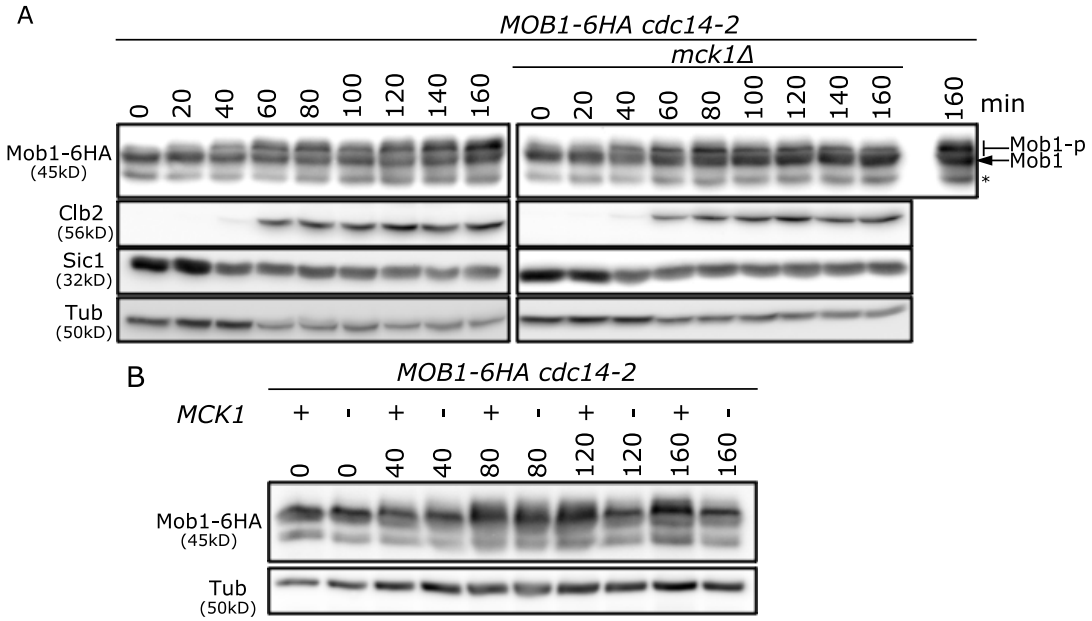

Figure. 3-28. Mob1 cannot be adequately phosphorylated in cells lacking Mck1. A) Cells were arrested in G_1 phase by alpha-factor synchronisation at 23°C and released in fresh medium at 37°C. Samples were collected at indicated time points to be analysed by western blotting. The immunoblots represent phosphorylation of Mob1, slower migrating forms are labelled as Mob1-p. Asterisk represents a non-specific band. Clb2 and Sic1 serve as markers for cell cycle progression and Tub is a loading control. B) Samples from A were run side by side.

Next, I decided to examine the phosphorylation status of Orc6, a component of the pre-RC, which is a substrate of Clb5-Cdc28 (Nguyen *et al.*, 2001; Henneke *et al.*, 2003; Ubersax *et al.*, 2003; Wilmes *et al.*, 2004). As Orc6 is also dephosphorylated by Cdc14 (Bloom and Cross, 2007b), I used the *cdc14-2* background to assess the phosphorylation status of Orc6 in cells depleted for Mck1. Orc6 migrated as a single band at 0 min until the cells start budding and Sic1 levels started dropping. At 40 minutes two bands corresponding to phosphorylated and unphosphorylated Orc6 were visible on the immunoblots (Figure. 3-29). As soon as the cells entered

metaphase and Clb2 accumulated (>40minutes), Orc6 migrated as a single slowly migrating band (Figure. 3-28; marked as Orc6-p). This was comparable between wild type and *mck1Δ* cells, suggesting that appropriate Orc6 phosphorylation could be achieved suitably in *mck1Δ* cells.

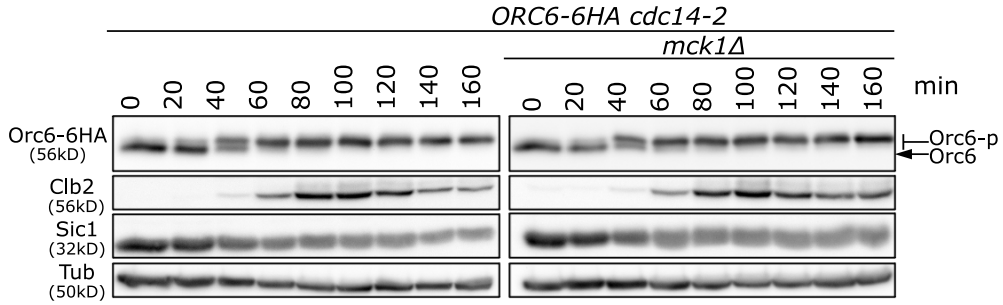

Figure. 3-29. Orc6 phosphorylation is not altered in *mck1Δ* cells. Cells were arrested in G_1 phase by alpha-factor synchronisation at 23°C and released in fresh medium at 37°C. Samples were collected at indicated time points to be analysed by western blotting. The immunoblots represent phosphorylation of Orc6, slower migrating forms are labelled as Orc6-p. Clb2 and Sic1 serve as markers for cell cycle progression and Tub is a loading control.

Together, this implies that cells deleted for *MCK1* are not compromised for Clb5-Cdc28 activity but may have slightly lower Clb2-Cdc28 activity. Further experiments using kinase assays, phospho-specific antibodies and more sensitive methods must be used to validate this conclusion.

3.10 Mck1 and its putative substrates

There may still be substrates of Mck1, other than Cdc6, that contribute to its role in inhibiting mitotic exit. To elucidate potential Mck1 substrates, I used different strategies along with Irem Polat, a Master's thesis student in the laboratory. Approaches like yeast-two hybrid analysis, Ubiquitin-based Split-protein sensor (USPS) (with Prof. Dr. Nils Johnson, University of Ülm), affinity-based mass spectrometry and tandem-fluorescent protein timer (tFT) based genome wide screening (with Prof. Dr. Michael Knop at the ZMBH, University of Heidelberg) were used*. The results from these analyses have been previously mentioned in her

Master's dissertation (which can be found in the heiDock repository of the University of Heidelberg (2021)).

3.10.1 Lte1 localises to bud neck in *mck1Δ* cells

I aimed to validate the results from the tFT screening, which gave us a list of proteins that were stabilised upon the deletion of *MCK1*. To do so, I, along with a student tagged the putative gene targets with yeGFP and looked at their protein localisation and levels via fluorescence microscopy and immunoblotting, respectively. Lte1 stood on top of that list of plausible Mck1 substrates.

Lte1 is a bud cortex localising protein, that inhibits Kin4 from binding the dSPB in the daughter compartment (Shirayama *et al.*, 1994a; Bardin *et al.*, 2000; Pereira *et al.*, 2000; Bertazzi *et al.*, 2011; Falk *et al.*, 2016) thereby, activating mitotic exit. Bud cortex localisation of Lte1 requires Cdc42 activity and phosphorylation by S/M-Cdk and dephosphorylation by Cdc14 renders its release from the cortex (Jensen *et al.*, 2002). Septins in yeast (Cdc12) have been shown to restrict Lte1 in the budding compartment (Jensen *et al.*, 2002). I looked at the localisation of Lte1 hoping to see higher levels of the protein in *mck1Δ* cells. In wild type cells, Lte1 localised to the emerging bud and the bud cortex until the disassembly of the mitotic spindle (Bardin *et al.*, 2000; Pereira *et al.*, 2000). Once the cell disassembled the mitotic spindle, Lte1 is diffused in both the mother and the daughter compartment (Bardin *et al.*, 2000) (Figure. 3-29A; marked by red arrows). Upon deleting *MCK1*, I observed that the bud specific localisation of Lte1 was retained, whereas, the cells did not exhibit any appreciable higher levels of Lte1 as compared to the wildtype (Figure. 3-29A). However, I observe that after spindle disassembly, when Lte1's asymmetric localisation is lost, it accumulated at the bud neck in *mck1Δ* cells (Figure. 3-30A).

Bud neck localisation of Lte1 has not been reported yet and therefore, is an interesting aspect to elucidate later.

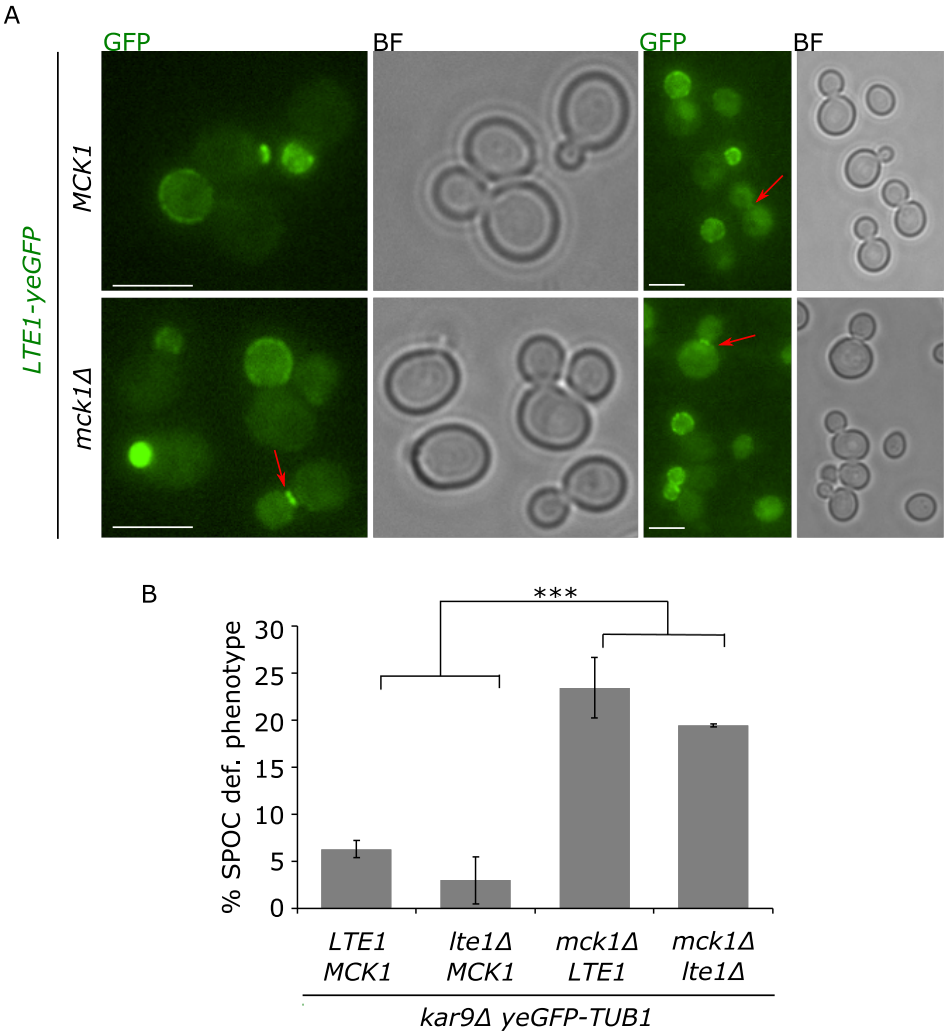

Figure. 3-30. Mck1 alters Lte1 localisation post spindle disassembly. A) Representative still images of Lte1-yeGFP localisation in cells with or without Mck1. Red arrows mark cells with Lte1 localisation diffused in both mother and daughter compartments. Scale bars- 5 µm; Images on the left are 2x magnified than ones in the right, for better visualisation and comparison. B) Graph represents the average percentage of SPOC deficient cells in indicated strains from three independent experiments. 100 anaphase cells were counted per strain and the error bars show standard deviation between the three experiments. Asterisks show significant difference as measured by Student's two-tailed t-test (* = p<0.05, ** = p<0.001, *** = p<0.0001).

I questioned if this aberrant localisation of Lte1 was a cause of mitotic exit in *mck1Δ* cells with misaligned spindles. Therefore, I conducted a SPOC assay and observed that *kar9Δ mck1Δ lte1Δ* cultures were as SPOC deficient as *kar9Δ mck1Δ* cells (Figure. 3-30B). This implies that the regulation of Mck1 on Lte1 localisation may not

be of importance in the context of SPOC. However, the bud neck localisation of Lte1 may contribute to other phenotypes of *mck1Δ* cells.

Further experiments need to be done in order to investigate the role of Mck1 in Lte1 regulation and cell polarisation, in general. Another possibility is that Mck1 could regulate the septin ring components that Lte1 binds to at the bud neck. Lte1 is also phosphorylated by Cla4 and Clb-Cdc28 (Höfken and Schiebel, 2002; Seshan *et al.*, 2002; Geymonat *et al.*, 2010). It would be of importance to observe the phosphorylation of Lte1 in cells lacking Mck1 as the cell cycle progresses. This could especially be of importance as *MCK1* deletion can rescue the cold sensitivity of *lte1Δ* cells.

4. Discussion

SPOC ensures proper alignment of the mitotic spindle along the mother-daughter polarity axis before cells decide to undergo mitotic exit (Adames and Cooper, 2000; Pereira *et al.*, 2000; Wang *et al.*, 2000; Caydasi and Pereira, 2012). The classical Kin4-dependent pathway activates the Bfa1-Bub2 GAP complex which inhibits cells with misaligned spindles from exiting mitosis (Geymonat *et al.*, 2002; D'Aquino *et al.*, 2005; Pereira and Schiebel, 2005). Although this pathway is extensively studied, recent studies have pointed toward mechanisms independent of Kin4 that can regulate SPOC (Falk *et al.*, 2016; Caydasi *et al.*, 2017; Kocakaplan *et al.*, 2021). My work has helped elucidate one such key SPOC component, Mck1, that controls SPOC and mitotic exit, exclusively of Kin4. Mck1 essentially sets a foreground for SPOC to function by keeping Cdc6 levels low as cells enter mitosis.

4.1 A new function of Mck1 in prompting SPOC by blocking MEN

Mck1 is one of the four GSK-3 kinase homologs in budding yeast. It was identified as a key meiotic and centromere regulatory kinase that activates early meiotic gene expression (Neigeborn and Mitchell, 1991; Shero and Hieter, 1991). Mck1 performs functions like sporulation, Protein kinase A (PKA) pathway and stress signalling redundantly with some of its homologs (Andoh *et al.*, 2000; Rayner *et al.*, 2002). However, here I concentrated on investigating the function of Mck1 in the mitotic checkpoint, SPOC.

Mck1 was recognised in a genome-wide screen as one of the key suppressors of mitotic exit in cells overexpressing *KIN4* (Caydasi *et al.*, 2010). I confirmed this and show that indeed the lethality caused by overproduced Kin4 is reversed upon *MCK1* deletion. *ELM1*, *RTS1*, *BMH1* and *SWR1*, were a few of the other genes besides *MCK1* that were found in this screen and were later implicated in SPOC regulation

(Caydasi *et al.*, 2010, 2014a, 2020). I, therefore, set out to examine if Mck1 could also monitor SPOC in budding yeast.

Based on the results mentioned in section 3.1, I conclude that Mck1 is essential to halt mitotic arrest in cells with misaligned spindles. I also examined if this SPOC function of Mck1 was shared with any of the other three GSK-3 homologs. Surprisingly, the role of Mck1 in engaging SPOC appears to be uniquely performed by it. Additionally, the protein levels of Mck1 remain unaltered throughout the cell cycle, suggesting that its function is not transcriptionally regulated. Like Kin4 and Bfa1, cells lacking Mck1 fail to sense the spindle misorientation and without prolonging the anaphase duration cause spindle disassembly leading to exit from mitosis (Results- 3.1). Opposite to what was predicted earlier (Drechsler *et al.*, 2015), I do not observe mispositioning of spindles when cells are devoid of Mck1 alone.

Here, I also show that Mck1 does not contribute to SPOC by modulating Kin4 localisation or activity *in vivo*. It also does not affect the phosphorylation of Bfa1 mediated by Kin4 or Cdc5 (Results- 3.2). These results suggested a role of Mck1 downstream of Bfa1. Hence, next, I investigated the localisation of MEN components in *mck1Δ* cells with mis-oriented anaphase spindles. Indeed, cells lacking Mck1 activate MEN as they accumulate Mob1 at the SPBs and cause a full release of Cdc14 upon spindle misalignment (Results- 3.3).

Furthermore, my data insists that Mck1 inhibits mitotic exit regardless of the spindle orientation, in cells with compromised mitotic exit. *MCK1* deletion could revert the synthetic lethality of the MEN temperature sensitive mutants and mitotic exit defects of cells overexpressing *BFA1* or cold sensitivity of cells devoid of Lte1 (Results- 3.5). Mck1 also requires FEAR to execute mitotic exit in these mutants (Results. 3-6). As reported earlier (McQueen *et al.*, 2012), at 23°C I observe that *mck1Δ* cells show a 15-minute delay in cycle progression. Nevertheless, Mck1 does not seem to have

any effect on normal cell cycle progression in cells with correctly aligned spindles at 30°C, which is a permissible temperature used for most of the experiments. An alternative explanation for this could be the existence of other pathways like FEAR, MEN and other polarity factors that cooperate in achieving successful mitotic exit (Höfken and Schiebel, 2002; Nelson and Cooper, 2007; Rock and Amon, 2009; Caydasi and Pereira, 2012; Scarfone and Piatti, 2015).

Taken together, my data identified a new role of Mck1 in activating spindle position checkpoint and inhibiting mitotic exit by blocking MEN. It still remains elusive if Mck1 cooperates with other mitotic exit inhibitors and/or directly blocks the MEN by interacting with its constituent components.

4.2 Mck1 inhibits FEAR-dependent MEN activation parallel to Kin4

Recent studies have claimed the existence of mechanisms working in parallel and independent of Kin4 to promote SPOC. As my work deciphers Mck1 as a novel SPOC component, I further questioned if Mck1 follows the conventional Kin4 based SPOC pathway or works unrelatedly of it.

Based on the results obtained, I detected some similarities between *kin4Δ* and *mck1Δ* cells. For example, deletion of both did not alter the anaphase duration upon spindle misalignment and also kept the SAC intact. Additionally, it became evident that similar to Kin4, Mck1 also becomes indispensable for SPOC in the absence of FEAR (Results- 3.4). This suggested a role of Mck1 in the Kin4 branch of SPOC, however, some other evidence proposed the contrary. Essentially, Mck1 does not modulate Kin4 activity and Bfa1 phosphorylation upon SPOC activation. Distinct from Mck1, Kin4 could not rescue the growth lethal phenotype of MEN temperature sensitive mutants, suggesting that Mck1 might be a more stringent inhibitor of MEN than Kin4. Furthermore, deletion of both *MCK1* and *KIN4* in FEARless cells leads to

SPOC deficiency (Results- 3.7), reinforcing the idea that the presence of either Kin4 or Mck1 is a must in *FEARΔ* cells to hold SPOC arrest. This evidence implies that Mck1 and Kin4 work independently to inhibit FEAR-dependent MEN activation and foster SPOC activity.

4.3 Cdc6 promotes mitotic exit via its N-terminal domain

The GSK-3 kinases are known to phosphorylate their substrates and target them for proteasomal degradation (Fiol *et al.*, 1987). As it became clearer that Mck1 kinase activity is essential for its SPOC function, I next aimed to decipher the substrates via which this function of Mck1 is executed. Amongst the known substrates of Mck1, Cdc6 has been implied in monitoring mitotic exit and therefore, became an interesting candidate to study.

Cdc6 is phosphorylated by S-Cdk and Mck1 which creates phospho-degrons targeting it for SCF^{Cdc4} mediated degradation (Drury *et al.*, 1997, 2000; Sánchez *et al.*, 1999; Mimura *et al.*, 2004; Ikui *et al.*, 2012; Al-Zain *et al.*, 2015). In accordance with previous studies (Ikui *et al.*, 2012; Al-Zain *et al.*, 2015), I observe higher levels of mitotic Cdc6 in cells lacking Mck1. Cdc6 binds to Clb2 via its N-terminal domain and this domain is crucial in promoting mitotic exit (Elsasser *et al.*, 1996; Calzada *et al.*, 2001; Örd *et al.*, 2019). My data also shows that Cdc6 abundance in mitosis seizes more Clb2 molecules in cells lacking Mck1 than in a wild type scenario (Results- 3.8). My results indicate that the regulation of Mck1 over Cdc6 in mitosis is crucial for cells to be able to engage SPOC and prohibit mitotic exit. Cells that overproduce Cdc6 early in mitosis, exhibit SPOC deficiency and mimic several phenotypes of *mck1Δ* cells. Of importance is that the DNA replication function of Cdc6 is performed mutually exclusively of its role in SPOC and mitotic exit. Surprisingly, SPOC deficiency of *mck1Δ* cells that overproduce the truncated version of Cdc6 lacking N

terminal region, *cdc6*$^{N\Delta}$ was reverted (Results- 3.8). Therefore, it is safe to conclude that Cdc6 contributes to SPOC and mitotic exit regulation via its N-terminal domain.

As the N-terminal domain of Cdc6 interacts with Clb2 and inhibits M-Cdk activity (Elsasser *et al.*, 1996; Calzada *et al.*, 2001; Archambault *et al.*, 2003), I proposed that cells devoid of Mck1 enter mitosis with higher Cdc6 and in turn lower M-Cdk activity. Indeed, in late anaphase, the hyperphosphorylation of Mob1, an M-Cdk substrate, is detected to a lesser extent in *mck1Δ* as compared to the wild type cells. But there is no detectable dissimilarity in the phosphorylation status of Orc6, an S-Cdk substrate (Results- 3.9). Altogether this supports the notion that cells deleted for *MCK1* may have lower M-Cdk activity, which leads to failure of SPOC and drives them out of mitosis.

Nevertheless, it still needs to be confirmed if Cdc6 could regulate mitosis via modulation of targets other than M-Cdk complexes.

4.4 Mck1 sets a stage for SPOC to function by keeping low Cdc6 in mitosis

Based on the aforementioned results and conclusions, I envision a model for SPOC and mitotic exit regulation through the Mck1-Cdc6 pathway (Figure. 4).

The model illustrates how Cdc6 protein levels are kept low throughout mitosis, via its proteasomal degradation at the G1/ S transition by S-Cdk and early in mitosis by Mck1 (Drury *et al.*, 1997; Ikui *et al.*, 2012). It is transcribed again in late mitosis, where it binds to Clb2 via its N-terminal domain and inhibits the M-Cdk activity (Elsasser *et al.*, 1996; McInerny *et al.*, 1997; Calzada *et al.*, 2001; Archambault *et al.*, 2003; Al-Zain *et al.*, 2015). In cells with misaligned spindles, under wild type conditions, the Kin4 branch of SPOC along with Mck1 inhibit the FEAR mediated MEN activation. The data also predicts a direct MEN inhibitory function for Mck1 (depicted by '?' in Figure. 4), although further evidence is needed to validate this

argument. Together, these regulations cause the arrest of cells in late anaphase upon spindle misorientation.

Contrarily, cells lacking Mck1 fail to degrade Cdc6 and its protein levels remain abundant throughout the cell cycle. Based on the results, I hypothesise a model where stabilised Cdc6 associates with more Clb2 moieties in mitosis. This association inhibits the Clb2-Cdk complex activity (M-Cdk) (Calzada *et al.*, 2001). Implying that abundant Cdc6 caters to lower M-Cdk activity as cells enter the M phase. Therefore, *mck1Δ* cells bear more Cdc6 and low M-Cdk activity as they commit to mitosis. Upon spindle misalignment, even though the Kin4 branch of SPOC is active, *mck1Δ* cells fail to engage SPOC and activate MEN to support the exit of cells from mitosis. Hence, Mck1 may be a more persuasive MEN inhibitor than Kin4. My conclusions support the earlier indications of the role of Cdc6 in mitotic exit and therefore, further explorations are needed into what targets besides M-Cdk does Cdc6 impede to regulate mitotic exit.

Additional experiments like kinase assays and antibodies derived against Cdk-dependent phosphorylation may help in improving the understanding of M-Cdk activity and phosphorylation profile of M-Cdk substrates in cells that have higher Cdc6 levels or are devoid of Mck1.

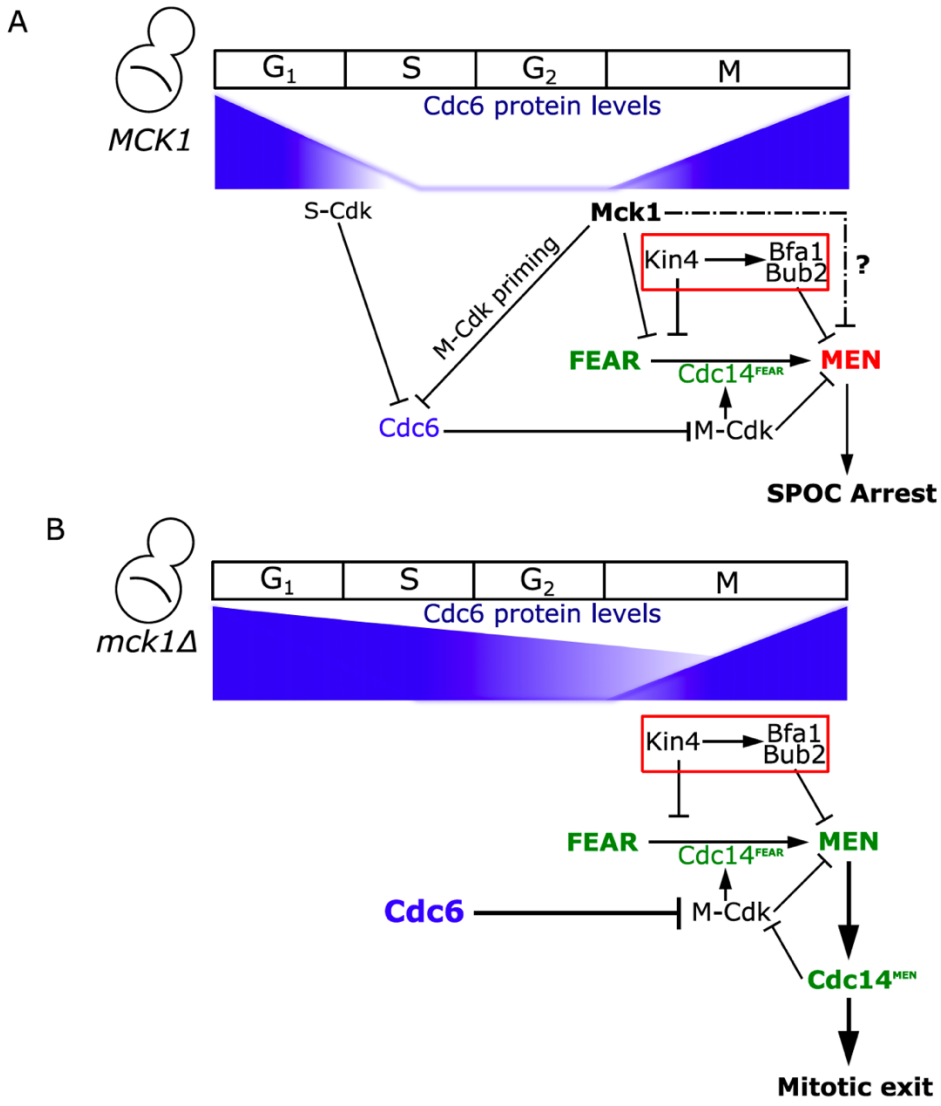

Figure. 4. Current model for Mck1-Cdc6 mediated regulation of SPOC and mitotic exit. The scheme shows Cdc6 regulation and protein levels (blue histogram) as cells progress through cell cycle. S-Cdk and Mck1 via M-Cdk priming cooperatively lead to the degradation of Cdc6 between G1 to early anaphase. In the red box is the conventional Kin4-dependent SPOC pathway. The figure also illustrates Mck1 in inhibiting mitotic exit and FEAR dependent activation of MEN, parallel to Kin4. It is a schematic representation of molecular understanding upon spindle misalignment in A) wild type or B) *mck1Δ* cells. Read text 4.4 for details.

4.5 Future perspectives

I have established Mck1 as a key spindle position checkpoint (SPOC) regulator which blocks MEN mutually exclusive of Kin4 upon spindle misorientation. This function of Mck1 is carried out primarily by sustaining Cdc6 degradation prior to mitosis.

However, other substrates of Mck1 that might contribute to its function in SPOC and mitotic exit need to be explored. Along with a master's student in the laboratory, I used several approaches to identify putative substrates of Mck1.

4.5.1 Plausible Mck1 targets

Using yeast two-hybrid assays, we found that Mck1 associates with MEN components like Tem1, Net1, Cdc14, Mob1 etc (Figure. 6-1). This is in accordance with a previous report that found Mck1 in the interaction network of Net1 and Cdc14 (Breitkreutz *et al.*, 2010). Using online software (PhosphoGRID), I was able to identify GSK-3 consensus sites in these proteins. During my work, I created Tem1 phospho-mimetic and phosphor-inhibitory at the GSK-3 sites (S5A/E and S240A/E). These were later checked for functionality but the relevance of these GSK-3 sites in Tem1 as well as other putative Mck1 substrates remains unclear.

Another approach we used to identify the proteins that were stabilised upon *MCK1* deletion, was a tandem-fluorescent protein timer (tFT) based genome-wide screen with help from Matthias Meurer from Michael Knop's lab at ZMBH, Heidelberg. Upon characterisation of the first few hits, Lte1, a bud confined protein made an interesting candidate. Comparable to wild type cells, the daughter cortex localisation of Lte1 as the bud emerges is persistent until late anaphase in *mck1Δ* cells. Surprisingly, only the cells lacking Mck1 gathered Lte1 at the bud neck post spindle disassembly (Results- 3.10). It appears that blocking Lte1 from localising to the bud neck might be one more function of Mck1, which may be of importance in cytokinesis or for cells to maintain polarity. Alternatively, Mck1 may also govern septin assembly at the bud neck that assists Lte1 localisation (Jensen *et al.*, 2002). Gic1 which is one of the Cdc42 effectors (Brown *et al.*, 1997), also interacted with Mck1 construct in our yeast two-hybrid assay (Figure. 6-2). As it is well established that Lte1 localisation requires

Cdc42 activity and Gic1 regulates mitotic exit (Jensen *et al.*, 2002; Höfken and Schiebel, 2004), Mck1 through its interaction with Gic1 may behave like a mediator for polarisation of cells thereby, modulating mitotic exit. Additional experiments need to be conducted to comprehend the consequences of these possibilities. It will also be of great importance to investigate the phosphorylation status of the putative Mck1 substrates with precise techniques and better biochemical approaches for eg. by using phospho-specific antibodies and phos-tag gels.

4.5.2 Mck1 and its involvement in several other checkpoints

Along with its newly discovered responsibility in monitoring SPOC, Mck1 has been previously reported to govern the cell wall integrity (CWI) and DNA damage checkpoint as well as the plasma-membrane stress signalling (Griffioen *et al.*, 2003; Archambault *et al.*, 2005; Kono *et al.*, 2016; Delgado and Toczyski, 2019). It has also been implicated in regulating osmotic stress stimulated Msn2/4-dependent response (Gutin *et al.*, 2019). Activation of this stress induced signalling leads to the translocation of transcription factors, Msn2/Msn4 into the nucleus (Görner *et al.*, 2002). I observe that cells lacking Kar9 did not portray any aberrancy in Msn2 and Msn4 cytosolic localisation (data not shown), implying that our SPOC background conditions do not illicit Msn2/Msn4-dependent stress response cascade. Therefore, the role of Mck1 in SPOC is independent to that of its significance in osmotic stress response.

Questions, however, arise as to how Mck1 orchestrates these surveillance mechanisms. Earlier studies and mine have looked at aspects of Mck1 under different conditions, singularly. It would be interesting to understand the default task of Mck1 by activating two or more checkpoints at the same time. The diverse pathways contributing to Mck1's varied functions may have overlapping components

and/or could be executed completely independent of each other. Therefore, further studies in this direction would deepen our interpretation of Mck1 as an essential cell cycle moderator.

4.5.3 Functional similarities of Mck1 and Cdc6 with their human orthologs

The sequence of GSK-3 kinase domain and active site is conserved from yeast to higher eukaryotes. Some of the functions identified for GSK-3 in budding yeast have been proven to be shared with the human GSK-3 (hGSK-3) orthologs. hGSK-3 is implied in maintaining microtubule dynamics and spindle morphology; GSK-3 has also been reported to establish mitotic checkpoint and abrogation of its activity induces chromosomal instability as well as mitotic exit in Hela cells (Wakefield *et al.*, 2003; Tighe *et al.*, 2007; Rashid *et al.*, 2018). More importantly, hGSK3 like Mck1 phosphorylates its targets at the GSK-3 consensus sites and marks them for subsequent ubiquitination and proteasomal degradation. An important target of the hGSK3-β is β-catenin which is stabilised upon inhibition of GSK-3 by Wnt-signalling (Aberle *et al.*, 1997; Taelman *et al.*, 2010; Stamos and Weis, 2013). In multicellular eukaryotes, Wnt-signalling is essential for early development and upholding adult tissue homeostasis (Clevers and Nusse, 2012). Moreover, recently it has been brought to light that Wnt-signalling also occurs by Wnt-mediated stabilisation of proteins (Wnt/STOP) other than β-catenin (Taelman *et al.*, 2010; Acebron *et al.*, 2014; Huang *et al.*, 2015; Stolz *et al.*, 2015; Acebron and Niehrs, 2016). Wnt/STOP is demonstrated to regulate mitosis and is crucial to preserve chromosomal integrity in human cells (Acebron *et al.*, 2014; Stolz *et al.*, 2015). Although yeast does not have Wnt-like ligands, these studies emphasise the importance of GSK-3 mediated protein degradation in moderating basic cellular processes.

Additionally, overexpression of human Cdc6 is detected in cancers of the brain and lung tissue where this overproduced Cdc6 also leads to DNA re-replication in tumour cells (Ohta, 2001; Vaziri *et al.*, 2003; Karakaidos *et al.*, 2004; Zhao *et al.*, 2021). Hence, it becomes evident that regulating Cdc6 protein levels in mammalian cells is also essential to maintain adequate cell proliferation.

Even though, in humans, Cdc6 has not been evaluated as a substrate of hGSK-3 kinases, these reports together portray similarities of functions with their orthologs in *S. cerevisiae*. Therefore, results obtained from this study may provide unique insights into how spindle dynamics, mitotic progression and integrity of diverse cellular checkpoints are governed in higher organisms.

5. Methods and Materials

5.1 Materials

5.1.1 Chemicals

Unless specified explicitly, the chemicals used in this study were bought from the following companies: Roth, Merck, Sigma-Aldrich, Roche, or Thermo-Fisher Scientific.

5.1.2 Antibiotics

Antibiotics were used for bacterial and yeast selection.

Antibody	**Working concentration**
Ampicillin	100 µg/ml
Kanamycin	25 µg/ml
Hygromycin B	250 µg/ml
ClonNAT (Nourseothricin) powder	200 µg/ml
Geneticine disulfate (G418)	200 µg/ml

5.1.3 Buffers and solutions

Buffer used for molecular biology and biochemical experiments:

- LiPEG: 100mM Lithium acetate, 1mM Ethylendiaminetetraacetic acid (EDTA) pH 8.0, 10mM Tris-HCl pH 8.0, 40% PEG3350. Filter sterilised and stored at 4°C
- LiSorb: 10mM Tris-HCl pH 8.0, 100mM Lithium acetate, 1mM EDTA pH 8.0, 1M Sorbitol, Filter sterilised and stored at room temperature
- Polymerase Chain Reaction (PCR) buffers for yeast tagging/deletion-cassettes:
  i. 10X Buffer 1: 500mM Tris-HCl, pH 9.2, 160mM $(NH_4)_2SO_4$, 17.5mM $MgCl_2$
  ii. 10X Buffer 2: 500mM Tris-HCl, pH 9.2, 160mM $(NH_4)_2SO4$, 22.5mM MgCl2
- 8% Paraformaldehyde (PFA): 4g PFA in 40ml H_2O, 600µl 1M NaOH, heated to 60°C to dissolve PFA. 7.5ml of 1M potassium phosphate (KPO) buffer pH 6.5 and filter sterilised.
- Agarose gel electrophoresis TAE buffer 50X: 1M Tris-HCl, 50mM EDTA, pH 7.7 adjusted with acetic acid
- 6X DNA loading dye: 0.25% Bromphenol-Blue, 0.25% Xylencyanol, 30% Glycerol
- Bacterial plasmid isolation solutions:
  i. P1: 20mM Tris-HCl pH 8.0, 10mM EDTA pH 8.0, 100µg/mL RNAse A (Sigma Aldrich)
  ii. P2: 0.2M NaOH, 1% (w/v) Sodium Dodecyl Sulfate (SDS)
  iii. P3: 3M potassium acetate

- Phosphate buffered saline (PBS) 1X: 137mM NaCl, 2.7mM KCl, 10mM Na_2HPO_4, 1.7mM KH_2PO_4, pH 7.4 adjusted with HCl
- High-Urea (HU) sample buffer: 0.1mM EDTA, 200mM Tris-HCl pH 6.8, 5% (w/v) SDS, 8M Urea and a small amount of Bromophenol-Blue. Just before use, add 15mg/ml (100mM) Dithiothreitol (DTT)
- SDS-Polyacrylamide Gel Electrophoresis (PAGE) running buffer: 0.1% (w/v) SDS, 25mM Tris-HCl, 192mM Glycine
- PBS-Tween (T): 0.01% (v/v) Tween 20 in PBS.
- Blotting buffer for semi-dry transfer: 0.025% (w/v) SDS, 20% (v/v) Methanol, 25mM Tris, 192mM Glycine
- Ponceau S: 0.2% Ponceau S, 3% Trichloroacetic acid (TCA)
- Enhanced chemiluminescence (ECL) solutions:
  i. 100mM Tris-HCl, 2.5mM p-Coumaric acid, 25mM Luminol, pH 8.5
  ii. 100mM Tris-HCl, 30% (w/w) H_2O_2, pH 8.5
  Solution i. and ii. must were stored at 4°C in dark bottles covered with Aluminium foil. Both the solutions were mixed 1:1 before use
- Stripping solution for Nitrocellulose membranes: 1% (w/v) SDS, 0.2M Gylcine pH 2.5 (25ml per membrane)

Media and agar plates for bacterial cultures:

- LB medium: 10g Bacto tryptone, 10g Bacto yeast extract, 5g NaCl, made the volume to 1 L with H_2O and autoclaved. Antibiotics were added to the autoclaved LB medium and stored at 4°C.
- LB-agar plates: 1 L LB medium, 20g agar and then autoclaved. Once the media cools down a little, respective antibiotics were added. These plates were stored at 4°C.

Media and agar plates for yeast cultures:

- 10-time amount SC-His-Trp-Leu-Ura drop out mix:

Adenine 5 g
Alanine 20 g
Arginine 20 g
Asparagine 20 g
Aspartic acid 20 g

Cystein 20 g
Glutamine 20 g
Glutamic acid 20 g
Glycin 20 g
Inositol 20 g
Isoleucine 20 g
Lysine 20 g
Methionine 20 g
para-Aminobenzoic acid 2 g
Phenylalanine 20 g
Proline 20 g
Serine 20 g
Threonine 20 g
Tyrosine 20 g
Valine 20 g
Mixed thoroughly for 12 h on rotor mixer and stored at 4°C.

- SC-X drop-out mix:

36.7g of the 10x SC-His-Trp-Leu-Ura drop out mix
And based on the specific drop outs:
Histidine 2 g
Leucine 4 g
Uracil 2 g
or Tryptophan 2 g
Mixed thoroughly before use and stored at 4°C.

- Yeast Peptone Dextrose (YPD) medium: 10g Bacto yeast extract, 20g Bacto Peptone, 20g Glucose, made the volume to 1 L with H_2O. Supplemented YPD media with 100g Adenine and autoclaved.
- YPD-agar plates: 1 L YPD, 20g agar autoclaved together. These plates were stored at 4°C.
- Synthetic Complete (SC) medium: 6.7g Bacto yeast nitrogen base w/o amino acids, 20g Glucose, 2g Drop-out mix, 100g Adenine, complete the volume to 1 L with H_2O and autoclaved.
- SC-agar plates: 1 L SC medium, 20g agar autoclaved together. These plates were stored at 4°C.

- In situations where (3%) Raffinose and/or (2%) Galactose were used as carbon source instead of Glucose, the media was sterilised using filters as they cannot be autoclaved.

5.1.4 Enzymes

Enzyme	Manufacturer
Taq DNA polymerase	New England Biolabs
Vent DNA polymerase	New England Biolabs
Q5 DNA polymerase	New England Biolabs
Pfu-Turbo DNA polymerase	Agilent technologies
Zymolyase 20T	Seikaga, Tokyo
T4 DNA ligase	New England Biolabs
RNAse A	Sigma-Aldrich
Restriction Endonucleases	New England Biolabs

5.1.5 Antibodies

- Primary Antibodies

Name	Host	Dilution	Reference
Anti-HA	Mouse	1:10	Labstock, 12CA5
Anti-Myc	Mouse	1:50	Labstock, 9E10
Anti-GFP	Mouse	1:800	Roche
Anti-Clb2	Rabbit	1:3000	Labstock
Anti-Sic1	Guinea Pig	1:200	Labstock
Anti-Tat1	Mouse	1:1000	Elspeth's lab
Anti-Mck1	Rabbit	1:200	Gift from J. Thorner (Dailey et al., 1990)
Anti-Nud1	Rabbit	1:100	Gift from E. Schiebel
Anti-Spc72	Rabbit	1:150	Gift from E. Schiebel
Anti-Cdc6	Mouse	1:500	Abcam
Anti-pMAPK/CDK substrates	Mouse	1:1000	Cell Signaling
Anti-Bfa1	Rabbit	1:1000	Gift from E. Schiebel

- Secondary Antibodies

Name	Host	Dilution	Reference

Anti-mouse Horseradish Peroxidase (HRP)	Goat	1:5000	Dianova
Anti-guinea pig HRP	Goat	1:5000	Dianova
Anti-rabbit HRP	Goat	1:5000	Dianova

5.1.6 Primers

100µM primers used in this study were ordered from Sigma-Aldrich and stored at -20°C. All the primer sequences can be found in the primer collection folder on the aggp server.

5.1.7 Plasmids

The following plasmids were made during the course of the study as described here:

Plasmid name	Description
pSPP01	**pJET1.2 –*MCK1***. MCK1 was amplified from ESM356 chr DNA using MCK1-3 &MCK-4 (product size :1778) and ligated with pJET 1.2. control digestion using BamHI and Xba1 enzymes cuts out the 1.8kb insert.
pSPP02	**pRS315-*MCK1*.** MCK1 was subcloned into pRS315/BamHI&XbaI, from pSPP01-4 (~1.8kb insert cut from pSPP01-4/BamHI&XbaI).
pSPP03	**pRS315-*mck1-KD (D164A).*** (MCK1 kinase dead). pSPP02-2 was mutated by point mutagenisis PCR using MCK1-D164-FW and MCK1-D164-Rw primers. Mutation was confirmed by sequencing using the MCK1-2H-fw and also MCK1-3 primers.
pSR01	**pRS305-*MCK1*.** MCK1 was subcloned into pRS305/BamHI & XbaI, from pSPP01-4 (~1.8kb insert cut from pSPP01-4/BamHI & XbaI.
pSR02	**pRS305-*mck1-KD (D164A).*** The kinase dead mutant was obtained from pSPP03-1 and cut with BamHI & Xba1 and cloned into pRS305. Confirmed by digestion with BamHI & XbaI.
pGW071	**pRS425-*CDC6***. The 2140 bp BamHI/XhoI fr. of CDC6 of pGW109 (pTopo-CDC6) was subcloned into pRS425/BamHI/XhoI. Confirmed by sequencing.
pSR9	**pRS316-*CDC6*.** Subcloned from pGW071 (pRS425-CDC6) 2140bp segment into pRS316 using BamHI/XhoI. Confirmed by sequencing.
pSR10	**pRS425-*cdc6NΔ (2-49)*.** Using PCR mutagenesis method with CDC6 Cdc6ΔN-Fw and Cdc6ΔN-Rv primers. Confirmed by sequencing.
pSR18	**pRS305-*cdc6NΔ* (2-49).** Used insert from pSR10 and subcloned into pRS305, both digested by BamHI and XhoI. Checked by restriction digestion and sequencing.

pSR22	**pRS305-*CDC6*.** Used insert from pGW071 and subcloned into pRS305, both digested by BamHI and XhoI. Checked by restriction digestion and sequencing.
pSR14	**pRS425-*CDC6^{KE} (K114E)*.** Using PCR mutagenesis method with CDC6 Cdc6-KE-Fw and Cdc6-KE-Rv primers. Confirmed by sequencing.
pSR24	**pRS425-*N50-CDC6***, only first 50 amino acids of *CDC6* were cloned with its own promoter. PCR fragment from Cdc6-1 and Cdc6-3 primers was cloned into BamHI-XhoI digested pRS425.

The following plasmids were used form the bacteria collection of the Pereira lab:

Plasmid name	Description
pBK067	pRS305-*mCherry-TUB1*
pAK011	pRS306-*mCherry-TUB1*
pTH17	pRS316-*LTE1*
pGW399	pRS316-*KAR9*
pSM926	pRS316-*MOB1*
pHM259-19a	pRS316-*CDC15*
pKA59	pRS316-*TEM1*
pMF164	pRS306-*cdc28-as*

5.1.8 Bacterial strains

DH5α: deoR endA1 gyrA96 hsdR17 (rκ-mκ-) recA1 relA1 supE44 thi-1Δ(lacZYA-argFV169) φ80δlacZΔM15 F- λ-

5.1.9 Yeast strains

Name	Genotype
BKY091	ESM356-1 *BFA1-3HA-hphNT1*
AKY887	ESM356-1 *BFA1-3HA-hphNT1 kin4Δ::HIS3MX6*
SRY194	ESM356-1 *BFA1-3HA-hphNT1 kin4Δ::HIS3MX6 mck1Δ::klTRP1*
SRY195	ESM356-1 *BFA1-3HA-hphNT1 mck1Δ::klTRP1*
AKY1798	ESM356-1 *BFA1-yeGFP-KanMX6 SPC42-eqFP-hphNT1 kar9Δ::klTRP1* pGW399 *kin4Δ::HIS3MX6 leu2Δ::mCherry-TUB1-LEU2*
BKY795	ESM356-1 *BFA1-yeGFP-KanMX6 SPC42-eqFP-hphNT1 kar9Δ::klTRP1* pGW399 *leu2Δ::mCherry-TUB1-LEU2*
SRY196	ESM356-1 *BFA1-yeGFP-KanMX6 SPC42-eqFP-hphNT1 kar9Δ::klTRP1* pGW399 *leu2Δ::mCherry-TUB1-LEU2 mck1Δ::HIS3MX6*
GPY160	ESM356-1 *bfa1Δ::KanMX6*
SHM1799	ESM356-1 *cdc15Δ::klTRP1* pHM259-19a

CJY521	ESM356-1 *CDC6-9MYC-natNT2*
SRY057	ESM356-1 *CDC6-9MYC-natNT2 mck1Δ::HIS3MX6*
SRY093	ESM356-1 *cdc6Δ::klTRP1* pSR9
SRY137	ESM356-1 c*dc15Δ::klTRP1* pHM259-19a *mck1Δ::HIS3MX6*
RDY301	ESM356-1 *kar9Δ::HIS3MX6 SPC42-eqFP-natNT2 MOB1-yeGFP-KanMX6* pGW399 *leu2Δ::mCherry-TUB1-LEU2*
RDY302	ESM356-1 *kar9Δ::HIS3MX6 SPC42-eqFP-natNT2 MOB1-yeGFP-KanMX6* pGW399 *leu2Δ::mCherry-TUB1-LEU2 kin4Δ::klTRP1*
SRY014	ESM356-1 *kar9Δ::HIS3MX6 SPC42-eqFP-natNT2 MOB1-yeGFP-KanMX6* pGW399 *leu2Δ::mCherry-TUB1-LEU2 mck1Δ::klTRP1*
SRY060	ESM356-1 *mck1Δ::HIS3MX6*
SRY191	ESM356-1 *mck1Δ::HIS3MX6 NUD1-6HA-klTRP1*
CKY329	ESM356-1 *mob1Δ::klTRP1* pSM926
SRY136	ESM356-1 *mob1Δ::klTRP1* pSM926 *mck1Δ::his3MX6*
SRY190	ESM356-1 *NUD1-6HA-klTRP1*
UJY011	ESM356-1 *SPC42-eqFP-KanMX6 natNT2*-Gal1-*yeGFP-KIN4 ura3::pMET25-KIN4-URA3*
UJY013	ESM356-1 *SPC42-eqFP-KanMX6 natNT2*-Gal1-*yeGFP-KIN4 ura3::pMET25-KIN4-URA3 bfa1Δ::klTRP1*
AKY1404	ESM356-1 *SPC42-eqFP-KanMX6 natNT2*-Gal1-*yeGFP-KIN4 ura3::pMET25-KIN4-URA3 mck1Δ::klTRP1*
SPP20	ESM356-1 *SPC42-eqFP-KanMX6 natNT2*-Gal1-*yeGFP-KIN4 ura3::pMET25-KIN4-URA3 mds1Δ::klTRP1*
SPP21	ESM356-1 *SPC42-eqFP-KanMX6 natNT2*-Gal1-*yeGFP-KIN4 ura3::pMET25-KIN4-URA3 mrk1Δ::klTRP1*
SPP19	ESM356-1 *SPC42-eqFP-KanMX6 natNT2*-Gal1-*yeGFP-KIN4 ura3::pMET25-KIN4-URA3 ygk3Δ::klTRP1*
RDY607	ESM356-1 *SPC42-mCherry-klTRP1 KIN4-mNeonGreen-hphNT1*
SRY061	ESM356-1 *SPC42-mCherry-klTRP1 KIN4-mNeonGreen-hphNT1 mck1Δ::HIS3MX6*
SRY192	ESM356-1 *SPC72-6HA-klTRP1*
SRY193	ESM356-1 *SPC72-6HA-klTRP1 mck1Δ::HIS3MX6*
MFY1506	ESM356-1 *SWI5-yeGFP-hphNT1*
SRY199	ESM356-1 *SWI5-yeGFP-hphNT1 mck1Δ::HIS3MX6*
MBY12	ESM356-1 tem1Δ::natNT2 pKA59
SRY144	ESM356-1 tem1Δ::natNT2 pKA59 *mck1Δ::HIS3MX6.*

SRY065	ESM356-1 *ura3::mCherry-TUB1-URA3 CDC6-yeGFP-HIS3MX6*
SRY103	ESM356-1 *ura3::mCherry-TUB1-URA3 CDC6-yeGFP-HIS3MX6 mck1Δ::klTrp1*
SRY147	ESM356-1 *ura3Δ::mCherry-TUB1-URA3 natNT2::Gal1-Cdc6-yeGFP-HIS3MX6*
ESM2139	ESM356-9 *lte1Δ::KanMX6 kin4Δ::hphNT1*
FAY145	ESM356-9 *lte1Δ::KanMX6* pTH17
SRY031	ESM356-9 *lte1Δ::KanMX6* pTH17 *mck1Δ::hphNT1*
BKY094	YPH499 *cdc14-2 BFA1-3HA-HIS3MX6*
SRY198-2	YPH499 *cdc14-2 BFA1-3HA-HIS3MX6 CDC28::pMF164*
IPY50	YPH499 *cdc14-2 BFA1-3HA-HIS3MX6 CDC28::pMF164 mck1Δ::klTRP1*
SRY197	YPH499 *cdc14-2 BFA1-3HA-HIS3MX6 mck1Δ::klTRP1*
SRY186	YPH499 *cdc14-2 mck1Δ::klTRP1 ORC6-6HA-HIS3MX6*
SRY180	YPH499 *cdc14-2 MOB1-6HA-HIS3MX6*
SRY181	YPH499 *cdc14-2 MOB1-6HA-HIS3MX6 mck1Δ::klTRP1*
SRY185	YPH499 *cdc14-2 ORC6-6HA-HIS3MX6*
ESM1278	YPH499 *cdc15-1*
SRY091	YPH499 *cdc15-1 CDC14-mCherry-HIS3MX6 ura3::yeGFP-TUB1-URA3 mck1Δ::klTRP1*
SRY090	YPH499 *cdc15-1 CDC14-mCherry-HIS3MX6 ura3::yeGFP-TUB1-URA3*
SRY092	YPH499 *cdc15-1 CDC14-mCherry-HIS3MX6 ura3::yeGFP-TUB1-URA3 spo12Δ::klTRP1 mck1Δ::hphNT1*
SRY089	YPH499 *cdc15-1 CDC14-mCherry-HIS3MX6 ura3::yeGFP-TUB1-URA3 spo12Δ::klTRP1*
YMY620	YPH499 *cdc15-1 kin4Δ::klTRP1*
YMY440	YPH499 cdc15-1 *mck1Δ::klTRP1*
CLY169-2	YPH499 *cdc5-10*
YMY468	YPH499 *cdc5-10 kin4Δ::klTRP1*
YMY442	YPH499 *cdc5-10 mck1Δ::klTRP1*
ESM1309	YPH499 *dbf2-2*
SRY006	YPH499 *kar9 Δ::klTRP1* pGW399 *ade2Δ::yeGFP-TUB1-ADE2 spo12Δ::hphNT1 mck1Δ::HIS3MX6*
IPY33	YPH499 *kar9Δ::HIS3MX6 x* YPH500 *kar9Δ::klTRP1 clb2Δ::hphNT1 yeGFP-TUB1-ADE2*
IPY30	YPH499 *kar9Δ::HIS3MX6 x* YPH500 *kar9Δ::klTRP1 yeGFP-TUB1-ADE2*
YMY343	YPH499 *kar9Δ::klTRP1* pGW399 ye*GFP-TUB1-ADE2 mck1Δ::HIS3MX6*

AKY1280	YPH499 *kar9Δ::klTRP*1 pGW399 *ade2Δ::*ye*GFP-TUB1-ADE2 spo12Δ::hphNT1*
SRY128	YPH499 *kar9Δ::klTRP1* pGW399 *ade2Δ::*ye*GFP-TUB1-ADE2 spo12Δ::hphNT1 mck1Δ::HIS3MX6 kin4Δ::natNT2*
AKY1279	YPH499 *kar9Δ::klTRP1* pGW399 *kin4Δ::HIS3MX6 ade2Δ::yeGFP-TUB1-ADE2 spo12Δ::hphNT1*
LYO45	*YPH499 kar9Δ::klTRP1* pGW399 *ade2Δ::mCherry-TUB1-ADE2 CDC6-yeGFP-HIS3MX6*
SRY062	*YPH499 kar9Δ::klTRP1* pGW399 *ade2Δ::mCherry-TUB1-ADE2 CDC6-yeGFP-HIS3MX6 mck1Δ::hphNT1*
AKY346	YPH499 *kar9Δ::klTRP1* pGW399 *ade2Δ::yeGFP-TUB1-ADE2*
IPY22	YPH499 *kar9Δ::klTRP1* pGW399 *ade2Δ::*ye*GFP-TUB1-ADE2 CDC14-mCherry-hphNT1*
IPY23	YPH499 *kar9Δ::klTRP1* pGW399 *ade2Δ::*ye*GFP-TUB1-ADE2 CDC14-mCherry-hphNT1 mck1Δ::HIS3MX6*
AKY351	YPH499 *kar9Δ::klTRP1* pGW399 *ade2Δ::yeGFP-TUB1-ADE2 kin4Δ::HIS3MX6*
SRY022	YPH499 *kar9Δ::klTRP1* pGW399 *ade2Δ::*ye*GFP-TUB1-ADE2 mck1Δ::HIS3MX6 leu2::LEU2-MCK1-9myc-hphNT1*
SRY055	YPH499 *kar9Δ::klTRP1* pGW399 *ade2Δ::yeGFP-TUB1-ADE2 mck1Δ::HIS3MX6 leu2::LEU2-MCK1-D164A-9myc-hphNT1*
SRY010	YPH499 *kar9Δ::klTRP1* pGW399 *ade2Δ::yeGFP-TUB1-ADE2 mds1Δ::HIS3MX6*
SRY012	YPH499 *kar9Δ::klTRP1* pGW399 *ade2Δ::yeGFP-TUB1-ADE2 mrk1Δ::HIS3MX6*
SRY011	YPH499 *kar9Δ::klTRP1* pGW399 *ade2Δ::yeGFP-TUB1-ADE2 ygk3Δ::HIS3MX6*
SRY105	YPH499 *kar9Δ::klTRP1 ade2Δ::yeGFP-TUB1-ADE2 mck1Δ::HIS3MX6* pSR9 *cdc6Δ::hphNT1*
SRY111	YPH499 *kar9Δ::klTRP1 ade2Δ::yeGFP-TUB1-ADE2 mck1Δ::HIS3MX6 pSR9 cdc6Δ::hphNT1 leu2Δ::CDC6-LEU2*
SRY113	YPH499 *kar9Δ::klTRP1 ade2Δ::yeGFP-TUB1-ADE2 mck1Δ::HIS3MX6 pSR9 cdc6Δ::hphNT1 leu2Δ::CDC6ΔN-LEU2*
IPY41	YPH499 *kar9Δ::klTRP1 ade2Δ::yeGFP-TUB1-ADE2 mck1Δ::hphNT1* x YPH500 *kar9Δ::klTRP1 mck1Δ::natNT2*
YMY455	YPH499 *kin4Δ::klTRP1*
AKY2914	YPH499 *lte1Δ::KanMX6* pRTH17 *spo12Δ::natNT2 ste20Δ::hphNT1*

THY309	YPH499 *lte1Δ::KanMX6* pTH17 *slk19Δ::klTRP1*
AKY2363	YPH499 *lte1Δ::KanMX6 pTH17 slk19Δ::klTRP1 kin4Δ::hphNT1*
SRY026	YPH499 *lte1Δ::KanMX6* pTH17 *slk19Δ::klTRP1 mck1Δ::hphNT1*
LYO58	YPH499 *lte1Δ::KanMX6* pTH17 *spo12Δ::HIS3MX6*
SRY174	YPH499 *lte1Δ::KanMX6* pTH17 *spo12Δ::HIS3MX6 ste20Δ::klTRP1 mck1Δ::hphNT1*
SRY177	YPH499 *lte1Δ::KanMX6* pTH17 *spo12Δ::HIS3MX6 ste20Δ::klTRP1 mck1Δ::hphNT1 bfa1Δ::natNT2*
SRY178	YPH499 *lte1Δ::KanMX6* pTH17 *spo12Δ::HIS3MX6 ste20Δ::klTRP1 mck1Δ::hphNT1 kin4Δ::natNT2*
SRY024	YPH499 *lte1Δ::KanMX6* pTH17 *spo12Δ::HIS3X6 mck1Δ::hphNT1*
AKY2362	YPH499 *lte1Δ::KanMX6 pTH17 spo12Δ::klTRP1 kin4Δ::hphNT1*
SRY172	YPH499 *lte1Δ::KanMX6* pTH17 *spo12Δ::klTRP1 ste20Δ::HIS3MX6 bfa1Δ::hphNT1*
SRY179	YPH499 *lte1Δ::KanMx6 spo12Δ::HIS3MX6 ste20Δ::klTrp1 kin4Δ::natNT2*
SRY200	ESM356-1 *ura3::mCherry-TUB1-URA3 CDC6-yeGFP-HIS3MX6 cdc55Δ::hphNT1*
SRY201	ESM356-1 *ura3::mCherry-TUB1-URA3 CDC6-yeGFP-HIS3MX6 mck1Δ::klTrp1 cdc55Δ::hphNT1*
IPY61	YPH499 *kar9Δ::klTRP1* pGW399 *ade2Δ::yeGFP-TUB1-ADE2 cdc55Δ::hphNT1*
IPY62	YPH499 *kar9Δ::klTRP1* pGW399 *ade2Δ::yeGFP-TUB1-ADE2 mck1Δ::HIS3MX6 cdc55Δ::hphNT1*
SRY202	ESM356-1 *LTE1-yeGFP- klTrp1 ura3::mCherry-TUB1-URA3*
SRY203	ESM356-1 *LTE1-yeGFP- klTrp1 mck1Δ::HIS3MX6 ura3::mCherry-TUB1-URA3*
CEY001	YPH499 *mck1Δ::klTRP1*
ESM1361	YPH499 *mob1-67*
YMY466	YPH499 *mob1-67 kin4Δ::klTRP1*
YMY441	YPH499 *mob1-67 mck1Δ::klTRP1*
ESM1249	YPH499 *tem1-3*
YMY626	YPH499 *tem1-3 kin4Δ::klTRP1*
CEY002	YPH499 *tem1-3 mck1Δ::klTRP1*
ESM356-9	MATa *ura3-52 his3Δ200 leu2Δ1*
ESM356-1	MATa *ura3-52 leu2Δ1 his3Δ200 trp1Δ63*
YPH499	MATa *ura3-52 lys2-801amber ade2-101ochre trp1Δ63 his3Δ200 leu2Δ1*

5.2 Methods and Materials

5.2.1 Molecular Biology

5.2.1.1 Amplification of DNA fragments with Polymerase Chain Reaction (PCR)

Amplification of DNA fragments from plasmid or genomic DNA was carried out by using the polymerase chain reaction (PCR). This technique is based on annealing of a pair of oligonucleotides to the DNA template. These oligonucleotides are known as the primers whose annealing temperature depends on their nucleotide composition and was calculated using the online NEB T_m calculator (n(A, T) x 2°C + n(G, C) x 4°C). All the PCRs were run in Thermocycler T-Personal (Biometra, Germany). Q5 (NEB) polymerase was used for regular DNA amplification and Pfu-Turbo (Agilent) was used to amplify DNA with site-directed mutations.

The following is the recipe for these reactions:

Q5	**Pfu**	
5-10 ng	50-100 ng	DNA template
2.5 µl	2.5 µl	10µM Forward primer
2.5 µl	2.5 µl	10µM Reverse primer
5 µl	5 µl	10X Q5/Pfu Buffer
5 µl	5 µl (freshly prepared)	2mM dNTPs
1 µl	1 µl	Q5/Pfu DNA polymerase
Fill upto 50 µl	Fill upto 50 µl	Nuclease free H_2O

The thermocycler was programmed as follows:

Step	**Temperature (°C)** **(Q5**/Pfu**)**	**Time** **(Q5**/Pfu**)**	**Number of cycles**
Initial denaturation	**98**/95	**30 s**/2 min	1
Denaturation	**98**/95	**10 s**/30 s	30
Annealing	**T_m+3**/60	**30 s**	
Extension	72	**30s/kb**/2min/kb	
Final Extension	72	**2 min**/10min	1
Pause	4	Hold	

5.2.1.2 Cloning with CloneJET PCR Cloning Kit

In situations where it was essential to improve the cloning efficiency, the CloneJET PCR cloning kit (Thermo-Scientific) was used. Blunt-end PCR fragments were ligated into linearised pJET1.2 blunt vectors using the protocol provided with the kit.

5.2.1.3 Restriction digestion of DNA fragments or plasmids

Restriction endonucleases (NEB) were used to cut DNA at specific sites in order to linearise plasmids, generate compatible DNA fragments for cloning and to identify the positive clones. The PCR amplified fragments were purified using QIAquick PCR purification kit prior to setting up the restriction digestion.

Cloning analysis	**Preparative plasmid and PCR fragments**	
100-500 ng	3-5 µg	DNA template
2-5 U	10-20 U	Restriction enzyme (NEB)
20 µl	50 µl	Total volume
90-120 mins	4-6 hours	Incubation time

The restriction-digested DNA fragments were checked by agarose gel electrophoresis.

5.2.1.4 Agarose gel electrophoresis

DNA fragments after PCR amplification and restriction digestion were resolved and visualised on a 0.8% agarose gel run in 1X TAE buffer at 100V for 15-30 minutes. The 6X loading dye is added to the samples prior to loading them in the gel. The samples were run alongside a 1kb DNA ladder (NEB). The gel was then incubated in a 1ng/ml Ethidium Bromide (EtBr) bath for 15mins. Once the gel was stained, the bands were visualised by a UV-illumination (Biometra, Analytik Jena).

5.2.1.5 DNA extraction from agarose gel

Restriction digested DNA upon Et-Br staining, were excised from the agarose gel and isolated using the gel extraction/ PCR clean up kit (Qiagen/Macherey and Nagel) following manufacturer's instructions.

5.2.1.6 DNA concentration determination

The concentration of purified, isolated or amplified DNA, was measured by the absorption at 260nm on a nanodrop (Perkin Elmer). The purity of DNA was estimated by the ratio of absorbance at 260nm/280nm (≈1.8 pure DNA).

5.2.1.7 Ligation of DNA fragments into linearised vector plasmid

Cloning an insert DNA into a vector backbone DNA was performed using a 3:1 ratio of insert: vector molar ratios, using the NEB ligation calculator. A 10 µl reaction volume was set up with 1 µl of the T4 DNA ligase (NEB). For sticky end restriction digested DNA fragments, ligation reaction was incubated at room temperature for 10 mins whereas, for blunt end, it was incubated at 16°C overnight. The ligation mix was then transformed into chemically competent *E. coli*, DH5α.

5.2.1.8 Chemically competent *E. coli* cells

To make chemically competent *E. coli*, a primary culture of 250ml was inoculated at 18°C while shaking at 150rpm until the optical reached 0.6 (OD_{600}). This primary culture was pelleted at 4°C at 1000g and then resuspended in ice-cold FTB solution- 250mM KCl, 15mM $MgCl_2$, 55$MnCl_2$, 10mM PIPES). Post incubation on ice for 10mins, the cells were pelleted again. This pellet was resuspended in 1/3rd volume of ice-cold FTP solution- 10mM RbCl, 75mM $CacCl_2$, 10mM MOPS, 12% glycerol (w/v)). Later, 7% DMSO was added to this and cells were incubated on ice for 10mins followed by freezing in liquid N_2 and stored at -80°C.

5.2.1.9 Transformation of DNA in chemically competent *E. coli* cells

Chemically competent *E. coli* (DH5α) were transformed with DNA using heat shock. 100g-1µg of DNA was added to 50 µl of aliquoted chemically competent *E. coli* cells. This mix was incubated for 30mins on ice after which the bacteria were heat shocked for 45 seconds at 42°C in a water bath. This was cooled on ice for 2mins to which 1ml of TY medium was added. The cells were incubated with shaking at 37°C for 1hours. This solution was plated onto a TY plate containing the antibiotic for selection and incubated for 12-16hours at 37°C.

5.2.1.10 Plasmid isolation from *E. coli* cells

A primary culture with single colonies inoculated in 4ml TY media-supplemented with respective antibiotics-was cultured at 37°C, overnight. This culture was pelleted at 14000rpm for 3mins at room temperature. This pellet was resuspended in 250 µl of ice cold P1 buffer. The cells were then lysed using the P2 buffer and mixed gently by flipping the Eppendorf tube 4-6 times. This solution was neutralised by adding buffer P3 and mixing gently again. This mix was centrifuged at 14000rpm for 10mins and

the supernatant was followed through silica membrane containing columns to adsorb DNA. This was followed by elution of the DNA from the columns using EB buffer or H_2O.

5.2.1.11 Sequencing of DNA

Samples for sequencing of DNA plasmids were sent to GATC Biotech – Eurofins Genomics. Results obtained from this were analysed using Snapgene Viewer.

5.2.1.12 Preparation of *E. coli* glycerol stocks

A single colony of bacteria was inoculated in 1.5ml TY media-supplemented with respective antibiotics with shaking at 37°C (12 hours-overnight). 700 µl of this culture was added to 700 µl of 50% glycerol and vortexed to freeze on dry ice and later stored at -80°C.

5.2.1.13 PCR protocol for yeast tagging/deletion-cassettes

The DNA polymerase used for cassette PCR was an enzyme mix- 8µl Taq DNA polymerase (5U/µl) + 4µl Vent DNA polymerase (2U/µl). Stored at -20°C.

5 µl	DNA template (20ng/µl)
3.2 µl	10µM Forward primer
3.2 µl	10µM Reverse primer
5 µl	10X PCR Buffer 1/2
8.75 /**10.62** µl	2mM dNTPs (Buffer1/**Buffer2**)
1 µl	Enzyme mix
Fill upto 50 µl	Nuclease free H_2O

PCR conditions:

Temperature (°C) (Buffer 1/Buffer 2**)**	**Time (Buffer 1**/Buffer 2**)**	**Number of cycles**
94/97	**2 min**/5 min	1
94/97	**20 s**/1 min	9
52/53	**30 s**	
68	**1min/kb**	
94/97	**30 s**/1 min	1
52/53	**30 s**	19
68	**1min/kb**	

4	Hold	

3 µl of the PCR product was analysed on 0.8% agarose gel.

Buffer 2 was used for cassettes with Nat selection, whereas, Buffer 1 was used for all cassettes containing all other selection markers.

Combination of primers for:

Tagging at C-terminus – S2/S3

Tagging at N-terminus – S1/S4

Deletion of genes – S1/S2

5.2.1.14 Chemically competent yeast cells

Cells were inoculated one day before in an appropriate medium and incubated at 30°C or 23°C with shaking at 150rpm. The cultures were diluted to 0.15 OD_{600} in 50ml fresh medium and incubated again until the OD_{600} reached 0.6-0.8.

The cultures were transferred to 50ml falcon tubes and centrifuged at 3200 rpm for 2mins at room temperature. After discarding the supernatant, cells were washed with 40 ml sterile H_2O and centrifuged as before. The resulting pellet was resuspended in 20-25 ml of LiSorb and subjected to centrifuge as earlier. Supernatant was discarded hereafter and excess of LiSorb was discarded.

The pellet was then resuspended in 300 µl LiSorb and $1/10^{th}$ of the volume of this solution, denatured salmon sperm DNA was added (Salmon sperm DNA was heated to 95°C for 3 mins and cooled on ice).

100 µl aliquots of this final cell suspension were made and put directly at -80°C.

5.2.1.15 Transformation of DNA in chemically competent yeast cells

Frozen competent yeast cells were first thawed at room temperature. 50 µl of cells were used per transformation. 5 µl PCR product of the deletion/tagging cassettes, 2-3 µl of 3-5 µg digested yeast integration plasmid and 1-3 µl of plasmid DNA was added to competent cells, mixed well and incubated at room temperature for 15mins. 300 µl of LiPEG was added and vortexed to incubate at room temperature for 15mins. 35 µl of DMSO was added to this and incubated straightaway in a 42°C water bath for 12 mins. The cells were later centrifuged at 3000 rpm for 2mins and supernatant was removed by aspiration. In cases of auxotrophs, the cell pellet was resuspended in 200 µl PBS/sterile H_2O and plated on appropriate selection plates. For antibiotic selection cassettes (kanamycin, hygromycin, natrunculin), cells were

resuspended in 1ml YPAD medium and incubated at 3-4hours at 30°C/4-5 hours at 23°C and 6-12hours at 30°C/ overnight at 23°C. Cells were spun and 800 µl medium was discarded. The residual media was used to resuspend the pellet and this was plated on the appropriate selection plate.

5.2.1.16 Colony PCR for yeast

Colony PCR was done to check for clones carrying the deletion of the target gene using primers pairs designed specifically for it.

Small quantity of freshly patched yeast cells was picked and dissolved in 50 µl of 0.01% Sarkosyl in 0.02N NaOH. This was boiled for 5 mins at 95°C and vortexed to freeze at -80°C. 1 µl of this cell suspension was used for the PCR reaction as mentioned below.

1 µl	Yeast cell suspension
1.25 µl	10µM Forward primer
1.25 µl	10µM Reverse primer
2.5 µl	10X PCR Buffer 1/2
2.5 µl	2mM dNTPs (Buffer1/**Buffer2**)
0.125 µl	Taq DNA polymerase
Fill upto 25 µl	Nuclease free H_2O

12.5 µl of this PCR product was analysed on 0.8% agarose gel.

PCR cycle conditions:

Temperature (°C) (Buffer 1/Buffer 2**)**	**Time (Q5**/Pfu**)**	**Number of cycles**
94/97	**5 min**/5 min	1
94/97	**30 s**/30 s	35
53/60	**30 s/**1 min	
68	**1 min/kb**	
68	**3 min**	1
4	Hold	

5.2.1.17 Plasmid isolation from yeast cells

Fresh yeast culture or cells directly from plate were used to isolate plasmid. The cells were resuspended in 750 µl of P1 buffer containing 0.15 mg of zymolyase 20T and 1 µl β-mercaptoethanol. This cell suspension was incubated at 37°C for an hour, while

mixing gently. After this 150 µl of P2 buffer was added, mixed carefully and incubated at 65°C for 20mins to facilitate cell lysis. The samples were then cooled on ice. Further, 150 µl of P3 buffer was added and mixed carefully to later incubate on ice for 15mins. Eventually, the samples were spun at 14000rpm for 5mins.

The supernatant from the earlier step was mixed with 450 µl of isopropanol in a new Eppendorf tube and incubated at room temperature for 5mins. The samples were subjected to centrifuge at 14000rpm for 1min and supernatant from this step was mixed with 70% ethanol to be incubated at room temperature for 10mins. After this the samples were subjected to centrifuge like before and the supernatant was discarded. The residual pellet was air-dried in a 37°C incubator for 30mins and later resuspended in 20 µl sterile H_2O.

5.2.1.18 Preparation of yeast glycerol stocks

Yeast cells were grown on an appropriate selection plate for 2-3 days. These were scrapped with 1ml glass pipettes and resuspended in 1 ml of 15% glycerol. They were frozen on dry ice and stored at -80°C.

5.2.2 Yeast specific methods

5.2.2.1 Culture and growth conditions

YP or SC media were used to culture yeast with the appropriate carbon sources, antibiotics and auxotrophic marker selections. Liquid cultures were made by inoculating fresh cells from agar plates into Erlenmeyer flasks containing media ($1/5^{th}$ of the total volume). This was generally incubated at 30°C on shaking at 150rpm, unless specified otherwise. Temperature sensitive strains were cultured at 23°C for normal cell cycle progressions. Media was autoclaved before usage and only filter sterilised media was used for fluorescence microscopy. Prior to any microscopic or biochemical experiments, cells were freshly streaked from -80°C onto agar plates and were inoculated from there into appropriate liquid media.

5.2.2.2 Synchronisations

Fresh cells were inoculated from agar plates two days prior to the synchronisation and maintained in log phase until the day of the experiment.

To synchronise yeast cells in G_1 phase, log phase (OD_{600}<1, 5 x 10^6 cells/ml) was used. Yeast cultures were treated with synthetic alpha-factor (10 µg/ml, Sigma-

Aldrich) for one and a half doubling time (maximum 2.5 hours at 30°C and 3 hours at 23°C), until >95% cells formed shmoo like structures and were arrested in G_1 phase. Experiments where cells needed to be released from the G_1 synchrony into normal cell cycle progression or to cause metaphase arrest, the cells were washed with pre-warmed alpha-factor fresh media twice and later resuspended in fresh flasks using alpha-factor free media.

To induce arrest of cells in metaphase, yeast cultures were treated with nocodazole (15 µg/ml, Sigma-Aldrich). In case of time course experiments samples were collected at specific time intervals and samples were taken both for biochemical analysis and budding index to insure the percentage of arrest. For end point analysis in metaphase, cells were harvested after 2.5-3 hours of nocodazole treatment at 30°C.

For inactivation of analog sensitive (as) Cdc28 mutant – Cdc28-as, PP1 analog II, 1NM-PP1 (25 µM, Sigma) was used.

5.2.2.3 Survival drop tests

To assess survival of various yeast strains, drop tests were performed.

The strains to be tested were inoculated in a 24 well plate with 1ml medium/ well, to get an overnight dense culture. The cultures of each strain were adjusted to get 1 OD_{600} (A, 2 x 10^7 cells/ml) using either sterile PBS or H_2O. Using this dilution, consecutive serial dilutions of 1:10 (B), 1:100 (C), 1:1000 (D), 1:10000 (E) were made in a 1.5ml Eppendorf tube or a 96 well plate. Each dilution was vortexed/mixed before proceeding to the next step.

Drops of 5-7 µl spotted on fresh air-dried agar plates from lowest (E) to the highest dilution (A). Once all the strains were spotted onto the specific agar plates, they were incubated at appropriate temperatures for 2-3 days.

In cases where cells were selected to grow in the absence of *URA3*-based plasmid, 5- fluoroorotic acid (5-FOA; 1mg/ml) was used in the plates.

5.2.2.4 SPOC assay

To ensure the integrity of SPOC in cells, they were deleted for Kar9 and the tubulin (TUB1) was tagged with yeGFP to visualise the microtubules in them. These strains were inoculated in filter sterilised media two days prior to conducting the assay at 23°C. They were maintained in log phase over the two days and at OD_{600} 0.2-0.3

were shifted to 30°C for 6 hours for population analysis of SPOC. After this, the cells are fixed with 4% Paraformaldehyde (PFA). The fixed samples were imaged under fluorescence microscopy to visualise tubulin. Approximately 100 anaphase cells were counted per strain and each experiment was done in biologically independent triplicates.

5.2.2.5 Cell fixation

Yeast cells were fixed by two ways: (i) 4% Paraformaldehyde (PFA) and (ii) 70% Ethanol.

PFA fixation was carried out in samples where protein localisation had to be visualised (with or without DAPI staining). Whereas, 70% Ethanol was suitable to fix samples only for budding index as this caused cells to dehydrate leading to obscure protein localisation for some proteins.

(i) For PFA fixation, 800 µl of cell culture was mixed with 800 µl of 8% PFA and incubated at room temperature for 10mins. The cells were spun at 5000 rpm for 3 mins and washed with sterile 1X PBS. In order to stain with DAPI, the pellet was resuspended in 500 µl of 1:1000 of DAPI made in 1X PBS (stored at 4°C) and incubated at room temperature for 1-2 hours. They were spun after that and resuspended in 5-10 µl of sterile 1X PBS to visualise under the microscope.

(ii) 300 µl of yeast cell culture was mixed with 700 µl of 100% Ethanol and incubated on ice to fix them. The cells were then spun and resuspended in 500 µl of 1:10,000 of DAPI in 1X PBS (stored at 4°C). After incubating for 10-30mins, the cells were spun again and visualised under the microscope.

5.2.2.6 Budding index

Budding index was calculated for experiments to estimate the percentage of cells in various cell cycle stages. This was achieved by staining ethanol fixed cells with 4 '6-diamidino-2-phenylindole (DAPI) (Sigma-Aldrich). 100 cells were counted for sample, each time point in case of time course experiments and cells with small bud-one DAPI, large bud-one DAPI and large bud-two DAPI were counted. These were plotted separately as percentage of total cells to understand the budding index of cultures.

5.2.2.7 Yeast two-hybrid

Yeast two-hybrid to identify the Mck1 interacting partners in a subset of genes was done along with a master's thesis student in the lab.

Plasmids coding for *LexA* and *Gal4* fusion proteins of the subset of genes that I wished to test for putative interactions with Mck1 and its kinase dead version. These plasmids were transformed into yeast strains of opposite mating types namely, YPH500 (MATα) and SGY37 (MATa). The transformants carrying *LexA* and *Gal4* encoding fusion proteins were selected on SC-Leu and SC-His plates, respectively. Multiple colonies from this were pooled together and streaked on selection plates. The strains carrying *LexA* fusion plasmids were mated with *Gal4* fusion carrying strains on YPD plates. These were replica-plated on double selection (SC-Leu-His) plates to be selected for diploid strains carrying both the selection plasmids. Two-three days after that, the replica plates were covered with an overlay solution to detect blue colour formation, indicating positive interaction between the two proteins carried by the plasmids.

Overlay solution: 0.4% low melting agarose, 1mM $MgCl_2$, 10mM KCl, 0.1% SDS, 0.25 NaPi buffer pH 7.0 and 0.04% X-Gal (5-Bromo-4-Chloro-3-Indolyl β-D-Galactopyranoside) (Invitrogen).

5.2.3 Biochemical and immunological methods

5.2.3.1 Yeast cell lysates using TCA precipitation

Yeast cells of known OD_{600} were harvested at 14000rpm for 2 min at room temperature and pellets were straightaway frozen on dry ice to either store at -20°C or continue with protein precipitation.

The frozen pellets were resuspended in 800 µl of sterile ice-cold H_2O and 150 µl of 1.85M NaOH was added immediately. The samples were vortexed well and 150 µl of 55% (w/w) Trichloroacetic acid (TCA) was added. This was vortexed again and incubated on ice for 10mins. The samples were subjected to centrifuge at 14000 rpm for 20mins at 4°C. After this, the supernatant was aspirated and centrifuged briefly. To remove excess supernatant.

The resulting pellets were resuspended with an equivalent amount of HU-DTT sample buffer. (In most cases, 1 OD_{600} of cells were resuspended with 75 µl of HU-DTT and for less abundant proteins like Bfa1 and Cdc6, 75 µl was used).

5.2.3.2 SDS-Polyacrylamide gel electrophoresis (PAGE)

Proteins from yeast lysates were separated based on their sizes using SDS-PAGE. The SDS-PAGE running set up, Mini-PROTEAN II, was obtained from Bio-Rab Laboratories. SDS-PAGE gels used in this study were self-prepared and stored at 4°C to be used within 1-2 weeks.

SDS-PAGE gel composition:

Ingredient	**Resolving gel** (5ml/gel)			**Stacking gel** (2ml/gel)
Acrylamide % in the gel	8	10	12	4
30% Acrylamide (Roth) (ml)	1.3	1.68	1.55	0.325
1.5M Tris-HCl pH 8.8 (ml)	1.25	1.25	1.25	-
0.5M Tris-HCl pH 6.8 (ml)	-	-	-	0.625
10% SDS (µl)	50	50	50	25
10% Ammonium persulfate (APS) (µl)	25	25	25	12.5
Tetramethylethylenediamine TEMED (Roth) (µl)	5	5	5	2.5
H_2O (ml)	2.38	2	1.7	1.55

Yeast cell lysates were heated at 65°C for 15mins, before loading on the SDS-PAGE gels. Samples were cooled down and then centrifuged at 14000rpm for 2mins. Generally, 15 µl was loaded for each sample per well. The gels were run at constant ampere (20mA/gel) and voltage was limited to 100V until the samples were stacked appropriately and entered the resolving gel. After this the voltage was limited to 150V. Molecular weight markers were used as standards – pre-stained, dual colour (Bio-Rad) or unstained (Fermentas).

8% SDS-PAGE gels were used to observe Bfa1-3HA phospho-shift and 10% SDS-PAGE gels for Mob1-6HA, Nud1-6HA, Pds1-6HA and Spc72-6HA. SDS-PAGE gels that were used to detect phosphorylated proteins were run in a cold room (4°C) at constant ampere (20mA/gel) and voltage was limited to 50V and increased to 100V once the sample entered resolving gel for 3-4 hours.

5.2.3.3 Semi-dry transfer of proteins

Semi-dry was used for detecting proteins separated by SDS-PAGE. Once the gels were run, the stacking gel was cut out of it and the remaining resolving gel along with

six Whatman papers (3mm) and a nitrocellulose membrane (GE Healthcare) for each gel were soaked in 1X blotting buffer. Three Whatman papers, a nitrocellulose membrane, the resolving SDS-PAGE gel and rest of the three Whatman papers were stacked together and placed in the semi-dry blotting apparatus. This was run at constant current-110mA and maximum voltage-16V for 1.5-2 hours.

The nitrocellulose membrane was stained with Ponceau S solution for 30secs to visualise the proteins on it. The membrane was de-stained using a PBST buffer and blocked for 30mins with 5% milk in PBST. After this the membrane was incubated with primary antibody (made in 3% PBST) overnight at 4°C. Membrane was washed with PBST 3 times for 5mins each and incubated with secondary antibody (made in 3% PBST) for 1 hour. The membrane was washed 3 times for 5mins each with PBST and probed with enhanced chemiluminescence (ECL) for one minute (self-made ECL solution 1: solution 2 (1:1) or ECL-plus (Thermo-Scientific) for less abundant proteins). The signal was detected using Amersham ImageQuant 800 documentation system by exposing the membrane between 30secs-1min for up to 10mins.

5.2.3.4 Co-immunoprecipitation protocol

Co-immunoprecipitation (Co-IP) technique was used to identify interaction partners of the target protein by using antibodies against that protein. This pulled down together captures other proteins likely bound to the target protein which can later be subjected to western blotting or MS for further analysis.

Cdc6-yeGFP Co-IP experiments:

Yeast pellets of 100 OD_{600} in ribolyser tubes were used per strain for Co-IP. 300 µl of IP buffer and ice-cold acid washed glass beads (Sigma-Aldrich) until the top of the liquid was added to the yeast cell pellets. The samples were lysed in FastPrep FP120 Cell Distributor (MP Biomedicals). The IP buffer constituted of 40mM HEPES pH 7.5, 220mM potassium acetate, 400mM NaCl, 1mM DTT, 100mM β-glycerophosphate (GP), 35 mg/ml benzamidine, 50mM sodium fluoride (NaF), 5mM sodium orthovanadate ($NaVO_3$), 10mM phenylmethylsulfonyl fluoride (PMSF), EDTA-free protease inhibitor cocktail- PhosSTOP (Roche) and 2 µg/ml DNase I. The lysates were checked under a light microscope to see clumps and check lysis. Once over 95% cells were lysed the tubes were subjected to centrifuge at 4000rpm for 1min at 4°C. Supernatant from this centrifuge were incubated with IP buffer containing detergents- 0.2% Tween20 and 0.4% Triton-X100, for 15mins on ice.

Centrifuge at 14000rpm for 10mins at 4°C was done to get the supernatant from here, which was the total cell extract (TCE).
Concentration of all the TCE was measured using Advanced reagent at 590nm wavelength in the spectrophotometer. The lysates were diluted equally and incubated with 40 µl of prewashed anti-GFP agarose slurry (GFP selector, Nanotag) for 1 hour with rotation (speed 7) at 4°C. The samples were spun at 2000rpm for 4mins and washed 5 times with IP buffer containing detergent. The final pellet was resuspended in HU-DTT buffer, boiled at 65°C for 15mins and later run on SDS-PAGE gels to visualise proteins on semi-dry transferred nitrocellulose membranes.

5.2.4 Microscopy and Image analysis

5.2.4.1 Fluorescence microscopy and Live cell imaging

Nikon Eclipse Ti2 Inverted Microscope Systems with Plan Apo 100x/1.40 Oil objective and an IRIS9 Scientific CMOS camera operating Nikon NIS-Elements Imaging Software was used for still imaging and live cell imaging of Cdc14-mCherry. Only for live cell imaging of yeGFP-tubulin strains, a wide-field fluorescence imaging system (DeltaVision RT; Applied Precision) with a 100x/1.40 NA UPLS Apo UIS2 oil immersion objective lens, a charge-coupled device camera (CoolSNAP HQ/ICX285; Photometrics), a quantifiable laser module, and SoftWoRx software (Applied Precision) was used.
Cells were imaged for 3 µm thickness with varying number z stacks depending on the fluorescent signal and localisation of the proteins. Sola lamp intensity and exposure time for still imaging and live cell imaging was (51% - 800ms-1s) and (5% - 300ms-500ms), respectively.
To perform live cell imaging experiments, temperature was maintained at 30°C and yeast cells were adhered onto the glass-bottom dishes (MatTek) using 6% concanavalin A-type IV (Sigma-aldrich).

5.2.4.2 Image processing and quantification

Images obtained from fluorescence microscopy were processed and analysed in FiJi (Schindelin *et al.*, 2012).For making figures and quantification the maximum Z projection feature in FiJi was used. Image contrast and brightness were adjusted in FiJi as well. Cell counting and intensity measurement from fluorescence microscopy and western blot images was also performed in FiJi.

Statistical analysis and data plotting was performed in Microsoft Excel. Images were assembled in Inkscape 1.2.

6. Supplementary figures

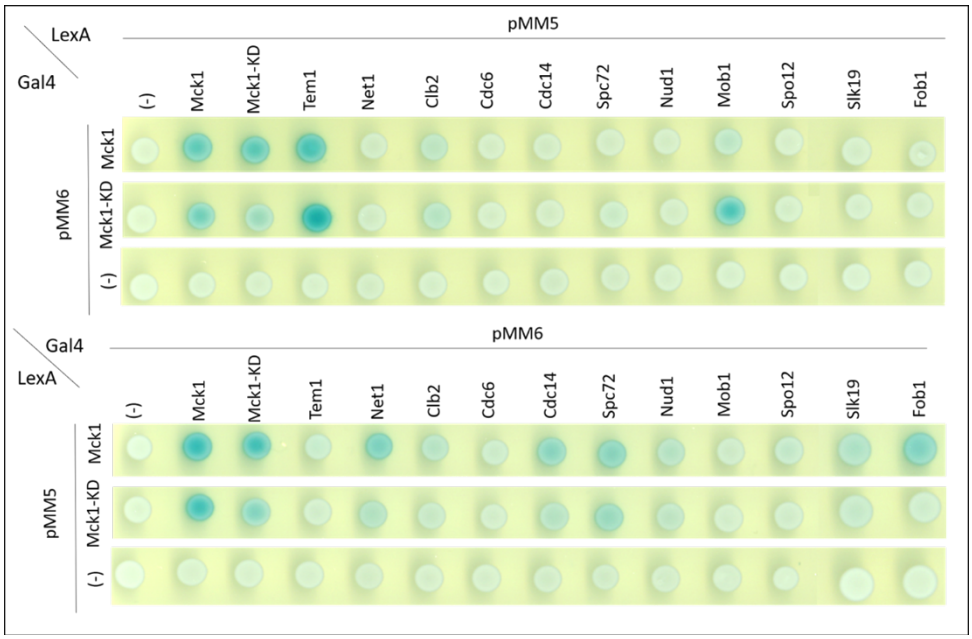

Figure 6-1. Yeast two-hybrid analysis of Mck1 and *mck1-KD* with target proteins. Blue colour formation indicates that two proteins could be interacting with each other. Protein-protein interactions are not the same because of the directionality of yeast two-hybrid assay. (Experiments were conducted with the help of Irem Polat).

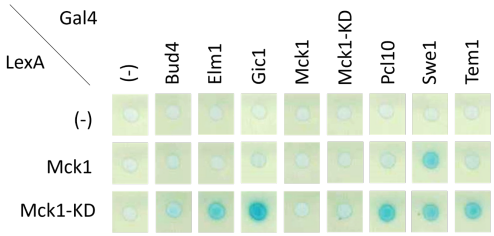

Figure 6-2. Yeast two-hybrid screen of Mck1 and *mck1-KD*. This screen was performed against the whole genome library. However, figure depicts positive interactions that are of interest for this study. Blue colour formation indicates that two proteins could be interacting with each other. (Experiments were conducted with the help of Irem Polat).

7. References

1. Aberle, H, Bauer, A, Stappert, J, Kispert, A, and Kemler, R (1997). β-catenin is a target for the ubiquitin–proteasome pathway. The EMBO Journal 16, 3797–3804.
2. Acebron, SP, Karaulanov, E, Berger, BS, Huang, YL, and Niehrs, C (2014). Mitotic Wnt Signaling Promotes Protein Stabilization and Regulates Cell Size. Molecular Cell 54, 663–674.
3. Acebron, SP, and Niehrs, C (2016). b-Catenin-Independent Roles of Wnt/LRP6 Signaling.
4. Adames, NR, and Cooper, JA (2000). Microtubule interactions with the cell cortex causing nuclear movements in Saccharomyces cerevisiae. J Cell Biol 149, 863–874.
5. Al-Zain, A, Schroeder, L, Sheglov, A, and Ikui, AE (2015). Cdc6 degradation requires phosphodegron created by GSK-3 and Cdk1 for SCFCdc4 recognition in Saccharomyces cerevisiae. Molecular Biology of the Cell 26, 2609–2619.
6. Andoh, T, Hirata, Y, and Kikuchi, A (2000). Yeast Glycogen Synthase Kinase 3 Is Involved in Protein Degradation in Cooperation with Bul1, Bul2, and Rsp5. Molecular and Cellular Biology 20, 6712.
7. Archambault, V, Ikui, AE, Drapkin, BJ, and Cross, FR (2005). Disruption of Mechanisms That Prevent Rereplication Triggers a DNA Damage Response. Molecular and Cellular Biology 25, 6707.
8. Archambault, V, Li, CX, Tackett, AJ, Wäsch, R, Chait, BT, Rout, MP, and Cross, FR (2003). Genetic and biochemical evaluation of the importance of Cdc6 in regulating mitotic exit. Mol Biol Cell 14, 4592–4604.
9. Asakawa, K, Yoshida, S, Otake, F, and Toh-e, A (2001). A novel functional domain of Cdc15 kinase is required for its interaction with Tem1 GTPase in Saccharomyces cerevisiae. Genetics 157, 1437–1450.
10. Azzam, R, Chen, SL, Shou, W, Mah, AS, Alexandru, G, Nasmyth, K, Annan, RS, Carr, SA, and Deshaies, RJ (2004). Phosphorylation by cyclin B-Cdk underlies release of mitotic exit activator Cdc14 from the nucleolus. Science 305, 516–519.
11. Balasubramanian, MK, Bi, E, and Glotzer, M (2004). Comparative analysis of cytokinesis in budding yeast, fission yeast and animal cells. Curr Biol 14.
12. Bardin, AJ, Visintin, R, and Amon, A (2000). A mechanism for coupling exit from mitosis to partitioning of the nucleus. Cell 102, 21–31.
13. Barr, FA, and Gruneberg, U (2007). Cytokinesis: placing and making the final cut. Cell 131, 847–860.
14. Bartek, J, Lukas, C, and Lukas, J (2004). Checking on DNA damage in S phase. Nat Rev Mol Cell Biol 5, 792–804.
15. Bell, SP, and Dutta, A (2003). DNA Replication in Eukaryotic Cells. Http://DxDoiOrg/101146/AnnurevBiochem71110601135425 71, 333–374.
16. Bertazzi, DT, Kurtulmus, B, and Pereira, G (2011). The cortical protein Lte1 promotes mitotic exit by inhibiting the spindle position checkpoint kinase Kin4. J Cell Biol 193, 1033–1048.
17. Bishop, AC et al. (2000). A chemical switch for inhibitor-sensitive alleles of any protein kinase. Nature 2000 407:6802 407, 395–401.
18. Bloecher, A, Venturi, GM, and Tatchell, K (2000). Anaphase spindle position is monitored by the BUB2 checkpoint. Nature Cell Biology 2000 2:8 2, 556–558.
19. Bloom, J, and Cross, FR (2007a). Multiple levels of cyclin specificity in cell-cycle control. Nature Reviews Molecular Cell Biology 2007 8:2 8, 149–160.
20. Bloom, J, and Cross, FR (2007b). Novel Role for Cdc14 Sequestration: Cdc14 Dephosphorylates Factors That Promote DNA Replication. Molecular and Cellular Biology 27, 842.
21. Boronat, S, and Campbell, JL (2007). Mitotic Cdc6 Stabilizes Anaphase-Promoting Complex Substrates by a Partially Cdc28-Independent Mechanism, and This Stabilization Is Suppressed by Deletion of Cdc55. Molecular and Cellular Biology 27, 1158–1171.

22. Breitkreutz, A et al. (2010). A global protein kinase and phosphatase interaction network in yeast. Science (1979) 328, 1043–1046.
23. Brown, JL, Jaquenoud, M, Gulli, MP, Chant, J, and Peter, M (1997). Novel Cdc42-binding proteins Gic1 and Gic2 control cell polarity in yeast. Genes & Development 11, 2972–2982.
24. Bücking-Throm, E, Duntze, W, Hartwell, LH, and Manney, TR (1973). Reversible arrest of haploid yeast cells in the initiation of DNA synthesis by a diffusible sex factor. Exp Cell Res 76, 99–110.
25. Bueno, A, and Russell, P (1992). Dual functions of CDC6: a yeast protein required for DNA replication also inhibits nuclear division. The EMBO Journal 11, 2167–2176.
26. Calzada, A, Sacristán, M, Sánchez, E, and Bueno, A (2001). Cdc6 cooperates with Sic1 and Hct1 to inactivate mitotic cyclin-dependent kinases. Nature 412, 355–358.
27. Castillon, GA, Adames, NR, Rosello, CH, Seidel, HS, Longtine, MS, Cooper, JA, and Heil-Chapdelaine, RA (2003). Septins have a dual role in controlling mitotic exit in budding yeast. Curr Biol 13, 654–658.
28. Caydasi, AK, Khmelinskii, A, Darieva, Z, Kurtulmus, B, Knop, M, and Pereira, G (2020). SWR1 Chromatin Remodeling Complex Prevents Mitotic Slippage during Spindle Position Checkpoint Arrest. BioRxiv, 749440.
29. Caydasi, AK, Khmelinskii, A, Duenas-Sanchez, R, Kurtulmus, B, Knop, M, and Pereira, G (2017). Temporal and compartment-specific signals coordinate mitotic exit with spindle position. Nature Communications 2017 8:1 8, 1–14.
30. Caydasi, AK, Kurtulmus, B, Orrico, MIL, Hofmann, A, Ibrahim, B, and Pereira, G (2010). Elm1 kinase activates the spindle position checkpoint kinase Kin4. The Journal of Cell Biology 190, 975.
31. Caydasi, AK, Micoogullari, Y, Kurtulmus, B, Palani, S, and Pereira, G (2014a). The 14-3-3 protein Bmh1 functions in the spindle position checkpoint by breaking Bfa1 asymmetry at yeast centrosomes. Mol Biol Cell 25, 2143–2151.
32. Caydasi, AK, Micoogullari, Y, Kurtulmus, B, Palani, S, and Pereira, G (2014b). The 14-3-3 protein Bmh1 functions in the spindle position checkpoint by breaking Bfa1 asymmetry at yeast centrosomes. Molecular Biology of the Cell 25, 2143.
33. Caydasi, AK, and Pereira, G (2009). Spindle Alignment Regulates the Dynamic Association of Checkpoint Proteins with Yeast Spindle Pole Bodies. Developmental Cell 16, 146–156.
34. Caydasi, AK, and Pereira, G (2012). SPOC alert--when chromosomes get the wrong direction. Exp Cell Res 318, 1421–1427.
35. Chang, F, Riera, A, Evrin, C, Sun, J, Li, H, Speck, C, and Weinreich, M (2015). Cdc6 ATPase activity disengages Cdc6 from the pre-replicative complex to promote DNA replication. Elife 4.
36. Clevers, H, and Nusse, R (2012). Wnt/β-Catenin Signaling and Disease. Cell 149, 1192–1205.
37. Cocker, JH, Piatti, S, Santocanale, C, Nasmyth, K, and Diffley, JFX (1996). An essential role for the Cdc6 protein in forming the pre-replicative complexes of budding yeast. Nature 379, 180–182.
38. Cottingham, FR, and Hoyt, MA (1997). Mitotic spindle positioning in Saccharomyces cerevisiae is accomplished by antagonistically acting microtubule motor proteins. J Cell Biol 138, 1041–1053.
39. Cross, FR (1995). Starting the cell cycle: what's the point? Current Opinion in Cell Biology 7, 790–797.
40. Dajani, R, Fraser, E, Roe, SM, Young, N, Good, V, Dale, TC, and Pearl, LH (2001). Crystal structure of glycogen synthase kinase 3 beta: structural basis for phosphate-primed substrate specificity and autoinhibition. Cell 105, 721–732.
41. Dalton, S, and Whitbread, L (1995). Cell cycle-regulated nuclear import and export of Cdc47, a protein essential for initiation of DNA replication in budding yeast. Proc Natl Acad Sci U S A 92, 2514–2518.

42. D'Amours, D, Stegmeier, F, and Amon, A (2004). Cdc14 and condensin control the dissolution of cohesin-independent chromosome linkages at repeated DNA. Cell 117, 455–469.
43. D'Aquino, KE, Monje-Casas, F, Paulson, J, Reiser, V, Charles, GM, Lai, L, Shokat, KM, and Amon, A (2005). The protein kinase Kin4 inhibits exit from mitosis in response to spindle position defects. Mol Cell 19, 223–234.
44. Daum, JR, Gomez-Ospina, N, Winey, M, and Burke, DJ (2000). The spindle checkpoint of Saccharomyces cerevisiae responds to separable microtubule-dependent events. Curr Biol 10, 1375–1378.
45. David O. Morgan (2007). Cell Cycle: Principles of Control, New Science Press.
46. Delgado, NS, and Toczyski, DP (2019). Mck1 kinase is a new player in the DNA damage checkpoint pathway. PLoS Genet 15.
47. Drechsler, H, Tan, AN, and Liakopoulos, D (2015). Yeast GSK-3 kinase regulates astral microtubule function through phosphorylation of the microtubule-stabilizing kinesin Kip2. Journal of Cell Science 128, 3910–3921.
48. van Driessche, B, Tafforeau, L, Hentges, P, Carr, AM, and Vandenhaute, J (2005). Additional vectors for PCR-based gene tagging in Saccharomyces cerevisiae and Schizosaccharomyces pombe using nourseothricin resistance. Yeast 22, 1061–1068.
49. Drury, LS, Perkins, G, and Diffley, JFX (1997). The Cdc4/34/53 pathway targets Cdc6p for proteolysis in budding yeast. EMBO J 16, 5966–5976.
50. Drury, LS, Perkins, G, and Diffley, JFX (2000). The cyclin-dependent kinase Cdc28p regulates distinct modes of Cdc6p proteolysis during the budding yeast cell cycle. Curr Biol 10, 231–240.
51. Elledge, SJ, and Harper, JW (1994). Cdk inhibitors: on the threshold of checkpoints and development. Curr Opin Cell Biol 6, 847–852.
52. Elsasser, S, Lou, F, Wang, B, Campbell, JL, and Jong, A (1996). Interaction between yeast Cdc6 protein and B-type cyclin/Cdc28 kinases. Mol Biol Cell 7, 1723–1735.
53. Epstein, CB, and Cross, FR (1992). CLB5: a novel B cyclin from budding yeast with a role in S phase. Genes Dev 6, 1695–1706.
54. Estruch, F, and Carlson, M (1993). Two homologous zinc finger genes identified by multicopy suppression in a SNF1 protein kinase mutant of Saccharomyces cerevisiae. Molecular and Cellular Biology 13, 3872.
55. Evans, T, Rosenthal, ET, Youngblom, J, Distel, D, and Hunt, T (1983). Cyclin: A protein specified by maternal mRNA in sea urchin eggs that is destroyed at each cleavage division. Cell 33, 389–396.
56. Falk, JE, Campbell, IW, Joyce, K, Whalen, J, Seshan, A, and Amon, A (2016). LTE1 promotes exit from mitosis by multiple mechanisms. Molecular Biology of the Cell 27, 3991–4001.
57. Falk, JE, Chan, LY, and Amon, A (2011). Lte1 promotes mitotic exit by controlling the localization of the spindle position checkpoint kinase Kin4. Proc Natl Acad Sci U S A 108, 12584–12590.
58. Fang, X, Yu, SX, Lu, Y, Bast, RC, Woodgett, JR, and Mills, GB (2000). Phosphorylation and inactivation of glycogen synthase kinase 3 by protein kinase A. Proc Natl Acad Sci U S A 97, 11960.
59. Farr, KA, and Cohen-Fix, O (1999). The metaphase to anaphase transition. European Journal of Biochemistry 263, 14–19.
60. Fiol, CJ, Mahrenholz, AM, Wang, Y, Roeske, RW, and Roach, PJ (1987). Formation of protein kinase recognition sites by covalent modification of the substrate. Molecular mechanism for the synergistic action of casein kinase II and glycogen synthase kinase 3. Journal of Biological Chemistry 262, 14042–14048.
61. Foley, EA, and Kapoor, TM (2013). Microtubule attachment and spindle assembly checkpoint signaling at the kinetochore. Nat Rev Mol Cell Biol 14, 25.
62. Forsburg, SL, and Nurse, P (1991). Cell cycle regulation in the yeasts Saccharomyces cerevisiae and Schizosaccharomyces pombe. Annu Rev Cell Biol 7, 227–256.

63. Fraschini, R, Venturetti, M, Chiroli, E, and Piatti, S (2008). The spindle position checkpoint: how to deal with spindle misalignment during asymmetric cell division in budding yeast. Biochem Soc Trans 36, 416–420.
64. Gachet, Y, Reyes, C, Goldstone, S, and Tournier, S (2006). The fission yeast spindle orientation checkpoint: a model that generates tension? Yeast 23, 1015–1029.
65. Gardner, RD, Poddar, A, Yellman, C, Tavormina, PA, Monteagudo, MC, and Burke, DJ (2001). The spindle checkpoint of the yeast Saccharomyces cerevisiae requires kinetochore function and maps to the CBF3 domain. Genetics 157, 1493–1502.
66. Geymonat, M, Jensen, S, and Johnston, LH (2002). Mitotic exit: the Cdc14 double cross. Curr Biol 12.
67. Geymonat, M, Spanos, A, Jensen, S, and Sedgwick, SG (2010). Phosphorylation of Lte1 by Cdk prevents polarized growth during mitotic arrest in S. cerevisiae. The Journal of Cell Biology 191, 1097.
68. Geymonat, M, Spanos, A, Walker, PA, Johnston, LH, and Sedgwick, SG (2003). In vitro regulation of budding yeast Bfa1/Bub2 GAP activity by Cdc5. J Biol Chem 278, 14591–14594.
69. Görner, W, Durchschlag, E, Wolf, J, Brown, EL, Ammerer, G, Ruis, H, and Schüller, C (2002). Acute glucose starvation activates the nuclear localization signal of a stress-specific yeast transcription factor. EMBO J 21, 135–144.
70. Griffioen, G, Swinnen, S, and Thevelein, JM (2003). Feedback inhibition on cell wall integrity signaling by Zds1 involves Gsk3 phosphorylation of a cAMP-dependent protein kinase regulatory subunit. J Biol Chem 278, 23460–23471.
71. Gruneberg, U, Campbell, K, Simpson, C, Grindlay, J, and Schiebel, E (2000). Nud1p links astral microtubule organization and the control of exit from mitosis. EMBO J 19, 6475–6488.
72. Gutin, J, Joseph-Strauss, D, Sadeh, A, Shalom, E, and Friedman, N (2019). Genetic screen of the yeast environmental stress response dynamics uncovers distinct regulatory phases. Molecular Systems Biology 15, e8939.
73. Hartwell, LH, Culotti, J, Pringle, JR, and Reid, BJ (1974). Genetic control of the cell division cycle in yeast. Science 183, 46–51.
74. Heil-Chapdelaine, RA, Oberle, JR, and Cooper, JA (2000). The Cortical Protein Num1p Is Essential for Dynein-Dependent Interactions of Microtubules with the Cortex. The Journal of Cell Biology 151, 1337.
75. Henneke, G, Koundrioukoff, S, and Hübscher, U (2003). Multiple roles for kinases in DNA replication. EMBO Rep 4, 252–256.
76. Hilioti, Z, Gallagher, DA, Low-Nam, ST, Ramaswamy, P, Gajer, P, Kingsbury, TJ, Birchwood, CJ, Levchenko, A, and Cunningham, KW (2004). GSK-3 kinases enhance calcineurin signaling by phosphorylation of RCNs. Genes Dev 18, 35–47.
77. Ho, Y et al. (2002). Systematic identification of protein complexes in Saccharomyces cerevisiae by mass spectrometry. Nature 415, 180–183.
78. Höfken, T, and Schiebel, E (2002). A role for cell polarity proteins in mitotic exit. EMBO J 21, 4851–4862.
79. Höfken, T, and Schiebel, E (2004). Novel regulation of mitotic exit by the Cdc42 effectors Gic1 and Gic2. Journal of Cell Biology 164, 219–231.
80. Hu, F, Wang, Y, Liu, D, Li, Y, Qin, J, and Elledge, SJ (2001). Regulation of the Bub2/Bfa1 GAP complex by Cdc5 and cell cycle checkpoints. Cell 107, 655–665.
81. Huang, YL, Anvarian, Z, Döderlein, G, Acebron, SP, and Niehrs, C (2015). Maternal Wnt/STOP signaling promotes cell division during early Xenopus embryogenesis. Proc Natl Acad Sci U S A 112, 5732–5737.
82. Huberman, JA (1996). Cell cycle control of S phase: A comparison of two yeasts. Chromosoma 1996 105:4 105, 197–203.
83. Ikui, AE, Rossio, V, Schroeder, L, and Yoshida, S (2012). A Yeast GSK-3 Kinase Mck1 Promotes Cdc6 Degradation to Inhibit DNA Re-Replication. PLOS Genetics 8, e1003099.

84. Janke, C et al. (2004). A versatile toolbox for PCR-based tagging of yeast genes: new fluorescent proteins, more markers and promoter substitution cassettes. Yeast 21, 947–962.
85. Jaspersen, SL, Charles, JF, and Morgan, DO (1999). Inhibitory phosphorylation of the APC regulator Hct1 is controlled by the kinase Cdc28 and the phosphatase Cdc14. Current Biology 9, 227–236.
86. Jaspersen, SL, Charles, JF, Tinker-Kulberg, RL, and Morgan, DO (1998). A late mitotic regulatory network controlling cyclin destruction in Saccharomyces cerevisiae. Mol Biol Cell 9, 2803–2817.
87. Jaspersen, SL, and Winey, M (2004). The budding yeast spindle pole body: structure, duplication, and function. Annu Rev Cell Dev Biol 20, 1–28.
88. Jensen, S, Geymonat, M, Johnson, AL, Segal, M, and Johnston, LH (2002). Spatial regulation of the guanine nucleotide exchange factor Lte1 in Saccharomyces cerevisiae. Journal of Cell Science 115, 4977–4991.
89. Jiang, W, Lim, MY, Yoon, HJ, Thorner, J, Martin, GS, and Carbon, J (1995). Overexpression of the yeast MCK1 protein kinase suppresses conditional mutations in centromere-binding protein genes CBF2 and CBF5. Mol Gen Genet 246, 360–366.
90. Johnson, DG, and Walker, CL (1999). Cyclins and cell cycle checkpoints. Annu Rev Pharmacol Toxicol 39, 295–312.
91. Jorgensen, P, Rupeš, I, Sharom, JR, Schneper, L, Broach, JR, and Tyers, M (2004). A dynamic transcriptional network communicates growth potential to ribosome synthesis and critical cell size. Genes Dev 18, 2491–2505.
92. Karakaidos, P et al. (2004). Overexpression of the replication licensing regulators hCdt1 and hCdc6 characterizes a subset of non-small-cell lung carcinomas: synergistic effect with mutant p53 on tumor growth and chromosomal instability--evidence of E2F-1 transcriptional control over hCdt1. The American Journal of Pathology 165, 1351–1365.
93. Khmelinskii, A, Lawrence, C, Roostalu, J, and Schiebel, E (2007). Cdc14-regulated midzone assembly controls anaphase B. J Cell Biol 177, 981–993.
94. Khmelinskii, A, Roostalu, J, Roque, H, Antony, C, and Schiebel, E (2009). Phosphorylation-dependent protein interactions at the spindle midzone mediate cell cycle regulation of spindle elongation. Dev Cell 17, 244–256.
95. Kim, DH, Zhang, W, and Koepp, DM (2012). The Hect domain E3 ligase Tom1 and the F-box protein Dia2 control Cdc6 degradation in G1 phase. J Biol Chem 287, 44212–44220.
96. Kishi, T, Ikeda, A, Nagao, R, and Koyama, N (2007). The SCFCdc4 ubiquitin ligase regulates calcineurin signaling through degradation of phosphorylated Rcn1, an inhibitor of calcineurin. Proc Natl Acad Sci U S A 104, 17418–17423.
97. Knop, M, Siegers, K, Pereira, G, Zachariae, W, Winsor, B, Nasmyth, K, and Schiebel, E (1999). Epitope tagging of yeast genes using a PCR-based strategy: more tags and improved practical routines. Yeast 15, 963–972.
98. Kocakaplan, D, Karabürk, H, Dilege, C, Kirdok, I, Bektaş, ŞN, and Caydasi, AK (2021). Protein phosphatase 1 in association with bud14 inhibits mitotic exit in saccharomyces cerevisiae. Elife 10.
99. Koch, C, Schleiffer, A, Ammerer, G, and Nasmyth, K (1996). Switching transcription on and off during the yeast cell cycle: Cln/Cdc28 kinases activate bound transcription factor SBF (Swi4/Swi6) at start, whereas Clb/Cdc28 kinases displace it from the promoter in G2. Genes Dev 10, 129–141.
100. König, C, Maekawa, H, and Schiebel, E (2010). Mutual regulation of cyclin-dependent kinase and the mitotic exit network. Journal of Cell Biology 188, 351–368.
101. Kono, K, Al-Zain, A, Schroeder, L, Nakanishi, M, and Ikui, AE (2016). Plasma membrane/cell wall perturbation activates a novel cell cycle checkpoint during G1 in Saccharomyces cerevisiae. Proc Natl Acad Sci U S A 113, 6910–6915.
102. Lechler, T, and Fuchs, E (2005). Asymmetric cell divisions promote stratification and differentiation of mammalian skin. Nature 437, 275–280.

103. Lee, L, Tirnauer, JS, Li, J, Schuyler, SC, Liu, JY, and Pellman, D (2000). Positioning of the mitotic spindle by a cortical-microtubule capture mechanism. Science 287, 2260–2262.
104. Lee, MG, and Nurse, P (1987). Complementation used to clone a human homologue of the fission yeast cell cycle control gene cdc2. Nature 1987 327:6117 327, 31–35.
105. Lee, SE, Frenz, LM, Wells, NJ, Johnson, AL, and Johnston, LH (2001a). Order of function of the budding-yeast mitotic exit-network proteins Tem1, Cdc15, Mob1, Dbf2, and Cdc5. Curr Biol 11, 784–788.
106. Lee, SE, Jensen, S, Frenz, LM, Johnson, AL, Fesquet, D, and Johnston, LH (2001b). The Bub2-dependent mitotic pathway in yeast acts every cell cycle and regulates cytokinesis. Journal of Cell Science 114, 2345–2354.
107. Lee, WL, Oberle, JR, and Cooper, JA (2003). The role of the lissencephaly protein Pac1 during nuclear migration in budding yeast. Journal of Cell Biology 160, 355–364.
108. Levine, K, Tinkelenberg, AH, and Cross, F (1995). The CLN gene family: central regulators of cell cycle Start in budding yeast. Prog Cell Cycle Res 1, 101–114.
109. Lew, DJ, and Burke, DJ (2003). The Spindle Assembly and Spindle Position Checkpoints. Http://DxDoiOrg/101146/AnnurevGenet37042203120656 37, 251–282.
110. Lew, DJ, and Reed, SI (1995). Cell cycle control of morphogenesis in budding yeast. Curr Opin Genet Dev 5, 17–23.
111. Li, R (1999). Bifurcation of the mitotic checkpoint pathway in budding yeast. Proc Natl Acad Sci U S A 96, 4989–4994.
112. Li, X et al. (2019). Mck1 defines a key S-phase checkpoint effector in response to various degrees of replication threats. PLOS Genetics 15, e1008136.
113. Luo, KQ, Elsasser, S, Chang, DC, and Campbell, JL (2003). Regulation of the localization and stability of Cdc6 in living yeast cells. Biochem Biophys Res Commun 306, 851–859.
114. Mackay, V, and Manney, TR (1974). Mutations affecting sexual conjugation and related processes in Saccharomyces cerevisiae. II. Genetic analysis of nonmating mutants. Genetics 76, 273–288.
115. Maekawa, H, Neuner, A, Rüthnick, D, Schiebel, E, Pereira, G, and Kaneko, Y (2017). Polo-like kinase Cdc5 regulates Spc72 recruitment to spindle pole body in the methylotrophic yeast Ogataea polymorpha. Elife 6.
116. Maekawa, H, Priest, C, Lechner, J, Pereira, G, and Schiebel, E (2007). The yeast centrosome translates the positional information of the anaphase spindle into a cell cycle signal. J Cell Biol 179, 423–436.
117. Maekawa, H, and Schiebel, E (2004). Cdk1-Clb4 controls the interaction of astral microtubule plus ends with subdomains of the daughter cell cortex. Genes Dev 18, 1709–1724.
118. Mah, AS, Jang, J, and Deshaies, RJ (2001). Protein kinase Cdc15 activates the Dbf2-Mob1 kinase complex. Proc Natl Acad Sci U S A 98, 7325–7330.
119. Malathi, K, Xiao, Y, and Mitchell, AP (1997). Interaction of yeast repressor-activator protein Ume6p with glycogen synthase kinase 3 homolog Rim11p. Molecular and Cellular Biology 17, 7230–7236.
120. McInerny, CJ, Partridge, JF, Mikesell, GE, Creemer, DP, and Breeden, LL (1997). A novel Mcm1-dependent element in the SWI4, CLN3, CDC6, and CDC47 promoters activates M/G1-specific transcription. Genes & Development 11, 1277–1288.
121. McQueen, J, van Dyk, D, Young, B, Loewen, C, and Measday, V (2012). The Mck1 GSK-3 kinase inhibits the activity of Clb2-Cdk1 post-nuclear division. Cell Cycle 11, 3421.
122. Meitinger, F, Palani, S, and Pereira, G (2012). The power of MEN in cytokinesis. Cell Cycle 11, 219–228.

123. Meitinger, F, Petrova, B, Mancini Lombardi, I, Trinca Bertazzi, D, Hub, B, Zentgraf, H, and Pereira, G (2010). Targeted localization of Inn1, Cyk3 and Chs2 by the mitotic-exit network regulates cytokinesis in budding yeast. J Cell Sci 123, 1851–1861.
124. Menssen, R, Neutzner, A, and Seufert, W (2001). Asymmetric spindle pole localization of yeast Cdc15 kinase links mitotic exit and cytokinesis. Curr Biol 11, 345–350.
125. Mewes, HW et al. (1997). Overview of the yeast genome. Nature 387, 737.
126. Miller, RK, D'Silva, S, Moore, JK, and Goodson, H v. (2006). The CLIP-170 orthologue Bik1p and positioning the mitotic spindle in yeast. Curr Top Dev Biol 76, 49–87.
127. Miller, RK, Heller, KK, Frisèn, L, Wallack, DL, Loayza, D, Gammie, AE, and Rose, MD (1998). The Kinesin-related Proteins, Kip2p and Kip3p, Function Differently in Nuclear Migration in Yeast. Molecular Biology of the Cell 9, 2051.
128. Miller, RK, and Rose, MD (1998). Kar9p Is a Novel Cortical Protein Required for Cytoplasmic Microtubule Orientation in Yeast. The Journal of Cell Biology 140, 377.
129. Mimura, S, Seki, T, Tanaka, S, and Diffley, JFX (2004). Phosphorylation-dependent binding of mitotic cyclins to Cdc6 contributes to DNA replication control. Nature 431, 1118–1123.
130. Mizunuma, M, Hirata, D, Miyaoka, R, and Miyakawa, T (2001). GSK-3 kinase Mck1 and calcineurin coordinately mediate Hsl1 down-regulation by Ca2+ in budding yeast. The EMBO Journal 20, 1074.
131. Mohl, DA, Huddleston, MJ, Collingwood, TS, Annan, RS, and Deshaies, RJ (2009). Dbf2-Mob1 drives relocalization of protein phosphatase Cdc14 to the cytoplasm during exit from mitosis. J Cell Biol 184, 527–539.
132. Molk, JN, Schuyler, SC, Liu, JY, Evans, JG, Salmon, ED, Pellman, D, and Bloom, K (2004). The Differential Roles of Budding Yeast Tem1p, Cdc15p, and Bub2p Protein Dynamics in Mitotic Exit. Molecular Biology of the Cell 15, 1519.
133. Monje-Casas, F, and Amon, A (2009). Cell polarity determinants establish asymmetry in MEN signaling. Dev Cell 16, 132–145.
134. Moore, JK, and Cooper, JA (2010). Coordinating mitosis with cell polarity: Molecular motors at the cell cortex. Semin Cell Dev Biol 21, 283–289.
135. Morgan, DO (1997). Cyclin-dependent kinases: engines, clocks, and microprocessors. Annu Rev Cell Dev Biol 13, 261–291.
136. Musacchio, A, and Salmon, ED (2007). The spindle-assembly checkpoint in space and time. Nature Reviews Molecular Cell Biology 2007 8:5 8, 379–393.
137. Nasmyth, K (1993). Control of the yeast cell cycle by the Cdc28 protein kinase. Curr Opin Cell Biol 5, 166–179.
138. Neigeborn, L, and Mitchell, AP (1991). The yeast MCK1 gene encodes a protein kinase homolog that activates early meiotic gene expression. Genes & Development 5, 533–548.
139. Nelson, SA, and Cooper, JA (2007). A novel pathway that coordinates mitotic exit with spindle position. Mol Biol Cell 18, 3440–3450.
140. Neuwald, AF, Aravind, L, Spouge, JL, and Koonin, E v. (1999). AAA+: A Class of Chaperone-Like ATPases Associated with the Assembly, Operation, and Disassembly of Protein Complexes. Genome Research 9, 27–43.
141. Nguyen, VQ, Co, C, and Li, JJ (2001). Cyclin-dependent kinases prevent DNA re-replication through multiple mechanisms. Nature 411, 1068–1073.
142. Nyberg, KA, Michelson, RJ, Putnam, CW, and Weinert, TA (2002). Toward maintaining the genome: DNA damage and replication checkpoints. Annu Rev Genet 36, 617–656.
143. Ohta, S (2001). Cdc6 expression as a marker of proliferative activity in brain tumors. Oncology Reports 8, 1063–1066.
144. Örd, M, Möll, K, Agerova, A, Kivi, R, Faustova, I, Venta, R, Valk, E, and Loog, M (2019). Multisite phosphorylation code of CDK. Nat Struct Mol Biol 26, 649–658.

145. Osborn, MJ, and Miller, RJ (2007). Rescuing yeast mutants with human genes. Brief Funct Genomic Proteomic 6, 104–111.
146. Pal, G, Paraz, MTZ, and Kellogg, DR (2008). Regulation of Mih1/Cdc25 by protein phosphatase 2A and casein kinase 1. Journal of Cell Biology 180, 931–945.
147. Pereira, G, Höfken, T, Grindlay, J, Manson, C, and Schiebel, E (2000). The Bub2p Spindle Checkpoint Links Nuclear Migration with Mitotic Exit. Molecular Cell 6, 1–10.
148. Pereira, G, Manson, C, Grindlay, J, and Schiebel, E (2002). Regulation of the Bfa1p–Bub2p complex at spindle pole bodies by the cell cycle phosphatase Cdc14p. Journal of Cell Biology 157, 367–379.
149. Pereira, G, and Schiebel, E (2004). Cdc14 phosphatase resolves the rDNA segregation delay. Nature Cell Biology 2004 6:6 6, 473–475.
150. Pereira, G, and Schiebel, E (2005). Kin4 kinase delays mitotic exit in response to spindle alignment defects. Mol Cell 19, 209–221.
151. Pereira, G, Tanaka, TU, Nasmyth, K, and Schiebel, E (2001). Modes of spindle pole body inheritance and segregation of the Bfa1p–Bub2p checkpoint protein complex. The EMBO Journal 20, 6359.
152. Perkins, G, and Diffley, JFX (1998). Nucleotide-dependent prereplicative complex assembly by Cdc6p, a homolog of eukaryotic and prokaryotic clamp-loaders. Mol Cell 2, 23–32.
153. Perkins, G, Drury, LS, and Diffley, JFX (2001). Separate SCFCDC4 recognition elements target Cdc6 for proteolysis in S phase and mitosis. The EMBO Journal 20, 4836.
154. Philip, J, Örd, M, Silva, A, Singh, S, Diffley, JF, Remus, D, Loog, M, and Ikui, AE (2022). Cdc6 is sequentially regulated by PP2A-Cdc55, Cdc14, and Sic1 for origin licensing in S. cerevisiae. Elife 11.
155. Piatti, S, Lengauer, C, and Nasmyth, K (1995). Cdc6 is an unstable protein whose de novo synthesis in G1 is important for the onset of S phase and for preventing a “reductional” anaphase in the budding yeast Saccharomyces cerevisiae. EMBO J 14, 3788–3799.
156. Piatti, S, Venturetti, M, Chiroli, E, and Fraschini, R (2006). The spindle position checkpoint in budding yeast: the motherly care of MEN. Cell Division 1, 2.
157. Puziss, JW, Hardy, TA, Johnson, RB, Roach, PJ, and Hieter, P (1994). MDS1, a dosage suppressor of an mck1 mutant, encodes a putative yeast homolog of glycogen synthase kinase 3. Mol Cell Biol 14, 831–839.
158. Queralt, E, Lehane, C, Novak, B, and Uhlmann, F (2006). Downregulation of PP2A(Cdc55) phosphatase by separase initiates mitotic exit in budding yeast. Cell 125, 719–732.
159. Rashid, MS, Mazur, T, Ji, W, Liu, ST, and Taylor, WR (2018). Analysis of the role of GSK3 in the mitotic checkpoint. Scientific Reports 2018 8:1 8, 1–16.
160. Rayner, TF, Gray, J v., and Thorner, JW (2002). Direct and novel regulation of cAMP-dependent protein kinase by Mck1p, a yeast glycogen synthase kinase-3. J Biol Chem 277, 16814–16822.
161. Rock, JM et al. (2013). Activation of the yeast Hippo pathway by phosphorylation-dependent assembly of signaling complexes. Science 340, 871–875.
162. Rock, JM, and Amon, A (2009). The FEAR network. Curr Biol 19.
163. Roostalu, J, Schiebel, E, and Khmelinskii, A (2010). Cell cycle control of spindle elongation. Cell Cycle 9, 1084–1090.
164. Rose, D, Price, BR, and Fink, GR (1986). Saccharomyces cerevisiae nuclear fusion requires prior activation by alpha factor. Molecular and Cellular Biology 6, 3490.
165. Rothstein, R (1991). Targeting, disruption, replacement, and allele rescue: integrative DNA transformation in yeast. Methods Enzymol 194, 281–301.
166. Rubin-Bejerano, I, Sagee, S, Friedman, O, Pnueli, L, and Kassir, Y (2004). The in vivo activity of Ime1, the key transcriptional activator of meiosis-specific genes in Saccharomyces cerevisiae, is inhibited by the cyclic AMP/protein kinase A signal

pathway through the glycogen synthase kinase 3-beta homolog Rim11. Mol Cell Biol 24, 6967–6979.
167. Sánchez, M, Calzada, A, and Bueno, A (1999). The Cdc6 Protein Is Ubiquitinated in Vivo for Proteolysis in Saccharomyces cerevisiae. Journal of Biological Chemistry 274, 9092–9097.
168. Scarfone, I, and Piatti, S (2015). Coupling spindle position with mitotic exit in budding yeast: The multifaceted role of the small GTPase Tem1. Small GTPases 6, 196–201.
169. Schindelin, J et al. (2012). Fiji: an open-source platform for biological-image analysis. Nature Methods 9, 676–682.
170. Seshan, A, Bardin, AJ, and Amon, A (2002). Control of Lte1 localization by cell polarity determinants and Cdc14. Curr Biol 12, 2098–2110.
171. Sharp, DJ, Rogers, GC, and Scholey, JM (2000). Microtubule motors in mitosis. Nature 407, 41–47.
172. Shero, JH, and Hieter, P (1991). A suppressor of a centromere DNA mutation encodes a putative protein kinase (MCK1). Genes Dev 5, 549–560.
173. Shirayama, M, Matsui, Y, Tanaka, K, and Toh-E, A (1994a). Isolation of a CDC25 family gene, MSI2/LTE1, as a multicopy suppressor of ira1. Yeast 10, 451–461.
174. Shirayama, M, Matsui, Y, and Toh-E, A (1994b). The yeast TEM1 gene, which encodes a GTP-binding protein, is involved in termination of M phase. Molecular and Cellular Biology 14, 7476–7482.
175. Shou, W, Seol, JH, Shevchenko, A, Baskerville, C, Moazed, D, Susan Chen, ZW, Jang, J, Shevchenko, A, Charbonneau, H, and Deshaies, RJ (1999). Exit from mitosis is triggered by Tem1-dependent release of the protein phosphatase Cdc14 from nucleolar RENT complex. Cell 97, 233–244.
176. Siller, KH, and Doe, CQ (2009). Spindle orientation during asymmetric cell division. Nat Cell Biol 11, 365–374.
177. Simanis, V (2003). Events at the end of mitosis in the budding and fission yeasts. J Cell Sci 116, 4263–4275.
178. Snead, JL, Sullivan, M, Lowery, DM, Cohen, MS, Zhang, C, Randle, DH, Taunton, J, Yaffe, MB, Morgan, DO, and Shokat, KM (2007). A coupled chemical-genetic and bioinformatic approach to Polo-like kinase pathway exploration. Chem Biol 14, 1261–1272.
179. Speck, C, Chen, Z, Li, H, and Stillman, B (2005). ATPase-dependent cooperative binding of ORC and Cdc6 to origin DNA. Nat Struct Mol Biol 12, 965–971.
180. Spellman, PT, Sherlock, G, Zhang, MQ, Iyer, VR, Anders, K, Eisen, MB, Brown, PO, Botstein, D, and Futcher, B (1998). Comprehensive identification of cell cycle-regulated genes of the yeast Saccharomyces cerevisiae by microarray hybridization. Mol Biol Cell 9, 3273–3297.
181. Stamos, JL, and Weis, WI (2013). The β-Catenin Destruction Complex. Cold Spring Harbor Perspectives in Biology 5.
182. Stegmeier, F, and Amon, A (2004a). Closing mitosis: the functions of the Cdc14 phosphatase and its regulation. Annu Rev Genet 38, 203–232.
183. Stegmeier, F, and Amon, A (2004b). Closing mitosis: the functions of the Cdc14 phosphatase and its regulation. Annu Rev Genet 38, 203–232.
184. Stegmeier, F, Visintin, R, and Amon, A (2002). Separase, polo kinase, the kinetochore protein Slk19, and Spo12 function in a network that controls Cdc14 localization during early anaphase. Cell 108, 207–220.
185. Stolz, A, Neufeld, K, Ertych, N, and Bastians, H (2015). Wnt-mediated protein stabilization ensures proper mitotic microtubule assembly and chromosome segregation. EMBO Rep 16, 490–499.
186. Strathern, JN, Jones, EW, and Broach, JR (1981). The Molecular biology of the yeast saccharomyces, life cycle and inheritance, Cold Spring Harbor, N.Y.: Cold Spring Harbor Laboratory.

187. Sullivan, M, and Morgan, DO (2007). Finishing mitosis, one step at a time. Nat Rev Mol Cell Biol 8, 894–903.
188. Surana, U, Yeong, FM, and Lim, HH (2002). MEN, destruction and separation: mechanistic links between mitotic exit and cytokinesis in budding yeast. Bioessays 24, 659–666.
189. Taelman, VF, Dobrowolski, R, Plouhinec, JL, Fuentealba, LC, Vorwald, PP, Gumper, I, Sabatini, DD, and de Robertis, EM (2010). Wnt signaling requires sequestration of glycogen synthase kinase 3 inside multivesicular endosomes. Cell 143, 1136–1148.
190. Tighe, A, Ray-Sinha, A, Staples, OD, and Taylor, SS (2007). GSK-3 inhibitors induce chromosome instability. BMC Cell Biology 8, 1–17.
191. Tomson, BN, Rahal, R, Reiser, V, Monje-Casas, F, Mekhail, K, Moazed, D, and Amon, A (2009). Regulation of Spo12 phosphorylation and its essential role in the FEAR network. Curr Biol 19, 449–460.
192. Ubersax, JA, Woodbury, EL, Quang, PN, Paraz, M, Blethrow, JD, Shah, K, Shokat, KM, and Morgan, DO (2003). Targets of the cyclin-dependent kinase Cdk1. Nature 425, 859–864.
193. Uhlmann, F, Lottspelch, F, and Nasmyth, K (1999). Sister-chromatid separation at anaphase onset is promoted by cleavage of the cohesin subunit Scc1. Nature 400, 37–42.
194. Valerio-Santiago, M, and Monje-Casas, F (2011). Tem1 localization to the spindle pole bodies is essential for mitotic exit and impairs spindle checkpoint function. Journal of Cell Biology 192, 599–614.
195. Vannini, M, Mingione, VR, Meyer, A, Sniffen, C, Whalen, J, and Seshan, A (2022). A novel hyperactive nud1 mitotic exit network scaffold causes spindle position checkpoint bypass in budding yeast. Cells 11.
196. Vaziri, C, Saxena, S, Jeon, Y, Lee, C, Murata, K, Machida, Y, Wagle, N, Hwang, DS, and Dutta, A (2003). A p53-dependent checkpoint pathway prevents rereplication. Molecular Cell 11, 997–1008.
197. Visintin, R, and Amon, A (2001). Regulation of the mitotic exit protein kinases CDc15 and Dbf2. Molecular Biology of the Cell 12, 2961–2974.
198. Visintin, R, Craig, K, Hwang, ES, Prinz, S, Tyers, M, and Amon, A (1998). The Phosphatase Cdc14 Triggers Mitotic Exit by Reversal of Cdk-Dependent Phosphorylation. Molecular Cell 2, 709–718.
199. Wakefield, JG, Stephens, DJ, and Tavaré, JM (2003). A role for glycogen synthase kinase-3 in mitotic spindle dynamics and chromosome alignment. Journal of Cell Science 116, 637–646.
200. Wang, Y, Hu, F, and Elledge, SJ (2000). The Bfa1/Bub2 GAP complex comprises a universal checkpoint required to prevent mitotic exit. Current Biology 10, 1379–1382.
201. Wang, Y, Shirogane, T, Liu, D, Harper, JW, and Elledge, SJ (2003). Exit from exit: resetting the cell cycle through Amn1 inhibition of G protein signaling. Cell 112, 697–709.
202. Wäsch, R, and Cross, FR (2002). APC-dependent proteolysis of the mitotic cyclin Clb2 is essential for mitotic exit. Nature 418, 556–562.
203. Weinreich, M, Liang, C, and Stillman, B (1999). The Cdc6p nucleotide-binding motif is required for loading mcm proteins onto chromatin. Proc Natl Acad Sci U S A 96, 441–446.
204. Whalen, J, Sniffen, C, Gartland, S, Vannini, M, and Seshan, A (2018). Budding Yeast BFA1 Has Multiple Positive Roles in Directing Late Mitotic Events. G3: Genes|Genomes|Genetics 8, 3397.
205. Wilmes, GM, Archambault, V, Austin, RJ, Jacobson, MD, Bell, SP, and Cross, FR (2004). Interaction of the S-phase cyclin Clb5 with an “RXL” docking sequence in the initiator protein Orc6 provides an origin-localized replication control switch. Genes Dev 18, 981–991.

206. Yamashita, YM, and Fuller, MT (2008). Asymmetric centrosome behavior and the mechanisms of stem cell division. J Cell Biol 180, 261–266.
207. Yeh, E, Skibbens, R v., Cheng, JW, Salmon, ED, and Bloom, K (1995). Spindle dynamics and cell cycle regulation of dynein in the budding yeast, Saccharomyces cerevisiae. J Cell Biol 130, 687–700.
208. Yoshida, S, Asakawa, K, and Toh-e, A (2002). Mitotic Exit Network Controls the Localization of Cdc14 to the Spindle Pole Body in Saccharomyces cerevisiae. Current Biology 12, 944–950.
209. Yuan, H, Chiang, CYA, Cheng, J, Salzmann, V, and Yamashita, YM (2012). Regulation of cyclin A localization downstream of Par-1 function is critical for the centrosome orientation checkpoint in Drosophila male germline stem cells. Developmental Biology 361, 57–67.
210. Zhao, H, Zhou, X, Yuan, G, Hou, Z, Sun, H, Zhai, N, Huang, B, and Li, X (2021). CDC6 is up-regulated and a poor prognostic signature in glioblastoma multiforme. Clinical and Translational Oncology 23, 565–571.